(19) **United States**

(12) **Patent Application Publication** (10) Pub. No.: **US 2007/0252082 A1**

Miller et al. (43) **Pub. Date: Nov. 1, 2007**

(54) **MOBILITY BASED APPARATUS AND METHODS USING DISPERSION CHARACTERISTICS, SAMPLE FRAGMENTATION, AND/OR PRESSURE CONTROL TO IMPROVE ANALYSIS OF A SAMPLE**

(75) Inventors: **Raanan A. Miller**, Chestnut Hill, MA (US); **Erkinjon G. Nazarov**, Lexington, MA (US); **Lawrence A. Kaufman**, Waltham, MA (US); **Douglas B. Cameron**, Wellesley, MA (US)

Correspondence Address:
FISH & NEAVE IP GROUP
ROPES & GRAY LLP
ONE INTERNATIONAL PLACE
BOSTON, MA 02110-2624 (US)

(73) Assignee: **SIONEX CORPORATION**, Bedford, MA

(21) Appl. No.: 11/724,953

(22) Filed: **Mar. 16, 2007**

Related U.S. Application Data

Publication Classification

(51) **Int. Cl.**
B01D 59/44 (2006.01)
(52) **U.S. Cl.** 250/282

(57) **ABSTRACT**

The invention relates generally to devices and methods for displaying ion mobility based analysis information using a processor that processes data from an ion mobility based analyzer and a display that displays the processed data in a three-dimensional representation.
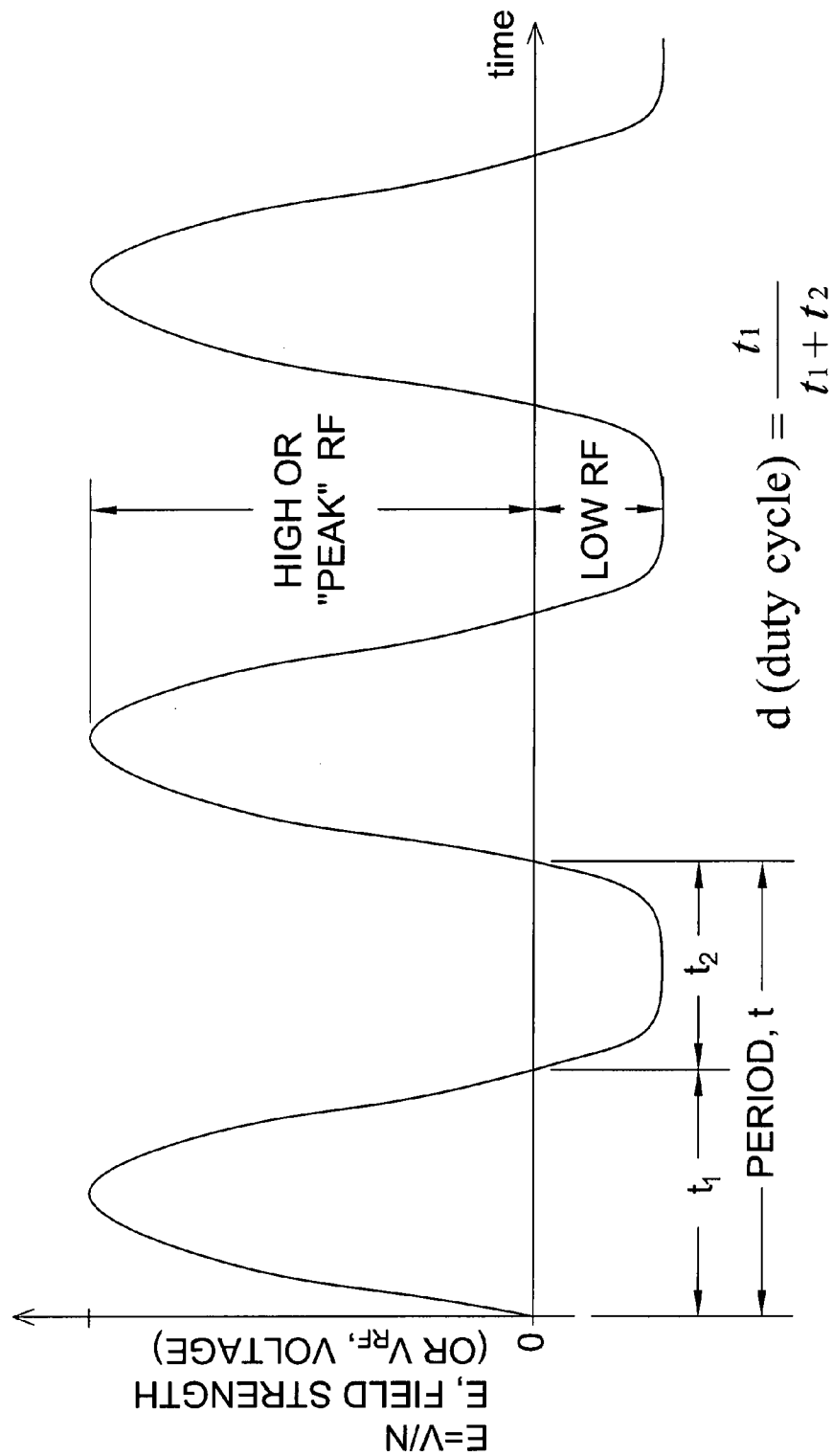
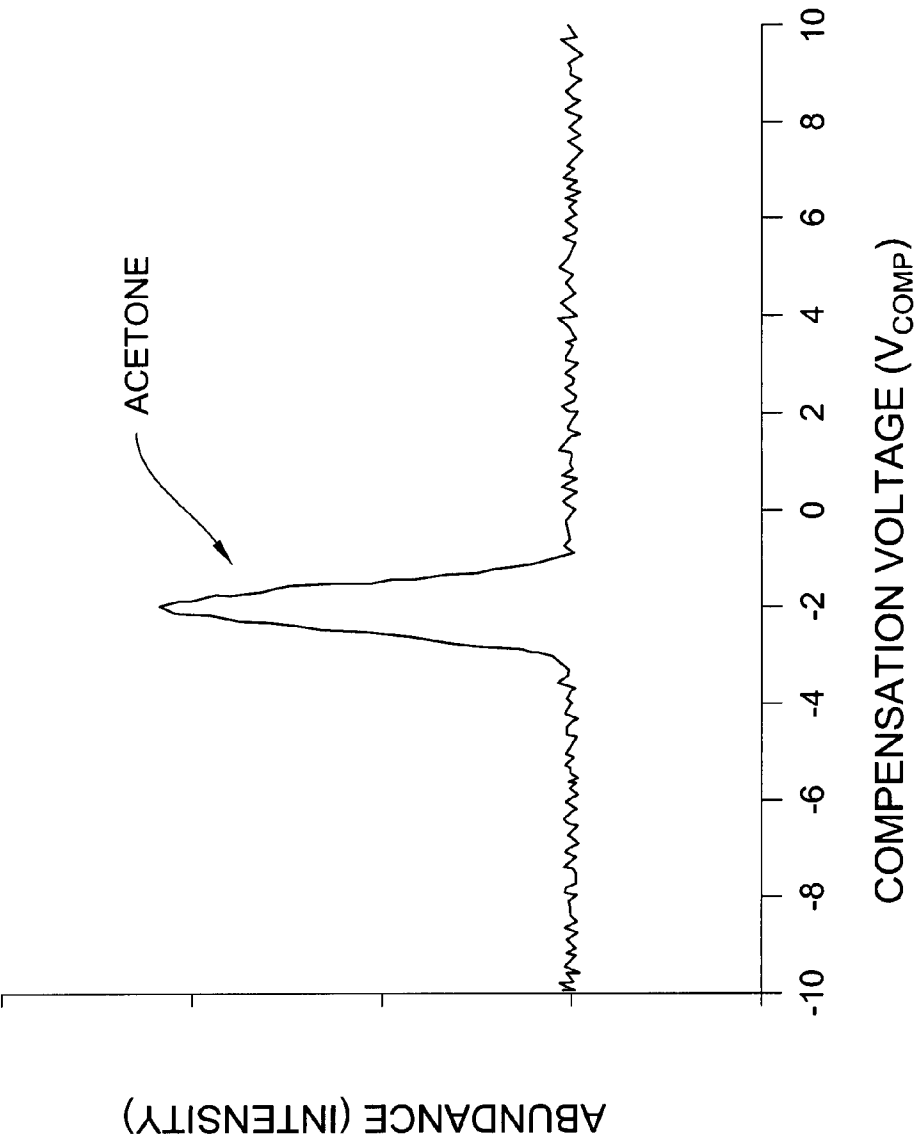$$d \text{ (duty cycle)} = \frac{t_1}{t_1 + t_2}$$
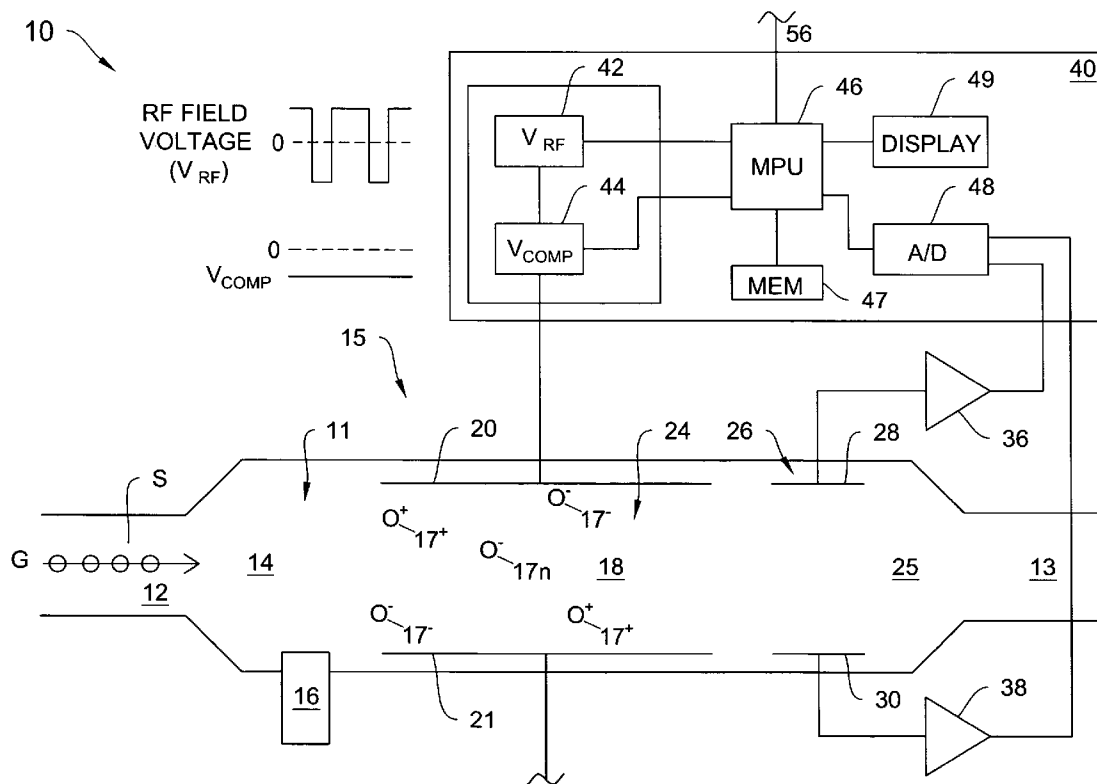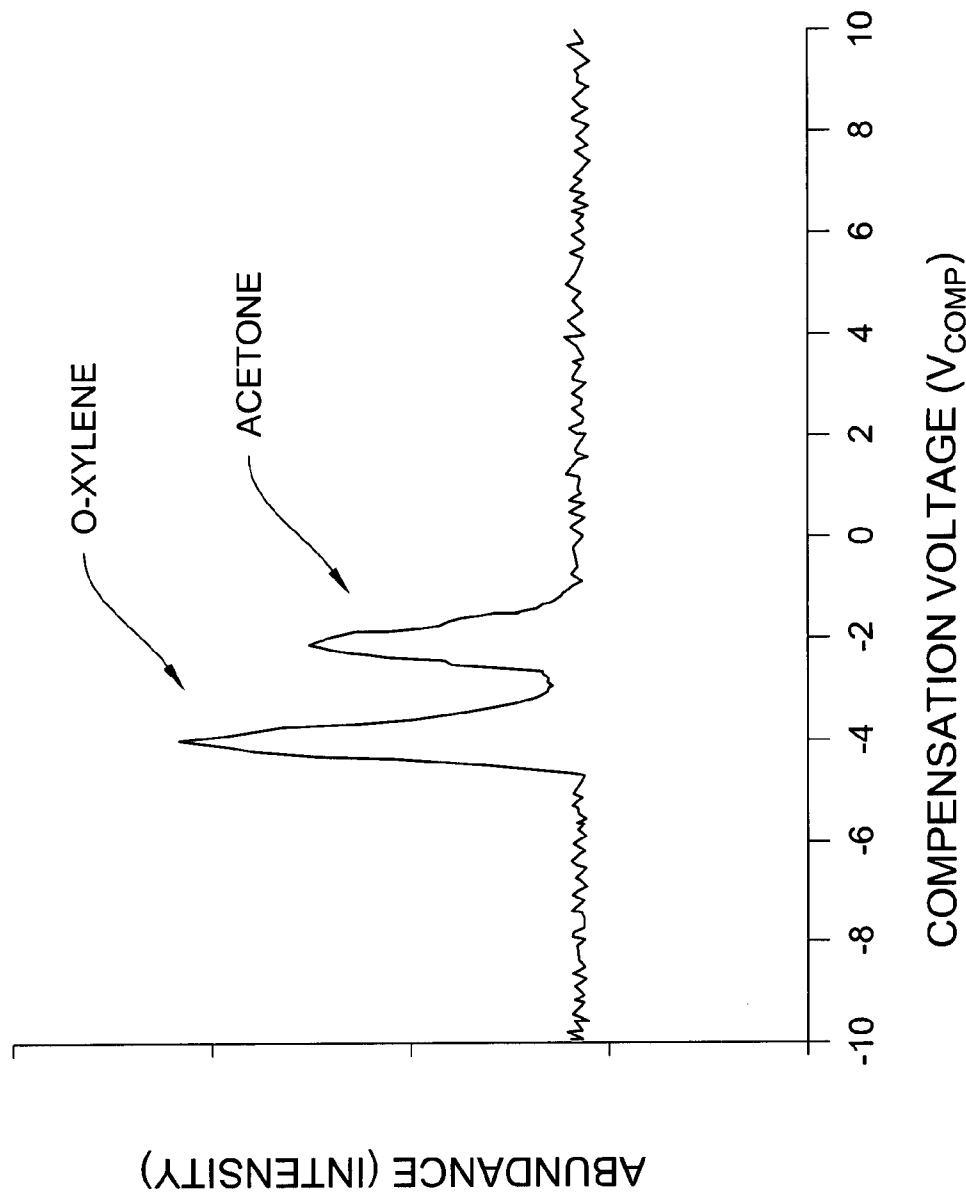
Figure 1 (prior art)

Figure 2A (prior art)
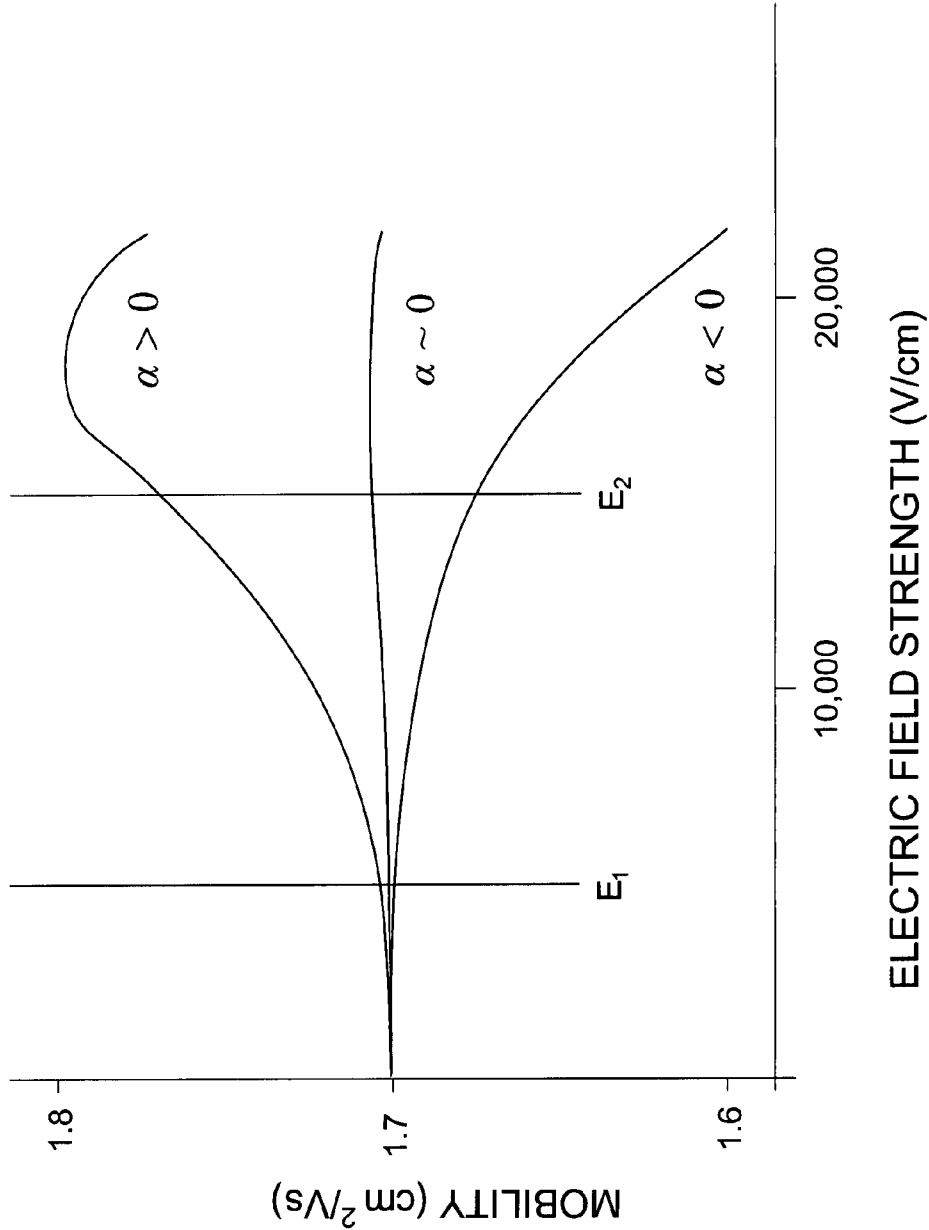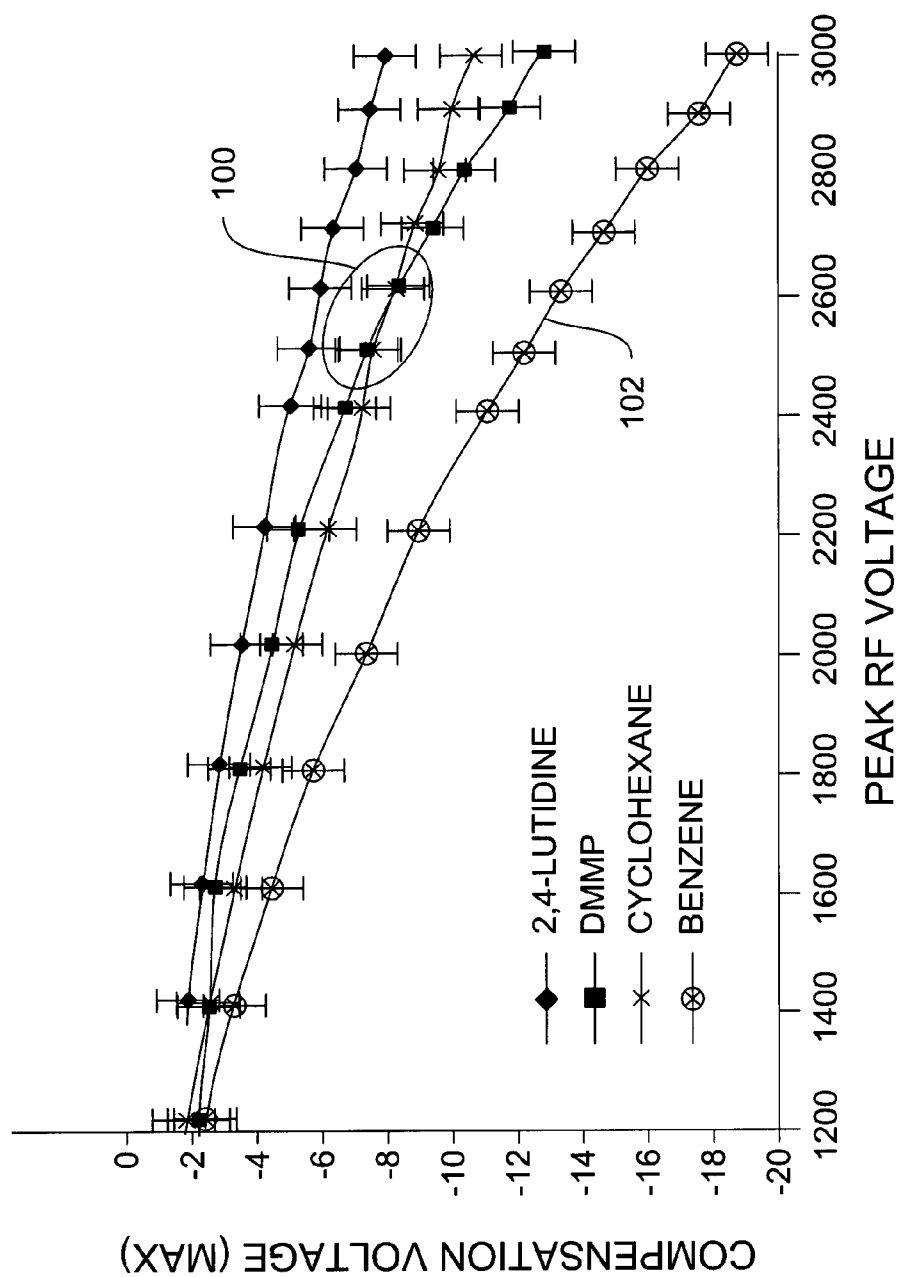
Figure 2B (prior art)

Figure 3 (prior art)

Figure 4
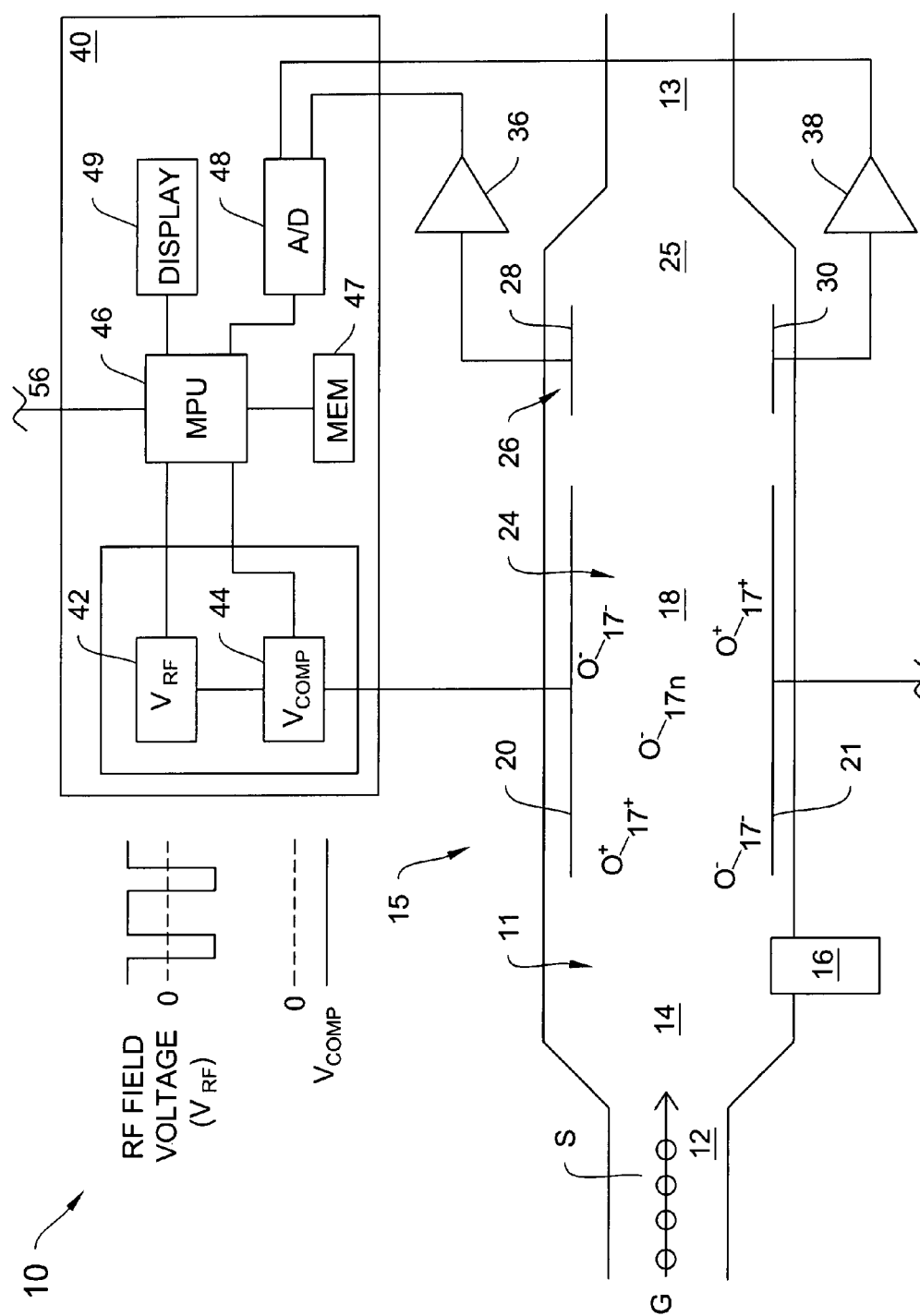
Figure 5

EFFECT OF VARYING METHANE CONCENTRATIONS ON ETHYL
MERCAPTAN SPECTRA
POSITIVE ION MODE
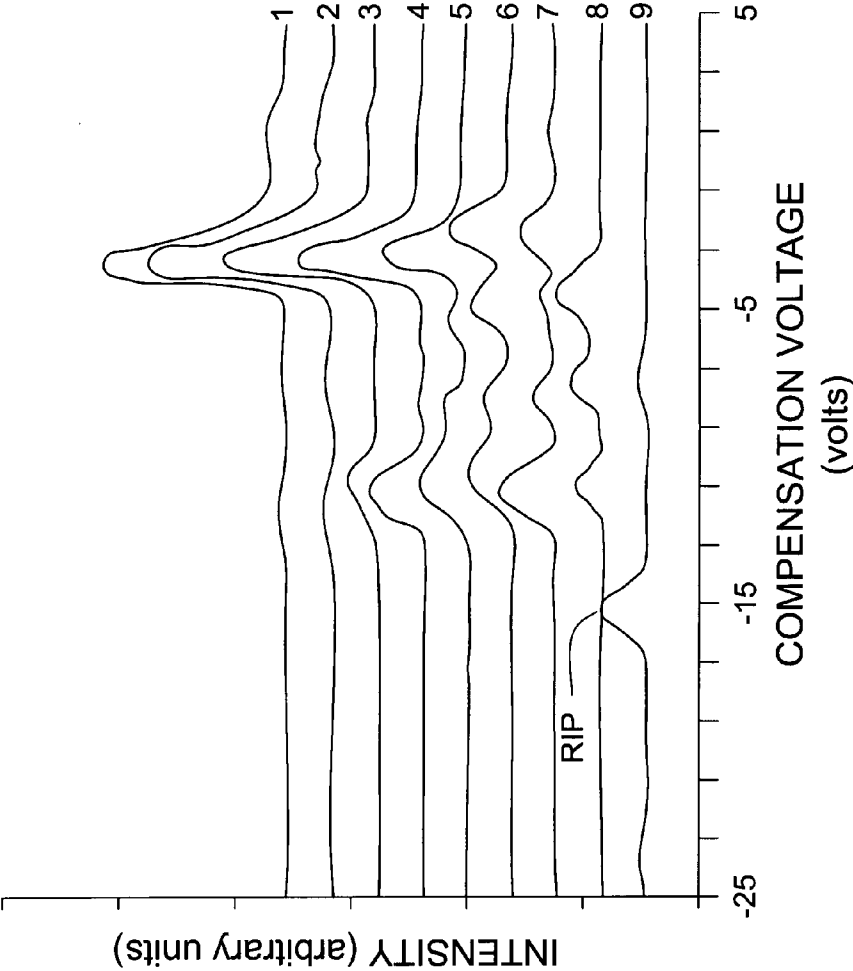
1	33% Methane	No Sample
2	33% Methane	6.36E-8 g Mercaptan
3	23% Methane	6.36E-8 g Mercaptan
4	15% Methane	6.36E-8 g Mercaptan
5	9% Methane	6.36E-8 g Mercaptan
6	5% Methane	6.36E-8 g Mercaptan
7	Trace Methane	6.36E-8 g Mercaptan
8	0% Methane	6.36E-8 g Mercaptan
9	0% Methane	0 g Mercaptan

Figure 6
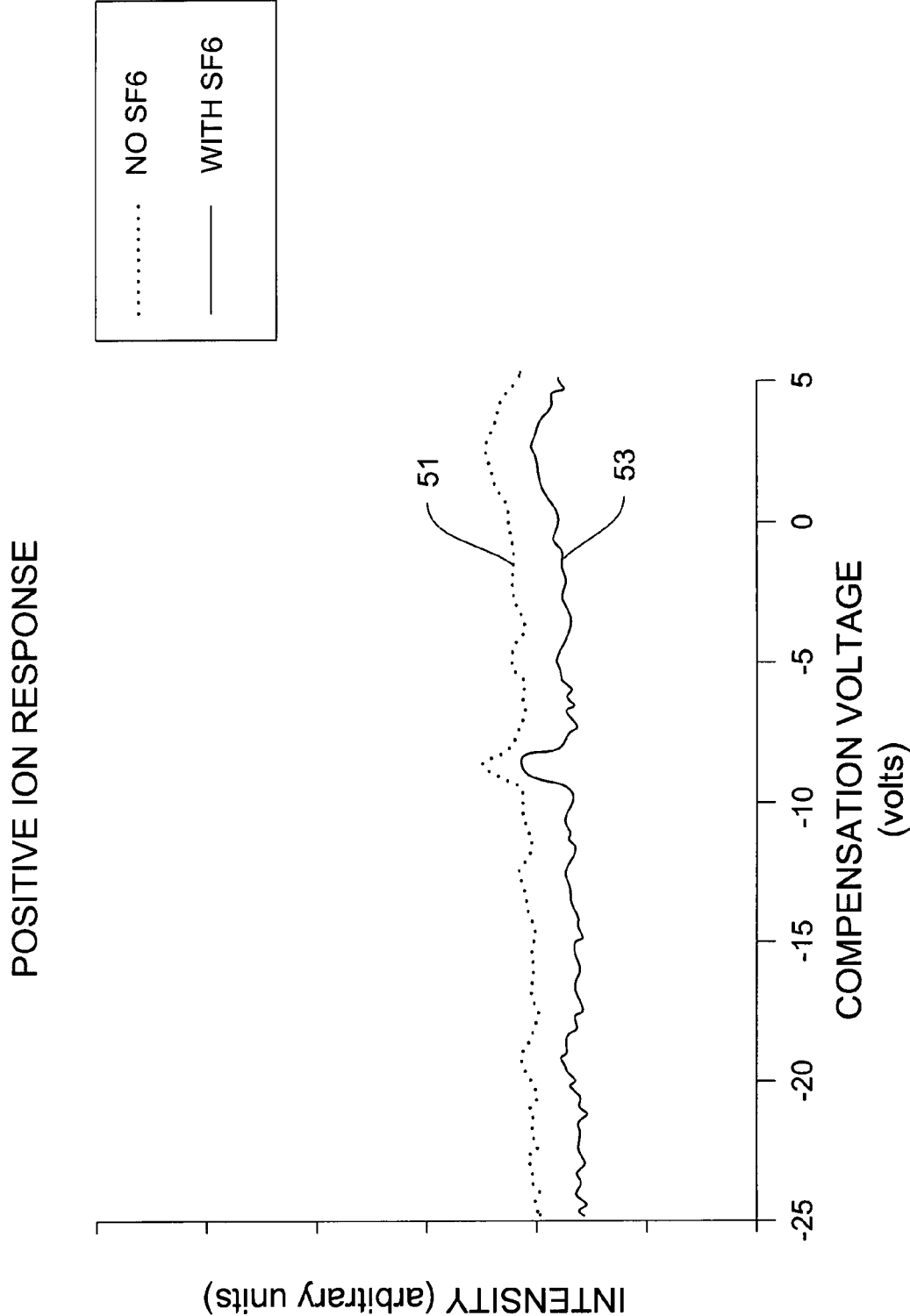
EFFECT OF VARYING METHANE CONCENTRATIONS ON ETHYL
MERCAPTAN SPECTRA
NEGATIVE ION MODE

1	33% Methane	No Sample
2	33% Methane	6.36E-8 g Mercaptan
3	23% Methane	6.36E-8 g Mercaptan
4	15% Methane	6.36E-8 g Mercaptan
5	9% Methane	6.36E-8 g Mercaptan
6	5% Methane	6.36E-8 g Mercaptan
7	Trace Methane	6.36E-8 g Mercaptan
8	0% Methane	6.36E-8 g Mercaptan
9	0% Methane	0 g Mercaptan

INTENSITY (arbitrary units)

COMPENSATION VOLTAGE (volts)

Figure 7

Figure 8

Figure 9
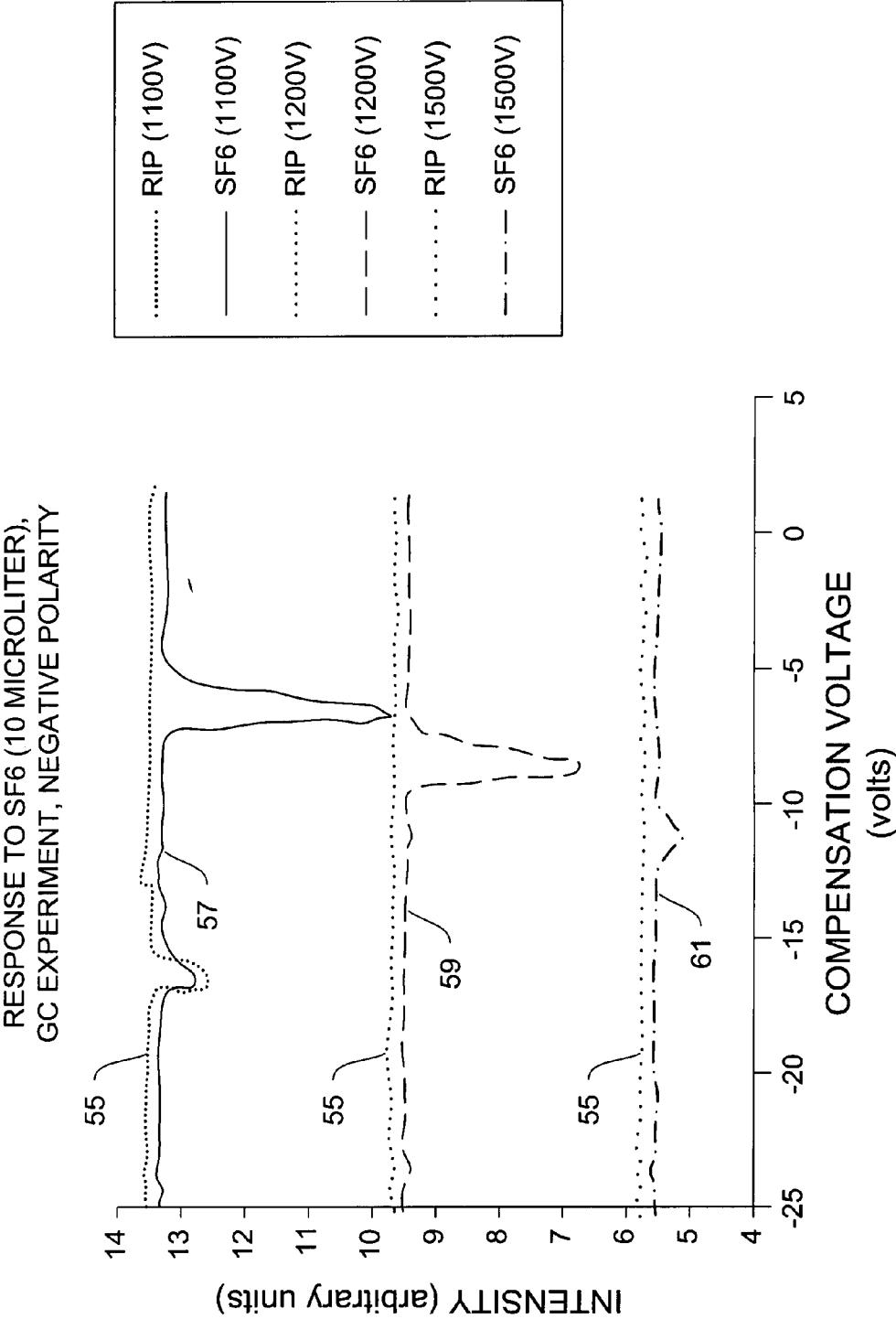
Figure 10
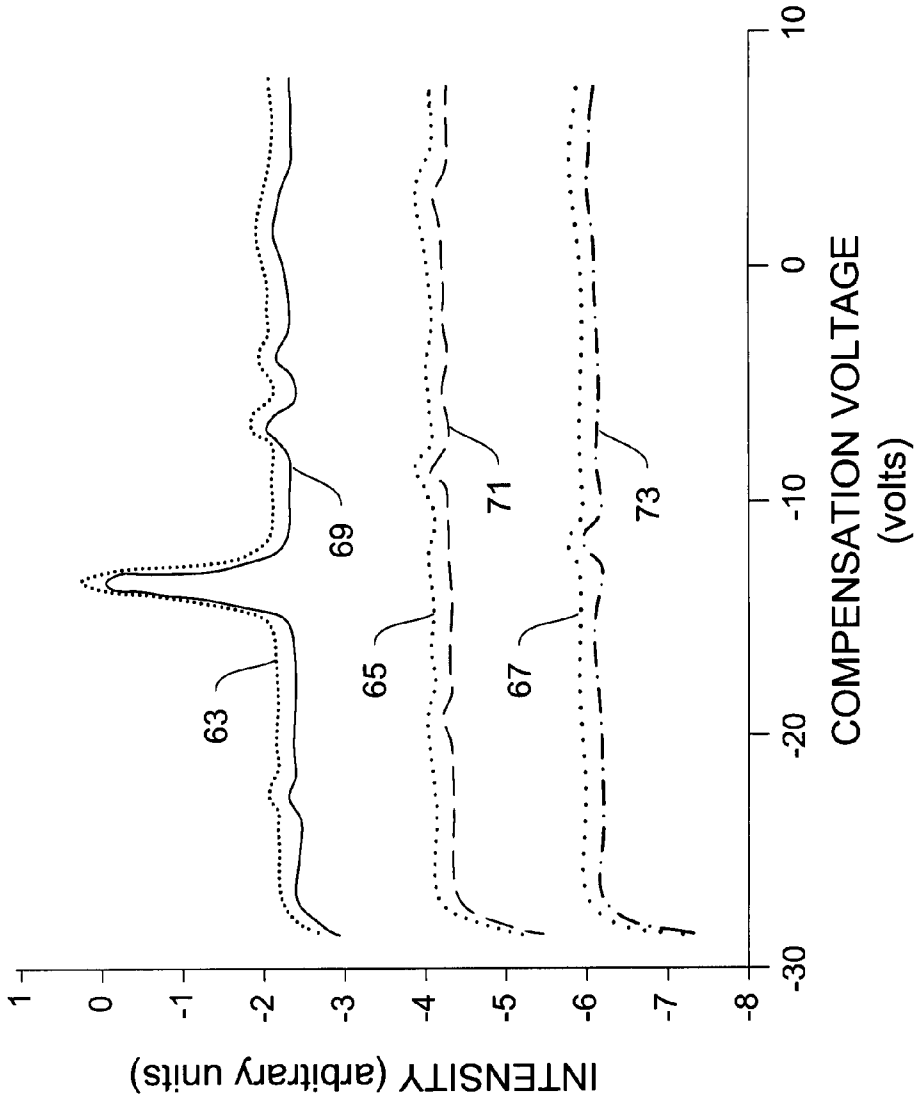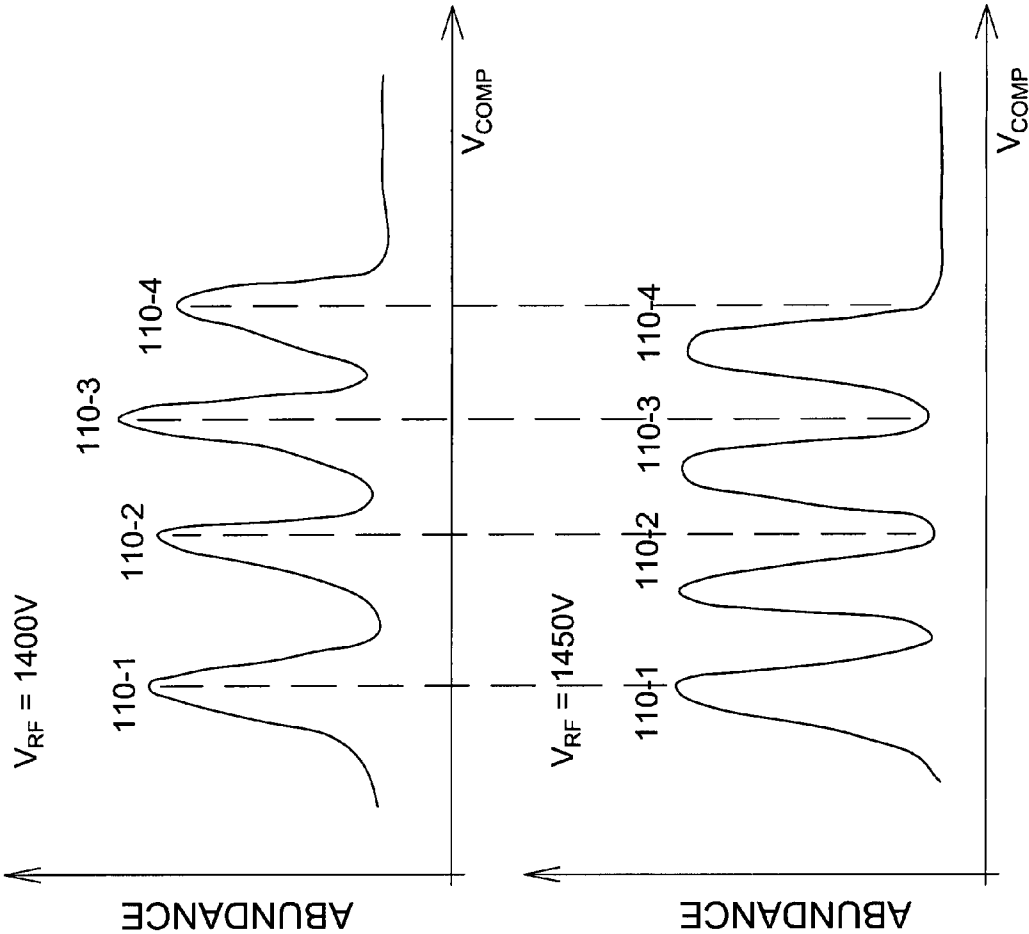
Figure 11

Figure 12

TUNABLE RESOLUTION
(XYLENES AT DIFFERENT E_{MAX} VALUES)

E_{MAX} = 24000 V/cm

ABUNDANCE

COMPENSATION VOLTAGE
(volts)

Figure 13B

E_{MAX} = 18000 V/cm

ABUNDANCE

COMPENSATION VOLTAGE
(volts)

Figure 13A

Figure 14A

Figure 14B

620

622

621

623

625

Figure 15A

V_c

V_{rf}

1000
800
600
400

METHYL SALICYLATE -
POSITIVE CHANNEL
0.33 mg/m³

$V_{rf} =$
[838,879]

627

629

Figure 15B

2.82
2.81
2.80
2.79
2.78
2.77
2.76

624

626

639

638

640

V_c

V_{rf}
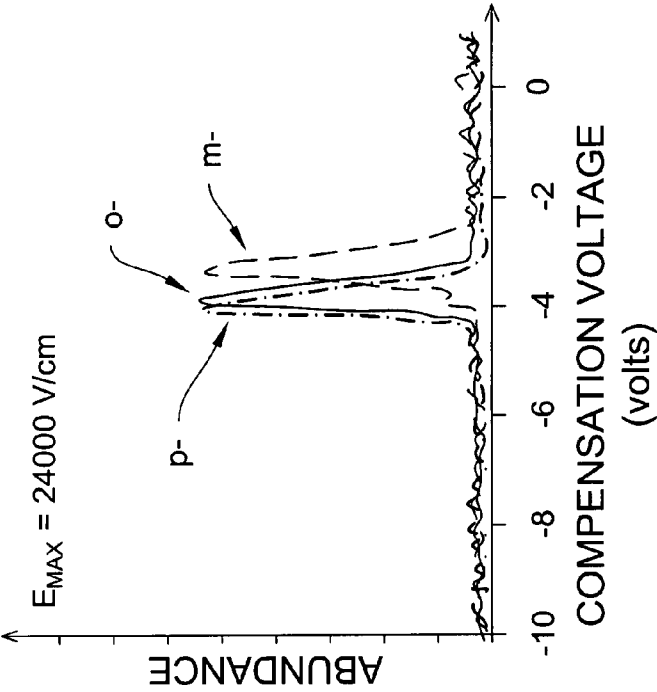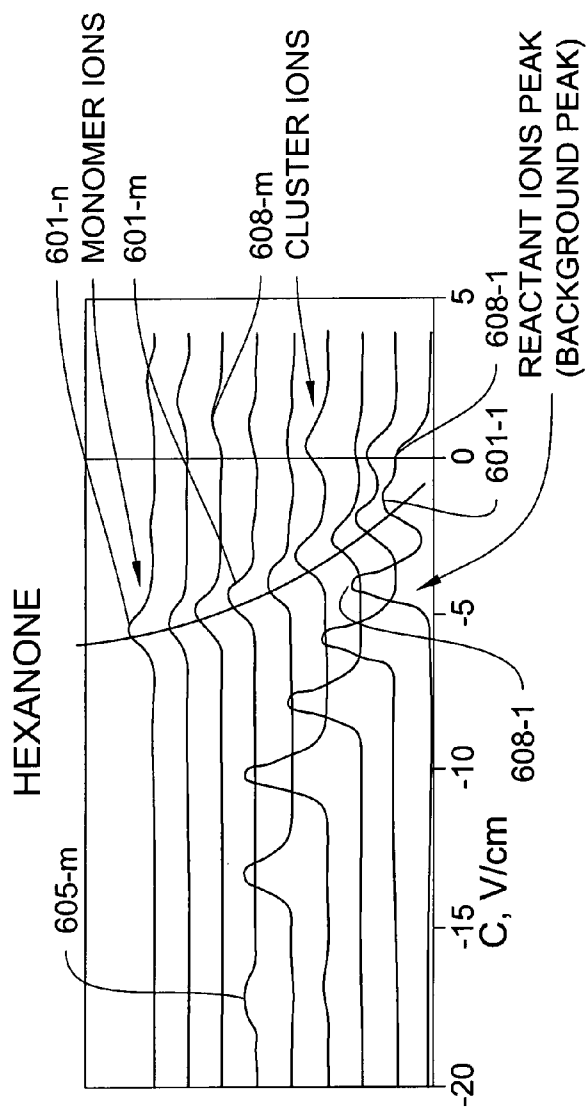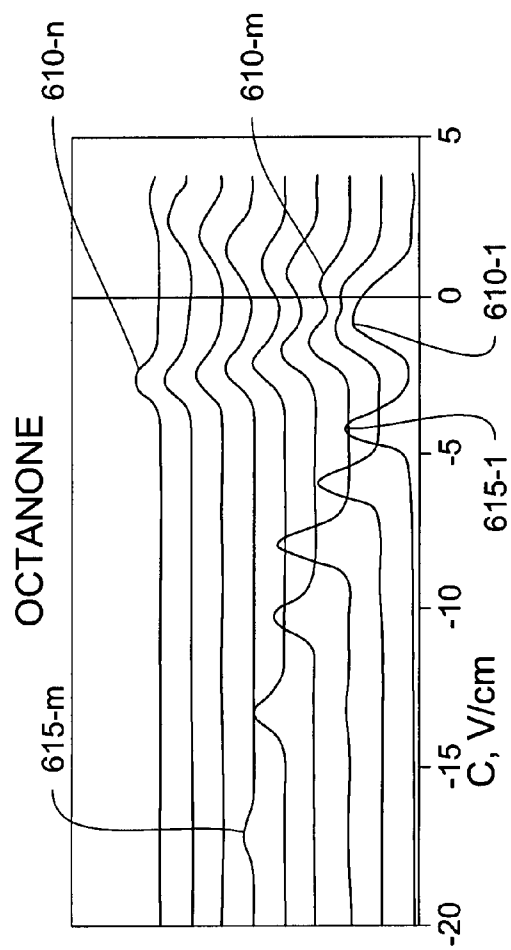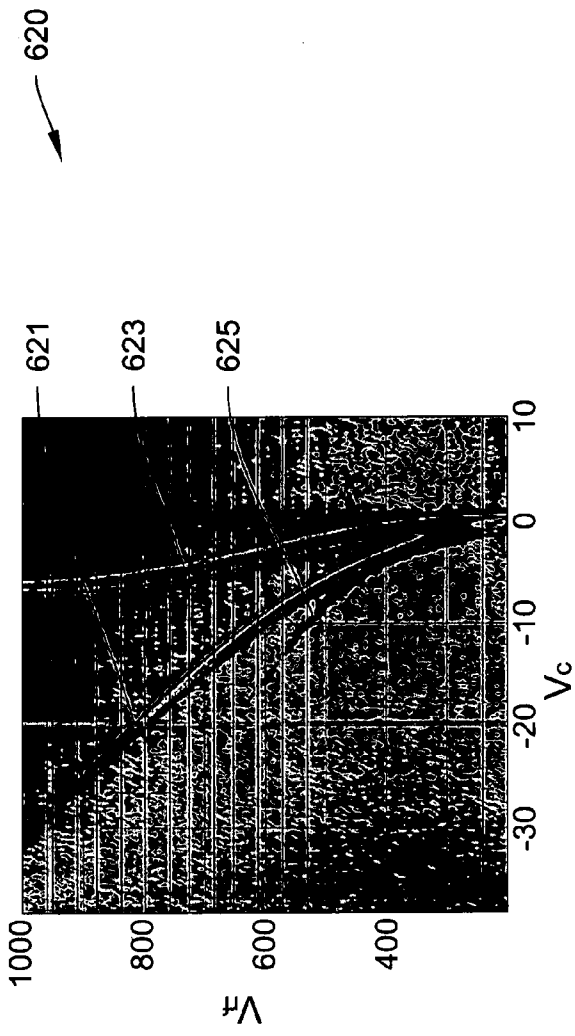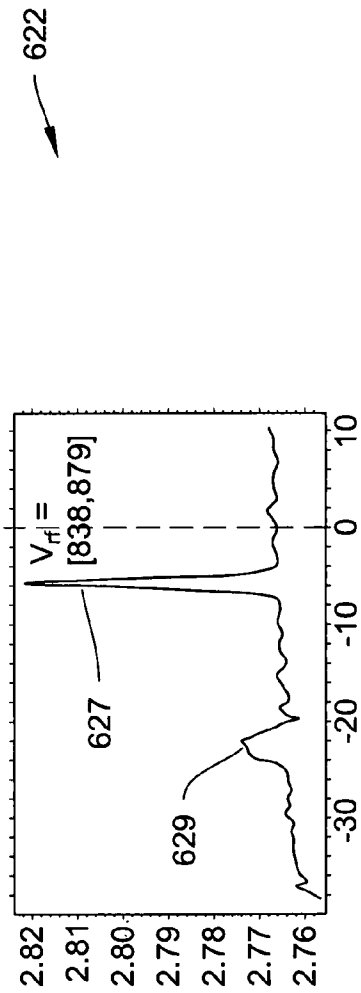
Figure 16A

Figure 16B

DMMP -
POSITIVE CHANNEL
0.16 mg/m^3

$V_{rf} =$
[838,879]

628

630

631

634

636

632

DIMP -
POSITIVE CHANNEL
0.3 mg/m³

Figure 17

Figure 18

$V_{rf} =$
[838,879]

EFFECT OF ELECTRIC FIELD ON ETHYL
MERCAPTAN RF SPECTRA

AMOUNT OF SAMPLE: 7.3ng

1450V
1430V
1340V
1230V
1120V
1000V

870V

620V

702
701-n
701-1
710

80
70
60
50
40
30
20
10
0

-30   -20   -10   0   10

COMPENSATION VOLTAGE
(volts)

Figure 19

712

716

714

INTENSITY

COMPENSATION VOLTAGE C_V (VOLTS)

-30

0
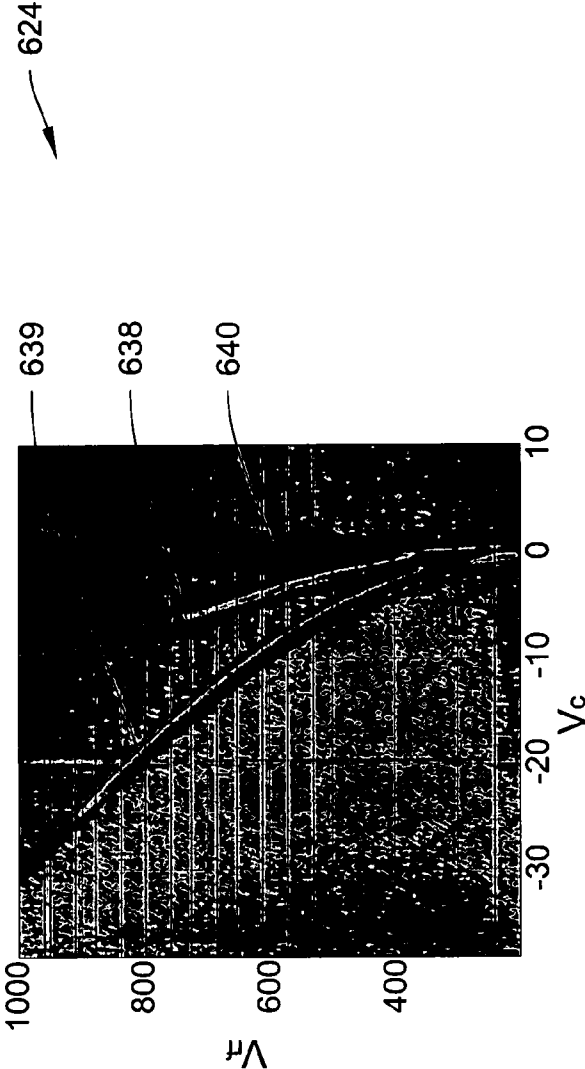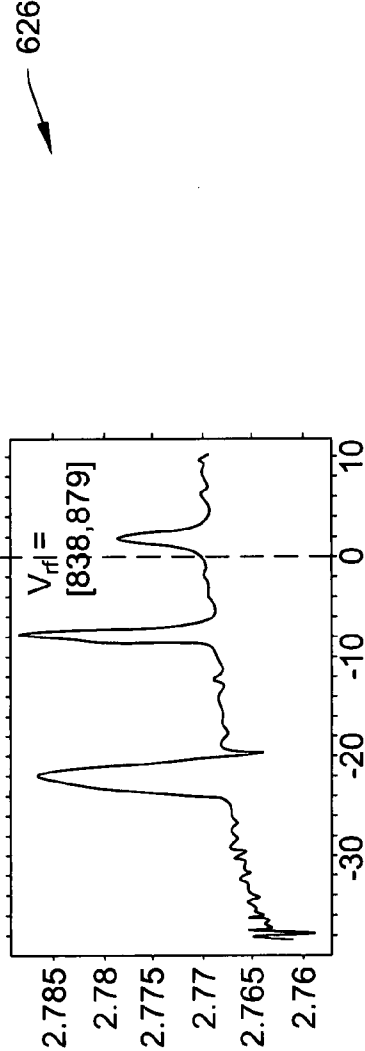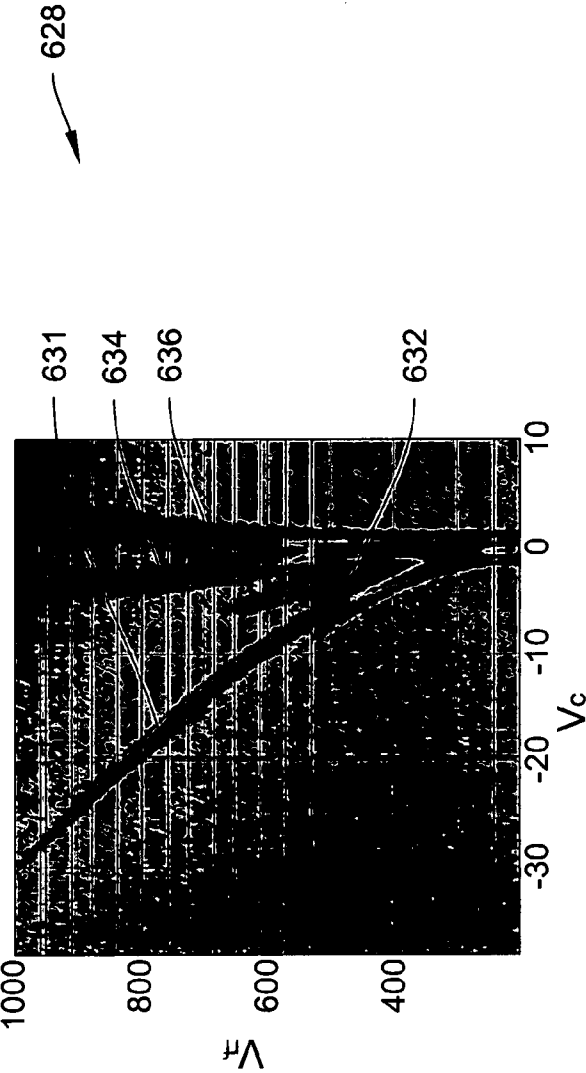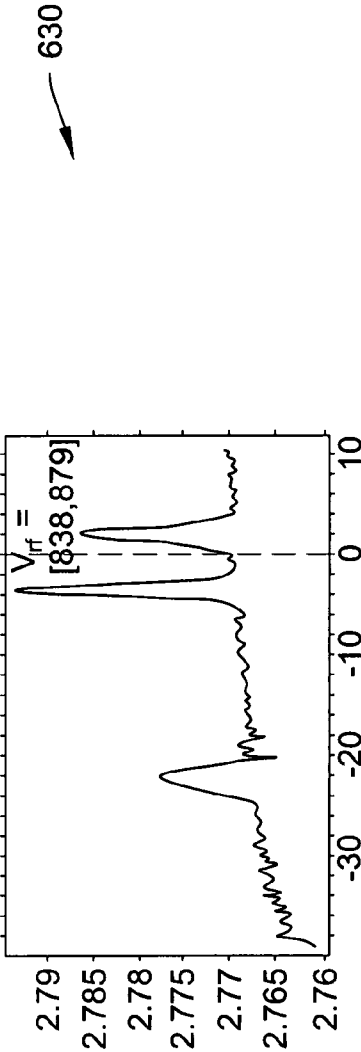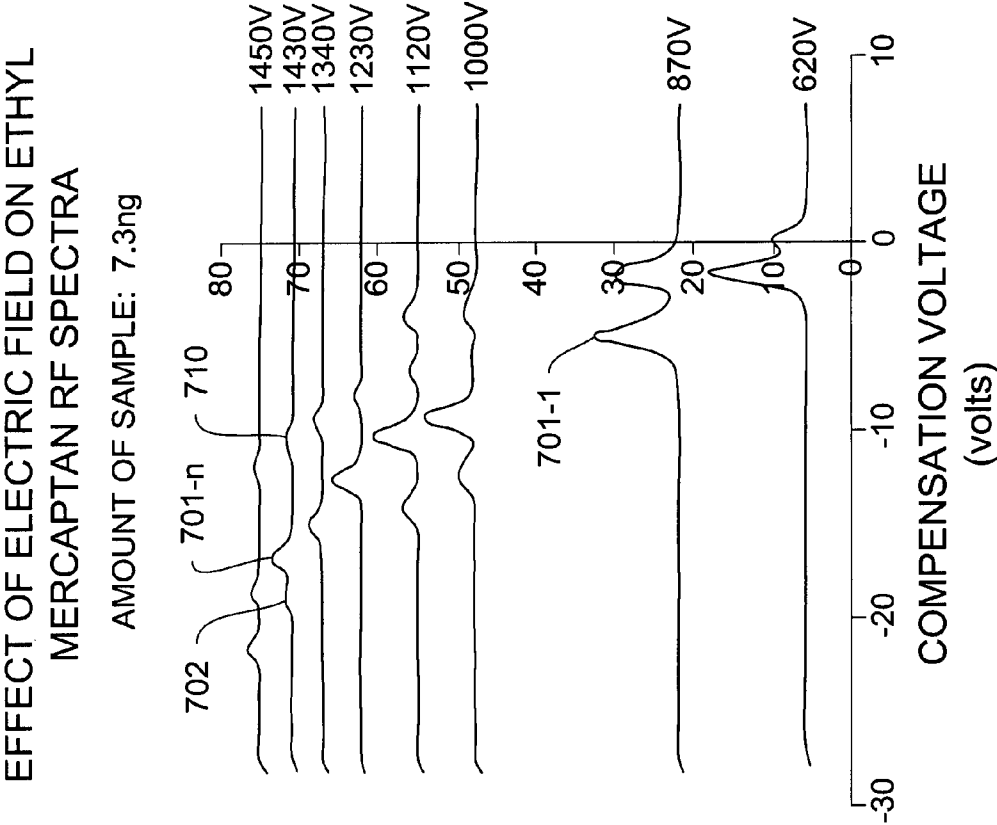
Figure 20A
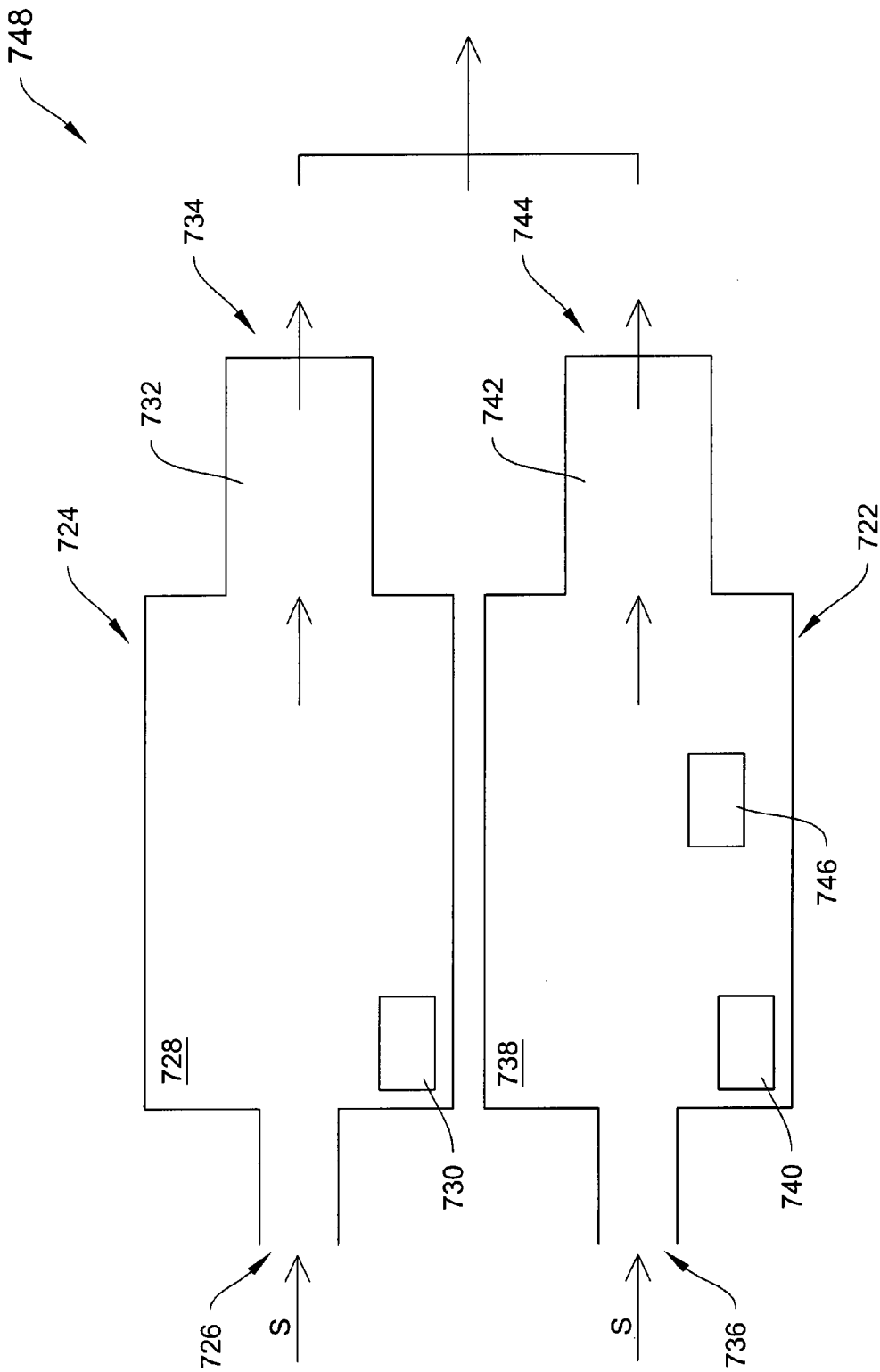
Figure 20B
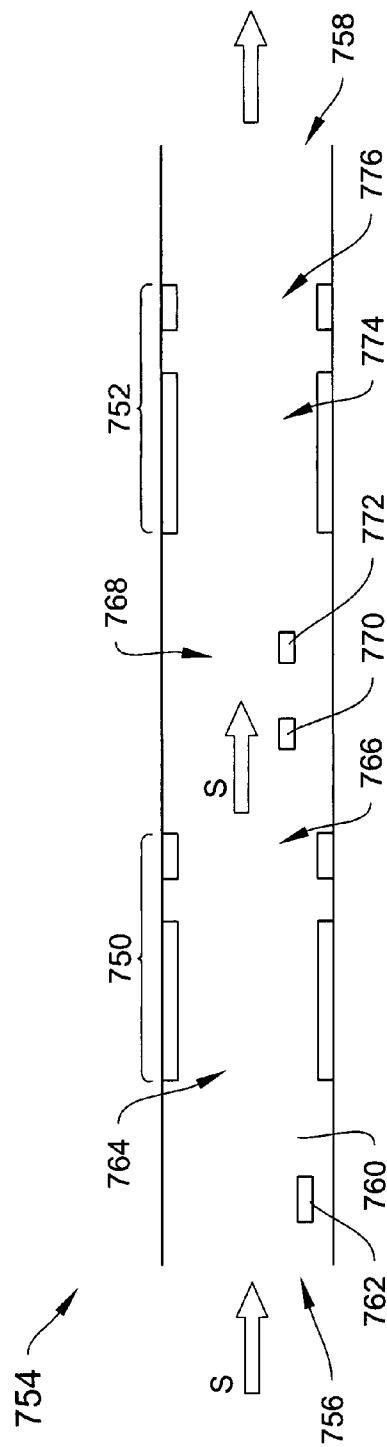
Figure 21

Figure 22

Figure 23A

Figure 23B

Figure 24

Figure 25

824

826

HIGH FIELD STRENGTH
GA FRAGMENTED

$V_{rf} = [1479, 1500]$

FRAGMENTS

Figure 26A

$V_{rf} = [1031, 1051]$

Figure 26B

828

830

$V_{rf} = [1381,1401]$

Figure 26C

$V_{rf} = [879, 899]$

Figure 26D

832

834

$V_{rf} = [1278, 1298]$

Figure 26E

$V_{rf} = [681, 702]$

LOW FIELD STRENGTH

Figure 26F

836

838

$V_{rf} = [1179, 1200]$

LOW FIELD
STRENGTH

Figure 26G

$V_{rf} = [500, 521]$

Figure 26H

POSITIVE MODE. FLOW RATE 300cc/min

| 500V/234mmHg |
| 510V/241mmHg |
| 540V/258mmHg |
| 575V/279mmHg |
| 640V/321mmHg |
| 730V/385mmHg |
| 670V/509mmHg |
| 920V/556mmHg |
| 950V/591mmHg |
| 1000V/637mmHg |
| 1010V/655mmHg |
| 1050V/760mmHg |

ION INTENSITY

COMPENSATION VOLTAGE (V)

Figure 27A

840

NEGATIVE MODE. FLOW RATE 300cc/min

| 500V/234mmHg |
| 510V/241mmHg |
| 540V/258mmHg |
| 575V/279mmHg |
| 640V/321mmHg |
| 730V/385mmHg |
| 670V/509mmHg |
| 920V/556mmHg |
| 950V/591mmHg |
| 1000V/637mmHg |
| 1010V/655mmHg |
| 1050V/760mmHg |

ION INTENSITY

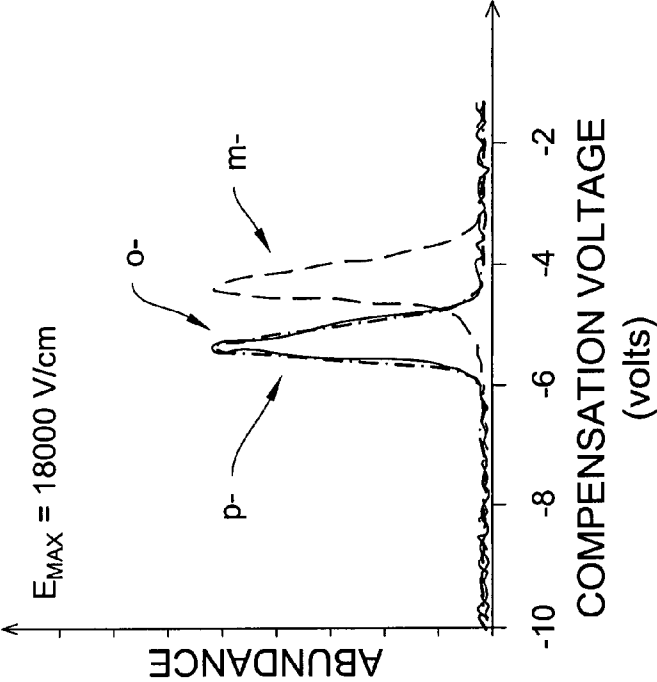COMPENSATION VOLTAGE (V)

Figure 27B

842

Figure 28A

Figure 28B

Figure 29A

Figure 29B

Figure 30A

Figure 30B

Figure 31

Figure 32A
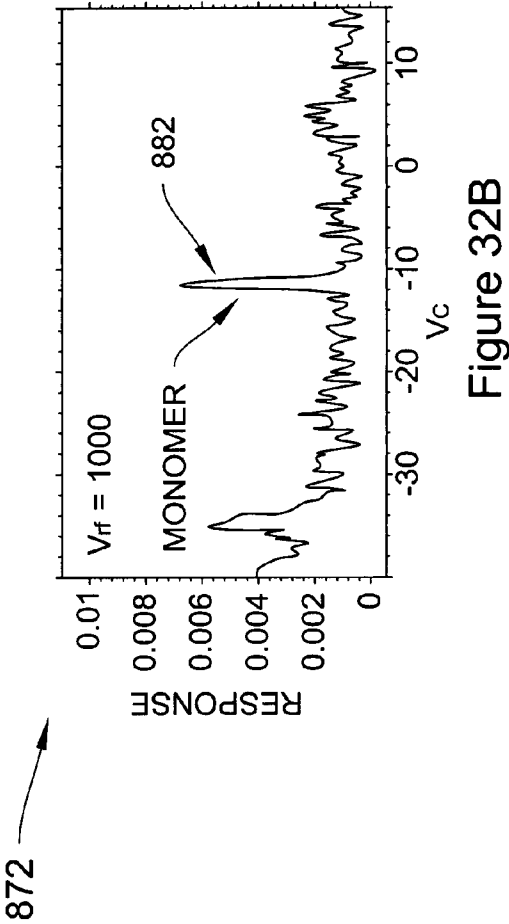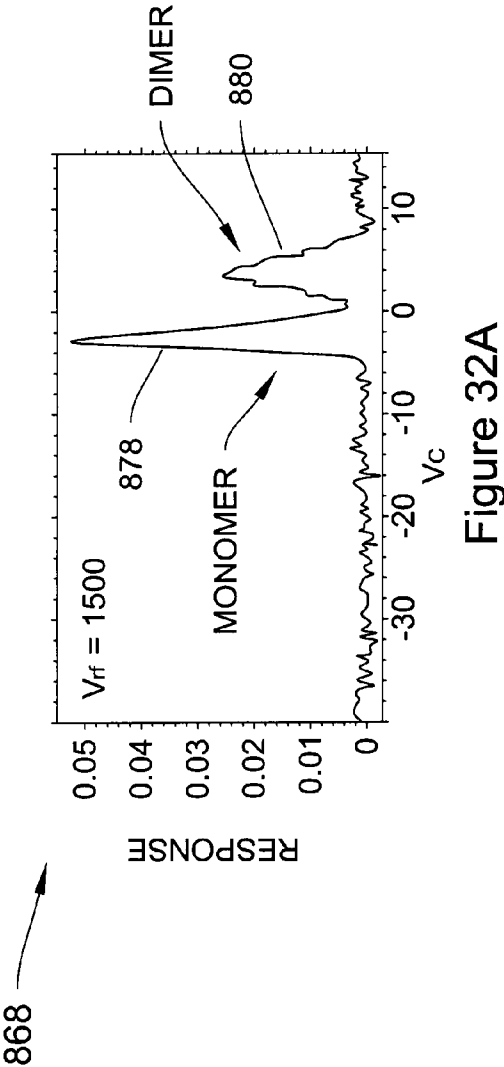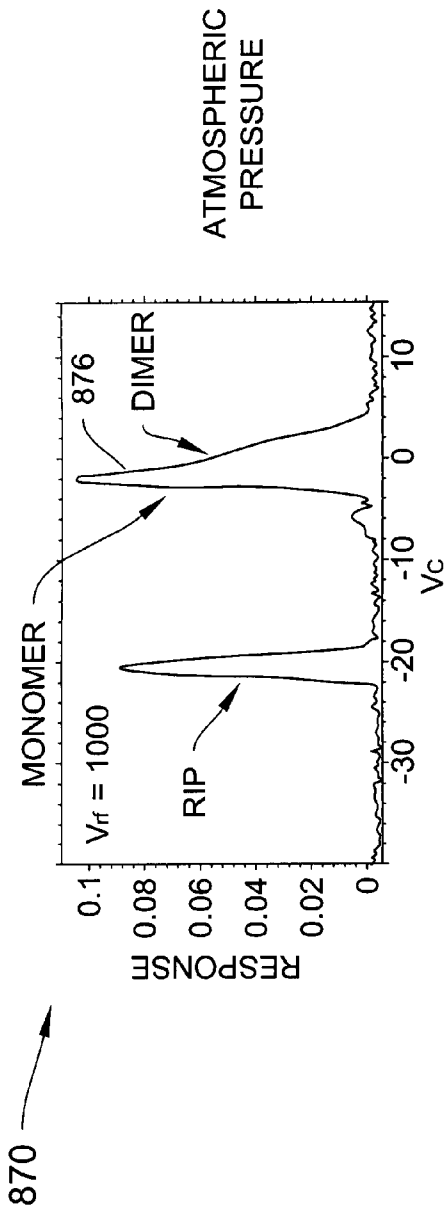
Figure 32B

Figure 32C

Figure 32D

Figure 34

Figure 33

Figure 35

Figure 36A

Figure 36B

Protonated Monomer

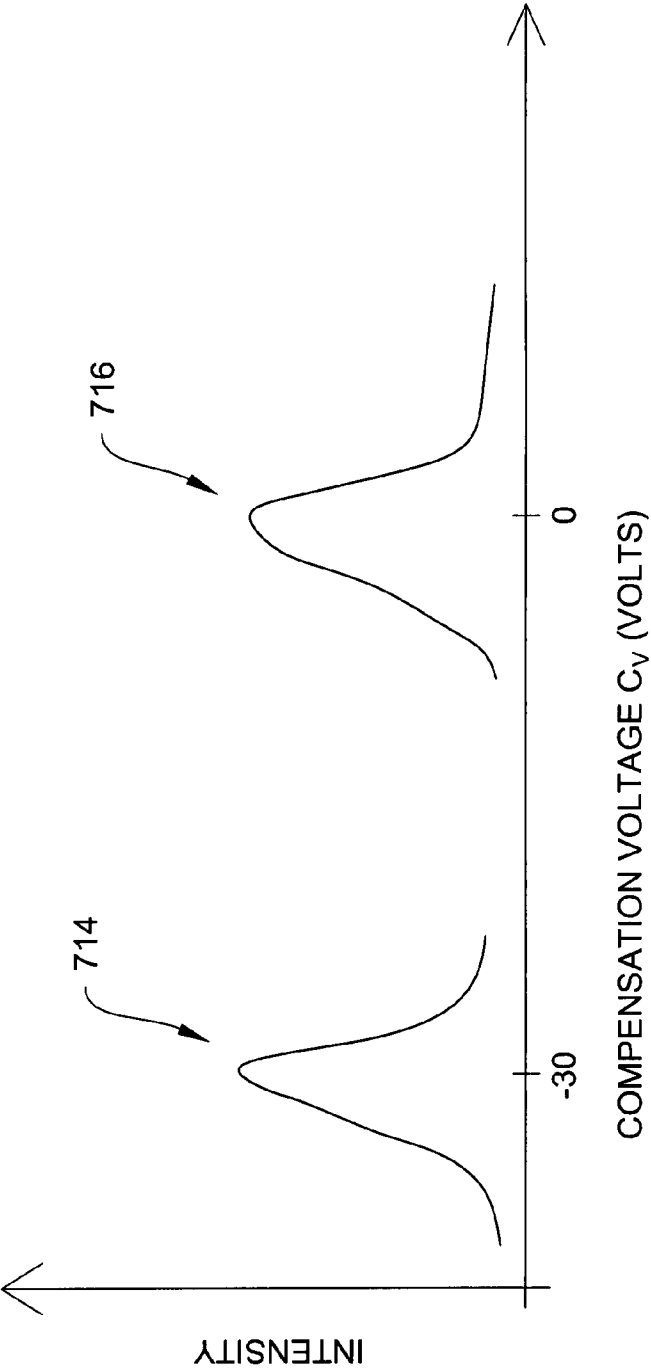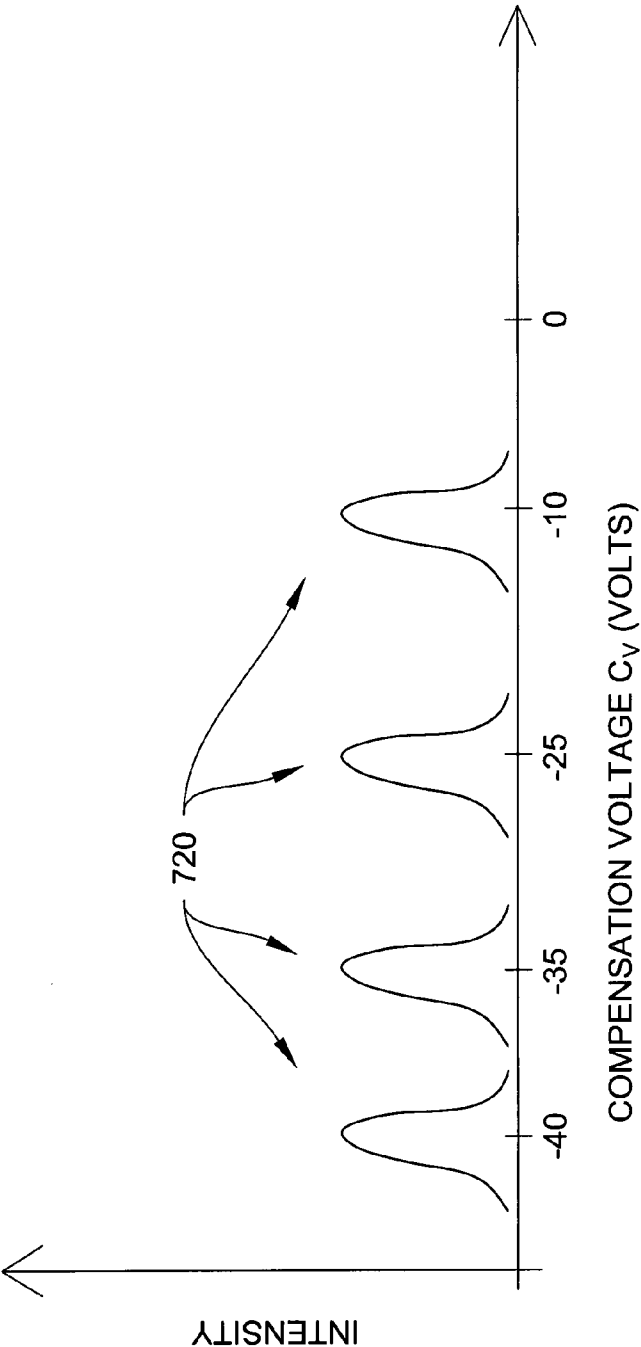|	Acetone	Butanone	Pentanone	Hexanone	Heptanone	Octanone	Nonanone	Decanone
Formula	$C_3H_6OH^+$	$C_4H_8OH^+$	$C_5H_{10}OH^+$	$C_6H_{12}OH^+$	$C_7H_{14}OH^+$	$C_8H_{16}OH^+$	$C_9H_{18}OH^+$	$C_{10}H_{20}OH^+$
m/z (amu)	59	73	87	101	115	129	143	157
α_2[% - Td]	3.14×10^{-3}	2.7×10^{-3}	2.1×10^{-3}	1.7×10^{-3}	1.2×10^{-3}	8.4×10^{-4}	6.5×10^{-4}	4.6×10^{-4}
α_4[% - Td]	-9.54×10^{-8}	-1.4×10^{-7}	-1.2×10^{-7}	-1.1×10^{-7}	-8.8×10^{-8}	-6.9×10^{-8}	-6.6×10^{-8}	-5.2×10^{-8}

Figure 37

Proton Bound Dimer

	Acetone	Butanone	Pentanone	Hexanone	Heptanone	Octanone	Nonanone	Decanone
Formula	$(C_3H_6O)_2H^+$	$(C_4H_8O)_2H^+$	$(C_5H_{10}O)_2H^+$	$(C_6H_{12}O)_2H^+$	$(C_7H_{14}O)_2H^+$	$(C_8H_{16}O)_2H^+$	$(C_9H_{18}O)_2H^+$	$(C_{10}H_{20}O)_2H^+$
m/z (amu)	117	145	173	201	229	257	285	303
α_2[% - Td]	1.34×10^{-3}	8.0×10^{-4}	1.9×10^{-4}	1.9×10^{-4}	2.5×10^{-5}	-3.5×10^{-5}	-2.2×10^{-4}	-3.5×10^{-4}
α_4[% - Td]	-1.77×10^{-7}	-1.2×10^{-7}	-6.0×10^{-8}	-8.0×10^{-8}	-6.8×10^{-8}	-6.9×10^{-8}	-4.8×10^{-8}	-3.2×10^{-8}

Figure 38

Figure 39A

Figure 39B

1018

IDENTIFY FEATURES
(PEAKS V_C, a)
$\forall V_{RF} \Rightarrow P$

1000

KNOWN
COMPOUND

1002

V_{COMP}, V_{DISP}
RANGES (b, e, s)

1004

$V_{DISP} = V_{DISPb}$ TO V_{DISPe} BY V_{DISPs}

1008

$V_{COMP} = V_{COMPb}$ TO V_{COMPe} BY V_{COMPs}

1010

STORE RESPONSE
AS VALUE (a)

1012

LAST
V_C?

NO   YES

1014

LAST
V_{RF}?

NO   YES

Figure 40A

Figure 40B

1220

IDENTIFY FEATURES
(PEAKS V_C, a)
$\forall V_{DISP} \Rightarrow P'$

1230

$\forall P'$

1240

COMPARE
P vs. P'

1250

PICK BEST
MATCH

1260

LOOK UP
COMPOUND
FIELD

1200

UNKNOWN
COMPOUND

1202

V_{COMP}, V_{DISP}
RANGES (b, e, s)

1206

$V_{DISP} = V_{DISPb}$ TO V_{DISPe} BY V_{DISPs}

1208

$V_{COMP} = V_{COMPb}$ TO V_{COMPe} BY V_{COMPs}

1210

STORE RESPONSE
AS VALUE (a)

1212

LAST
V_C?

NO

YES

1214

LAST
V_{RF}?

NO

YES

Figure 40C

1270

FOR
∀ A ∈ P'

1272

CURVE FIT
Z' = β' + γ'

1274

MATCH β', γ'
TO BEST β, γ

1020

FOR
∀ A ∈ P

1022

Z={∨$_{C11}$, a$_{11}$}{∨$_{C12}$, a$_{12}$}...{∨$_{C1m}$, a$_{1m}$}

1024

CURVE FIT
Z ⟹
y^2 = β x^2 + γ (β, γ)

1026

STORE
β, γ

Figure 40D

P

COMPOUND ID				
V_{RF1}	V_{C11}, A_{11}, L_{11}	V_{C12}, A_{12}, L_{12}	⋯	V_{C1n}, A_{1n}, L_{1n}
V_{RF2}	V_{C21}, A_{21}, L_{21}	V_{C22}, A_{22}, L_{22}	⋯	V_{C2n}, A_{2n}, L_{2n}
	⋯	⋯		⋯
V_{RFm}	V_{Cm1}, A_{m1}, L_{m1}	V_{Cm2}, A_{m2}, L_{m2}	⋯	V_{Cmn}, A_{mn}, L_{mn}
V_{FRAG}				

$L = \{monomer, cluster, RIP\}$

Figure 40E

1321

L = RIP

1331

L = CLUSTER

1320

YES

PEAK DETECT
WITH NO
COMPOUND
APPLIED?

• • • • • NO

1310

YES

PEAK SHIFT
RIGHT AT
V_{RF}

NO

1332

L = MONOMER

Figure 40F

1280

A & P'

1282

COMPARE
MONOMER
(P', P')

1284

SCORE S_m

1286

COMPARE
CLUSTER
(P', P')

1288

SCORE S_c

1290

$S_f = W_m S_m + W_c S_c$
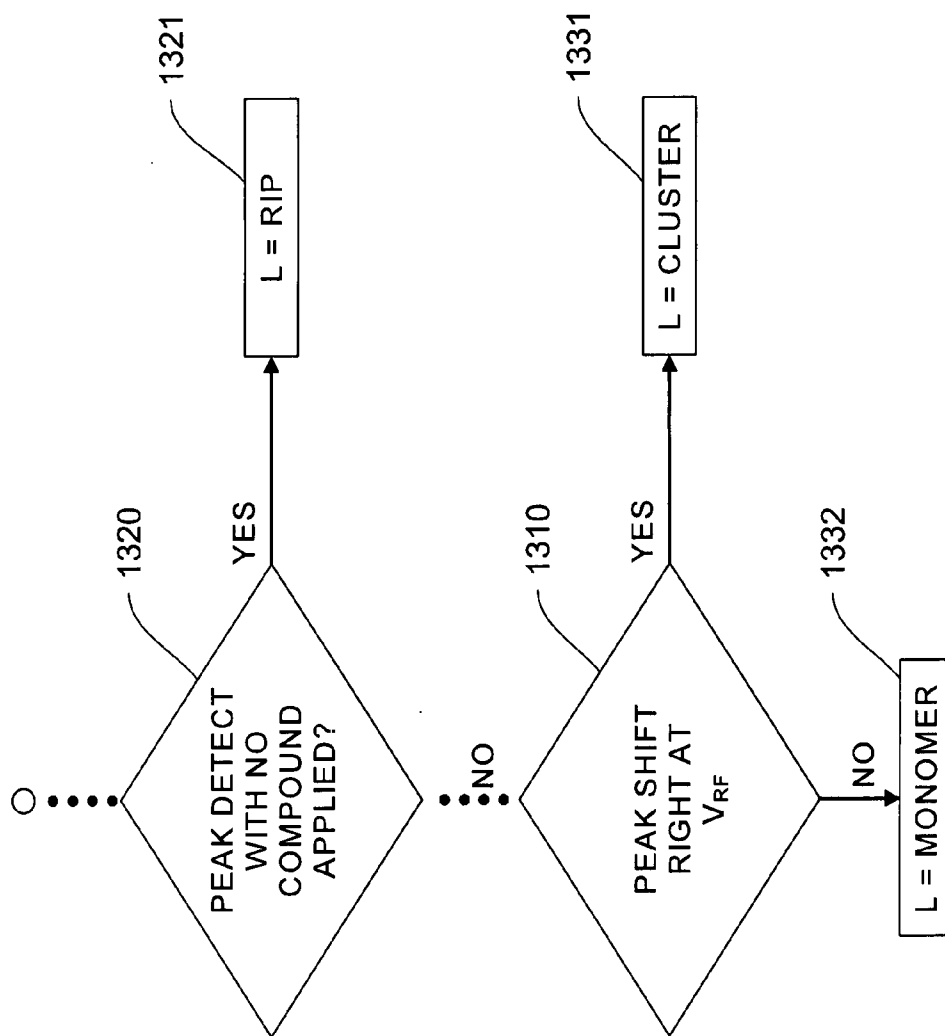
Figure 40G

Figure 41

Figure 42

1750

Figure 43

1476

1486

1484

MOLECULAR SIEVE

PUMP

1482

1480

MOLECULAR SIEVE

FILTERED AIR OR GAS

1498

1478

DMS

1488

1496

1494

EXHAUST

1492

S

1490

Figure 44

Figure 45

1546

1548

NEUTRALS

1544

1542

1538

1536

1532

1534

S

CLEAN
TRANSPORT
GAS

1540

1530

Figure 46

Figure 47

Figure 48

Figure 49

Figure 50

Figure 51

1672

1692

MS

PUMP

1686

1682

1674

1690

1688

1680

1678

1694

PUMP

1676

1698

+ +

+

+ +

S

1684

1700

1704

1702

MS

1696

MS

Figure 52

Figure 53

MOBILITY BASED APPARATUS AND METHODS USING DISPERSION CHARACTERISTICS, SAMPLE FRAGMENTATION, AND/OR PRESSURE CONTROL TO IMPROVE ANALYSIS OF A SAMPLE

REFERENCE TO RELATED APPLICATIONS

[0001] This application is a continuation of U.S. patent application Ser. No. 10/998,344, filed on Nov. 24, 2004, which claims the benefit of and priority to: U.S. Provisional Application No. 60/524,830, filed on Nov. 25, 2003, entitled "System for Identification of Ion Species in an Electric Field"; U.S. Provisional Application No. 60/549,004, filed on Mar. 1, 2004, entitled "Chemical Agent Detector"; and U.S. Provisional Application No. 60/549,952, filed on Mar. 4, 2004, entitled "Tunable Chemical Agent Detector"; U.S. Provisional Application No. 60/556,349, filed on Mar. 25, 2004, entitled "Tunable DMS Recirculation System"; and U.S. Provisional Application No. 60/556,198, filed on Apr. 28, 2004, entitled "Reduced Pressure DMS." The entire teachings of the above referenced applications are incorporated herein by reference.

[0002] This application also incorporates by reference the entire contents of the following co-pending U.S. patent applications: U.S. Ser. No. 10/187,464, filed on 28 Jun. 2002; U.S. Ser. No. 10/215,251, filed on 7 Aug. 2002; U.S. Ser. No. 10/462,206, filed on 13 Jun. 2003; U.S. Ser. No. 10/684,33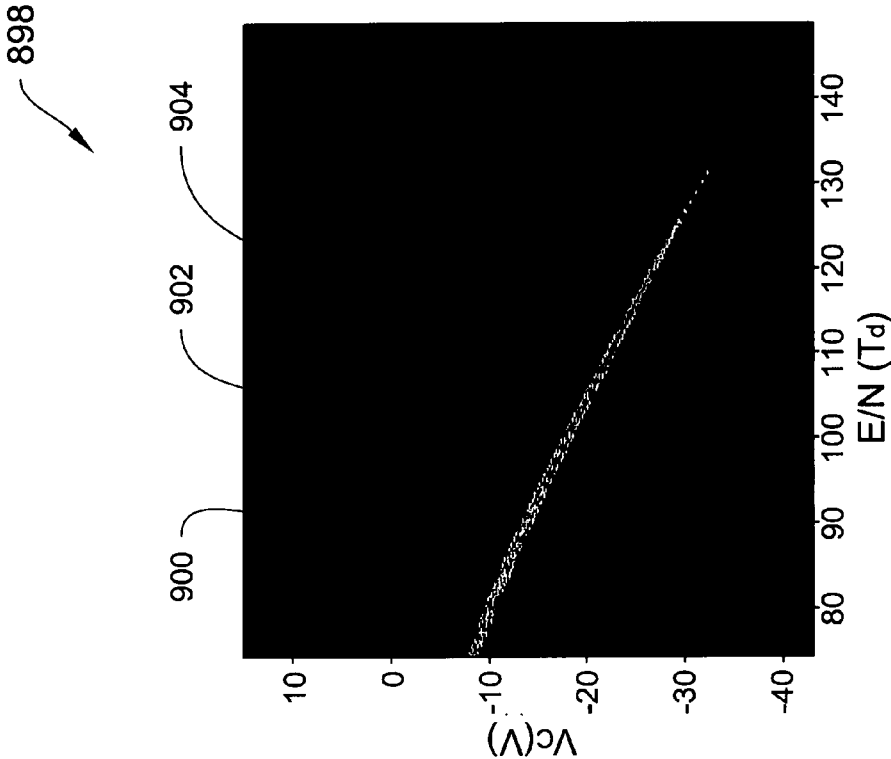2, filed on 10 Oct. 2003; U.S. Ser. No. 10/734,499, filed on 12 Dec. 2003; U.S. Ser. No. 10/738,967, filed on 17 Dec. 2003; U.S. Ser. No. 10/797,466, filed on 10 Mar. 2004; U.S. Ser. No. 10/821,812, filed on 8 Apr. 2004; U.S. Ser. No. 10/824,674, filed on 14 Apr. 2004; U.S. Ser. No. 10/836,432, filed on 30 Apr. 2004; U.S. Ser. No. 10/840,829, filed on 7 May 2004; U.S. Ser. No. 10/866,645, filed on 10 Jun. 2004; U.S. Ser. No. 10/887,016, filed on 8 Jul. 2004; U.S. Ser. No. 10/894,861, filed on 19 Jul. 2004; U.S. Ser. No. 10/903,497, filed on 30 Jul. 2004; U.S. Ser. No. 10/916,249, filed on 10 Aug. 2004; U.S. Ser. No. 10/932, 986, filed on 2 Sep. 2004; U.S. Ser. No. 10/943,523, filed on 17 Sep. 2004; and U.S. Ser. No. 10/981,001, filed on 4 Nov. 2004.

FIELD OF THE INVENTION

[0003] The invention relates generally to mobility-based systems, methods and devices for analyzing samples. More particularly, in various embodiments, the invention relates to improving sample collection, filtration, detection, measurement, identification and/or analysis (collectively "analysis") using, for example: dispersion characteristics (2-, 3-, and n-dimensional); sample fragmentation; and/or variations in flow channel/filter field conditions. Such conditions may include, without limitation: pressure; temperature; humidity; field strength, duty cycle, and/or frequency; and/or compensation voltage.

BACKGROUND

[0004] There are a number of different circumstances in which it is desirable to perform analysis to identify compounds in a sample. Such samples may be taken directly from the environment or they may be provided by front end specialized devices to separate or prepare compounds before analysis. There exists, a demand for low cost, compact, low-power, accurate, easy to use, and reliable devices capable of detecting compounds in a sample.

[0005] One class of known analyzers are mass spectrometers (MS). Mass spectrometers are generally recognized as being the most accurate type of analyzers for compound identification. However, mass spectrometers are quite expensive, easily exceeding a cost of $100,000 or more and are physically large enough to become difficult to deploy everywhere the public might be exposed to dangerous chemicals. Mass spectrometers also suffer from other shortcomings such as the n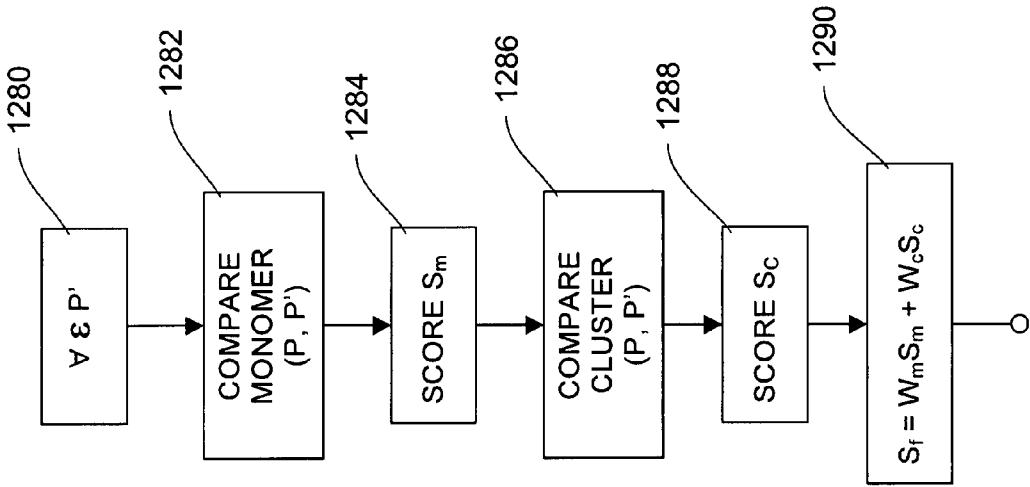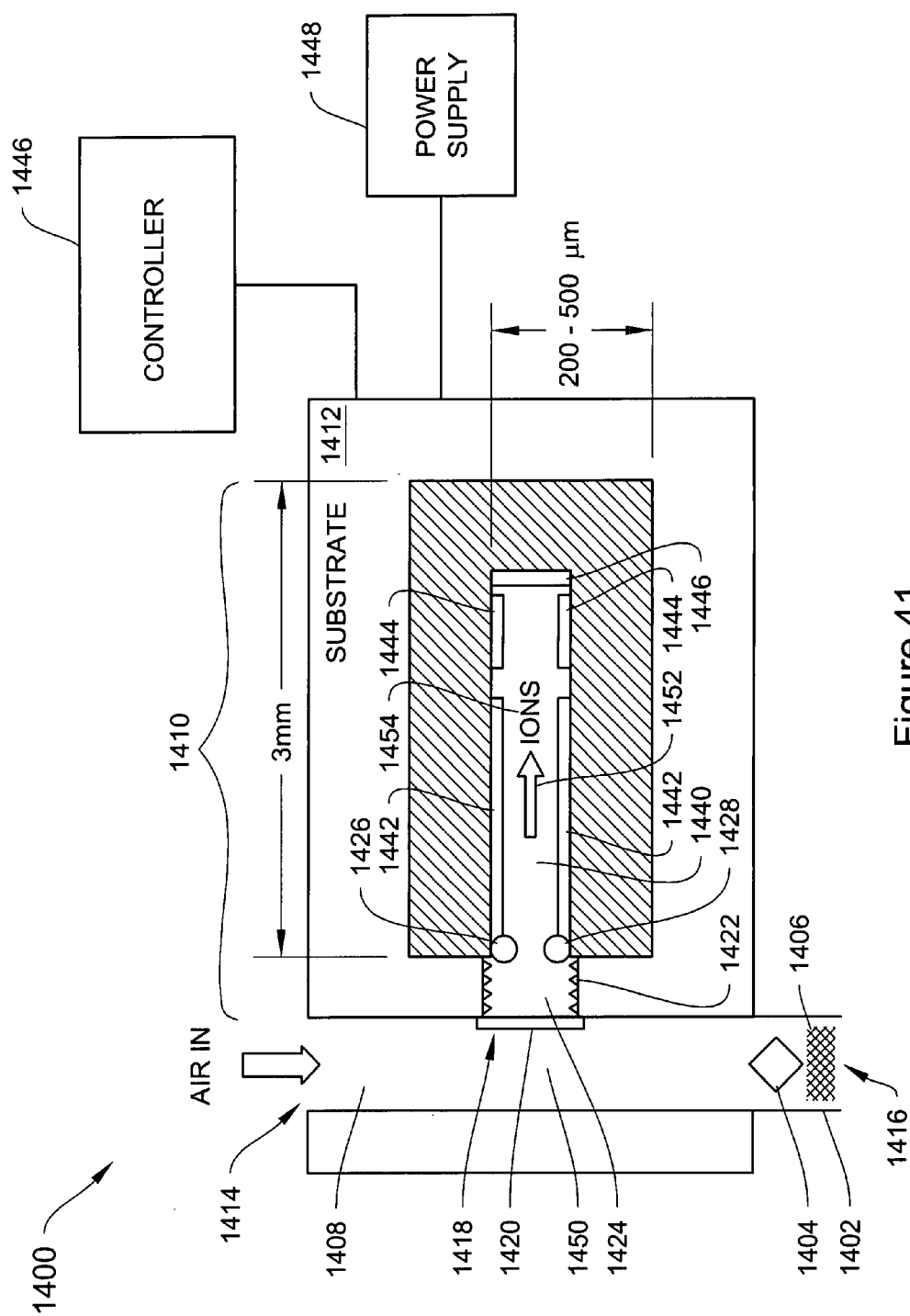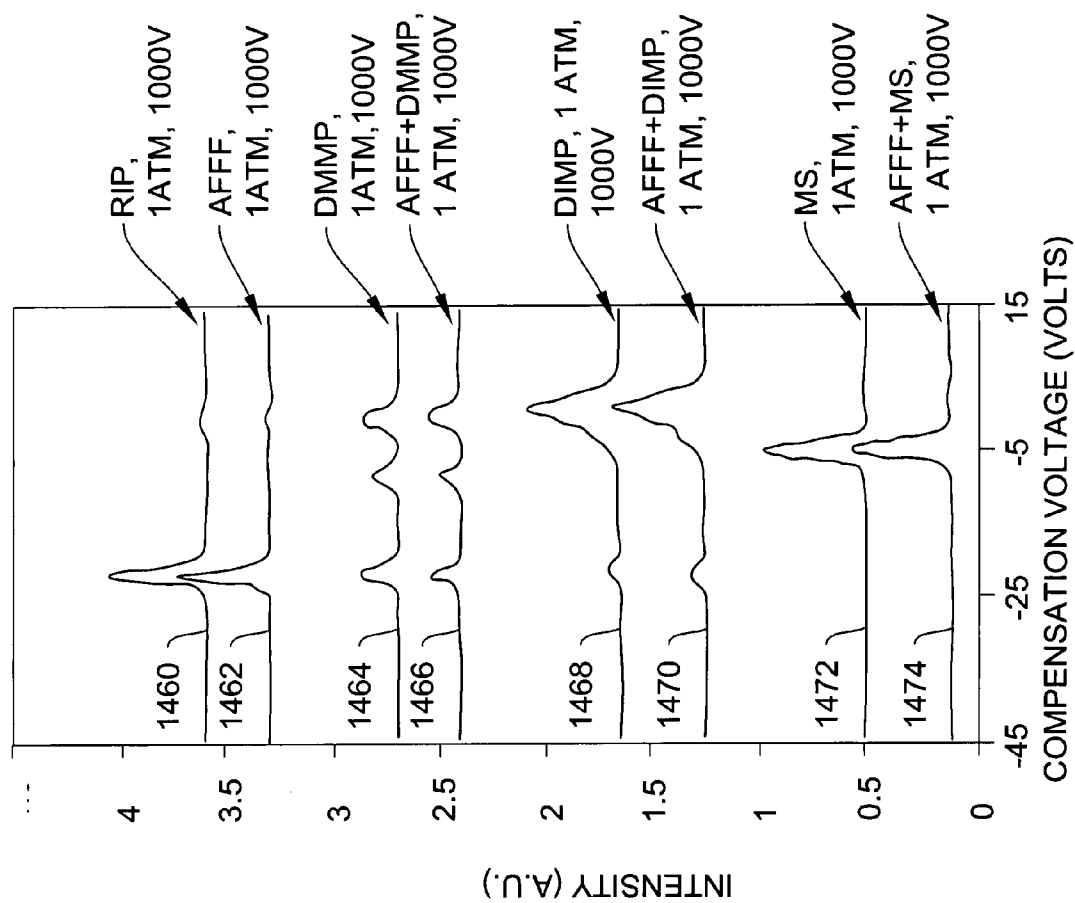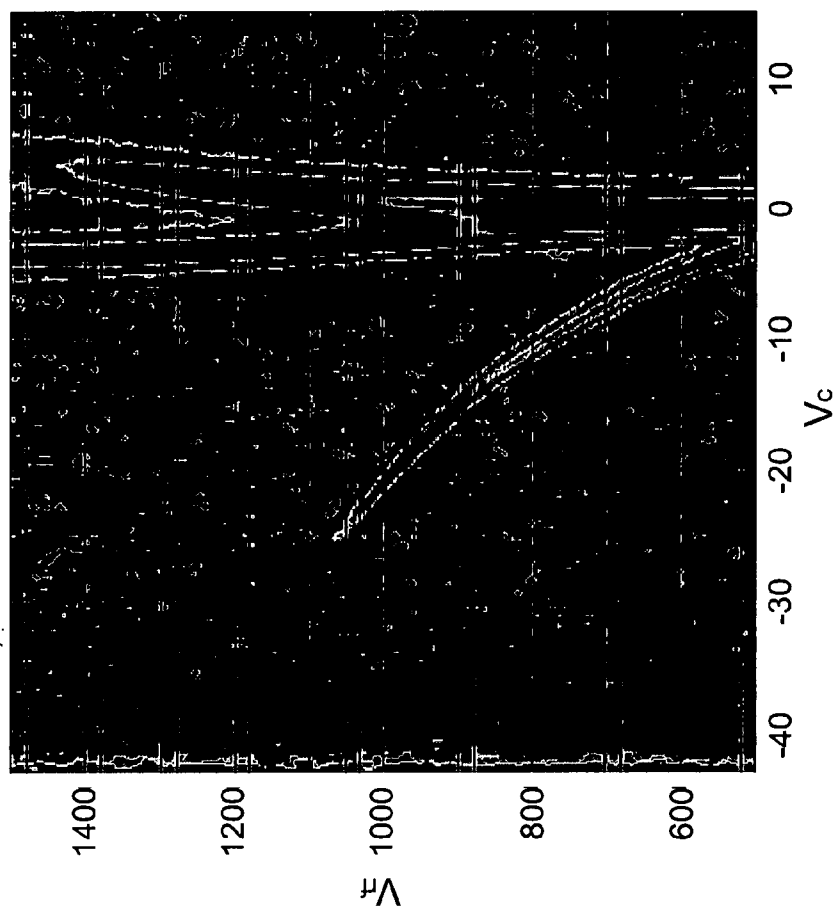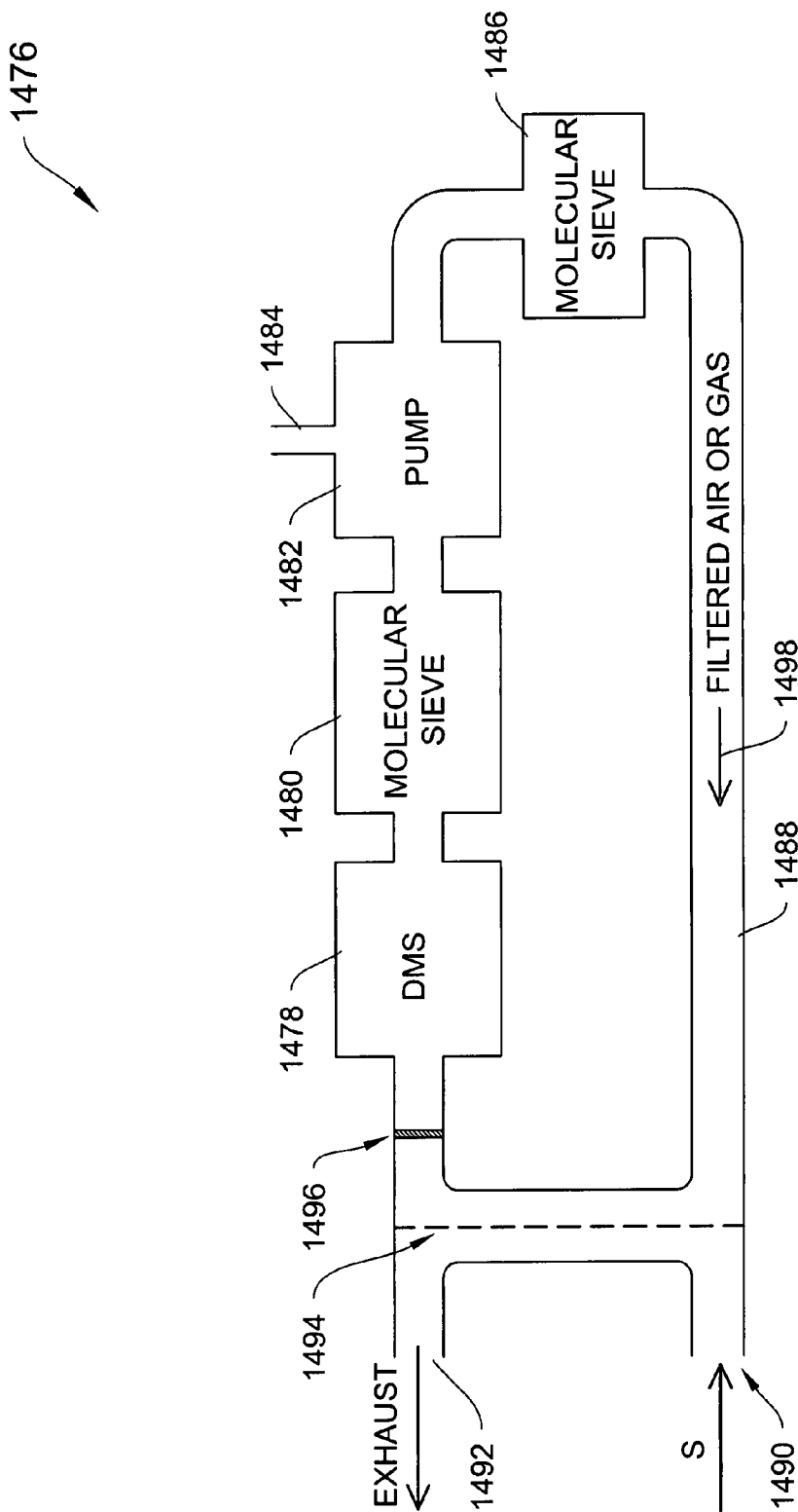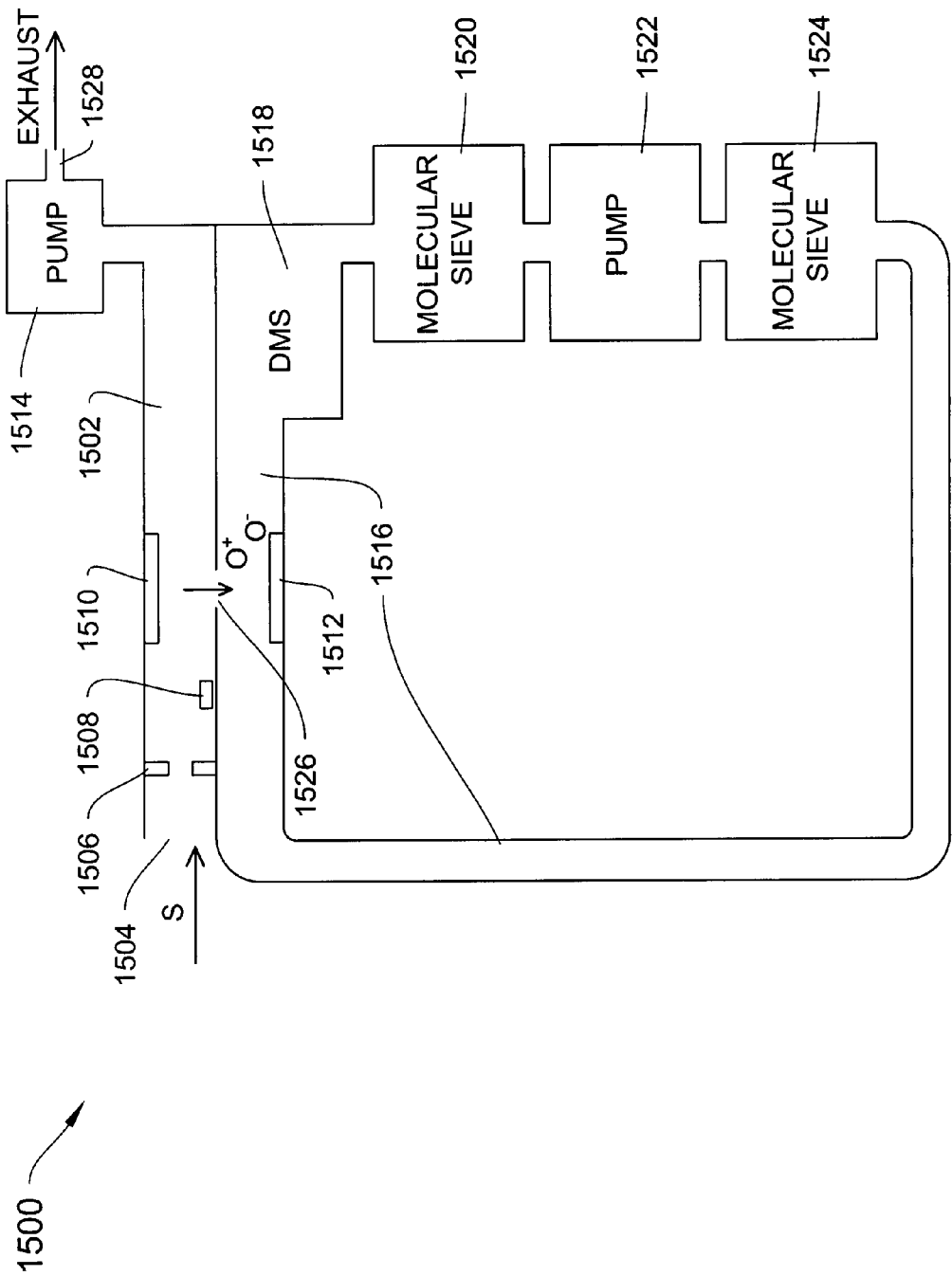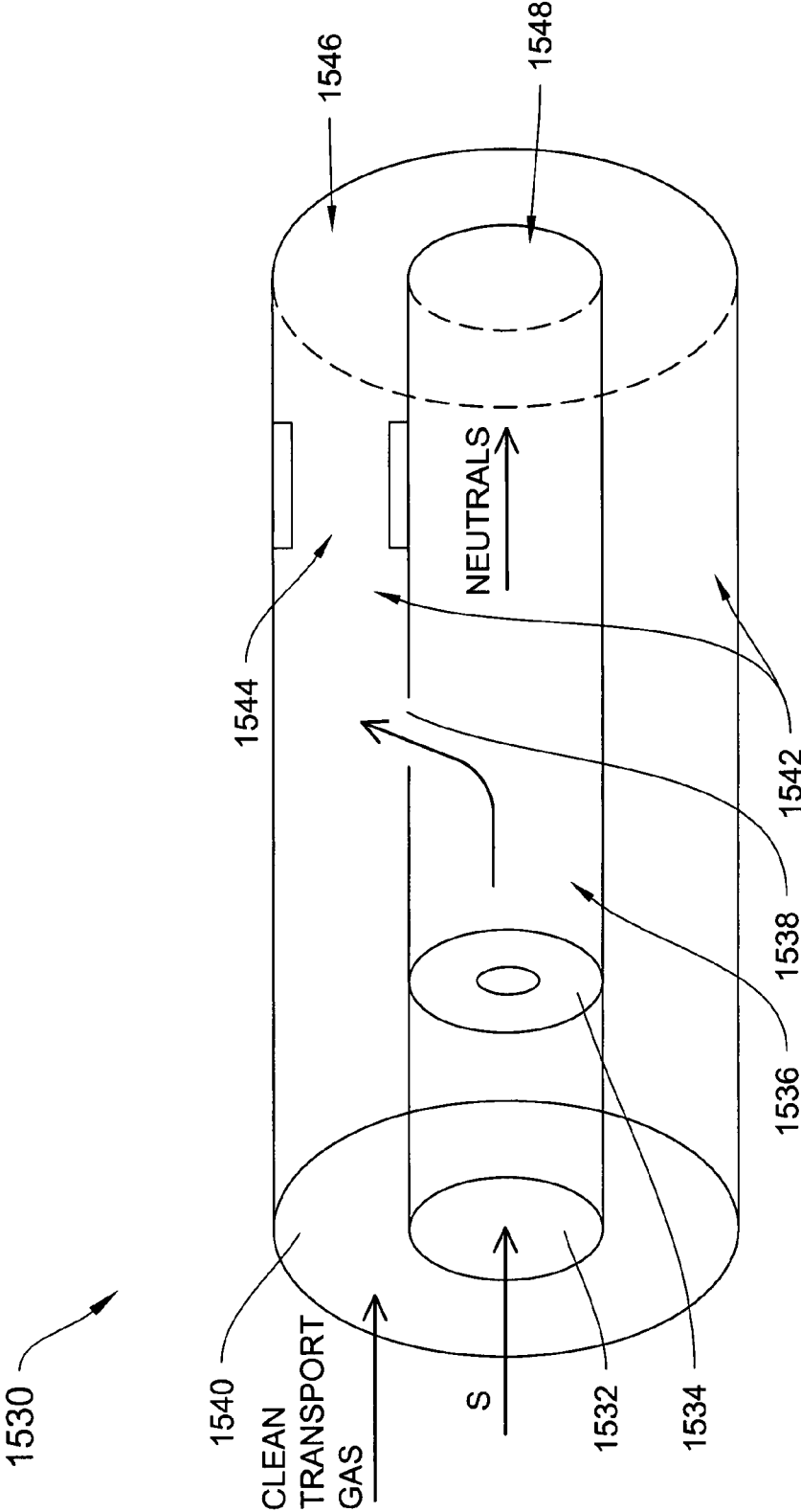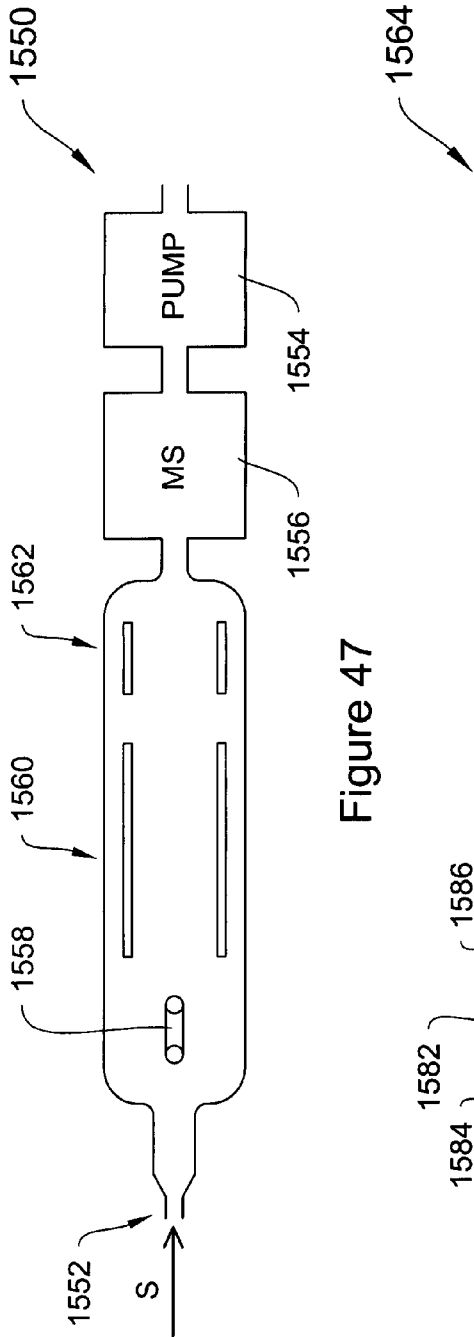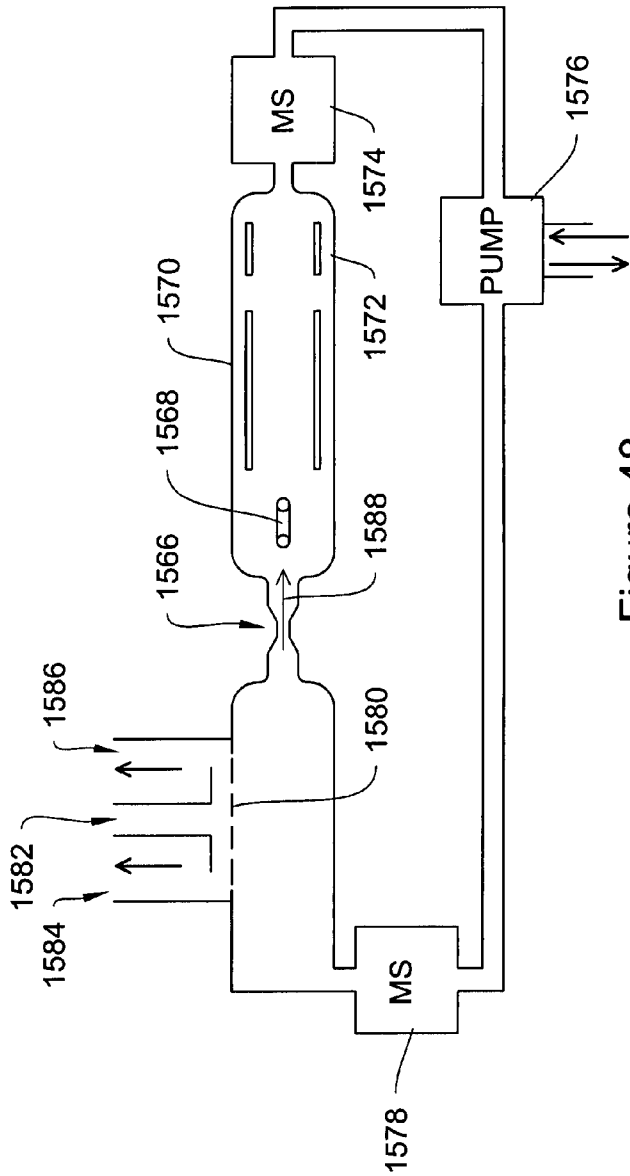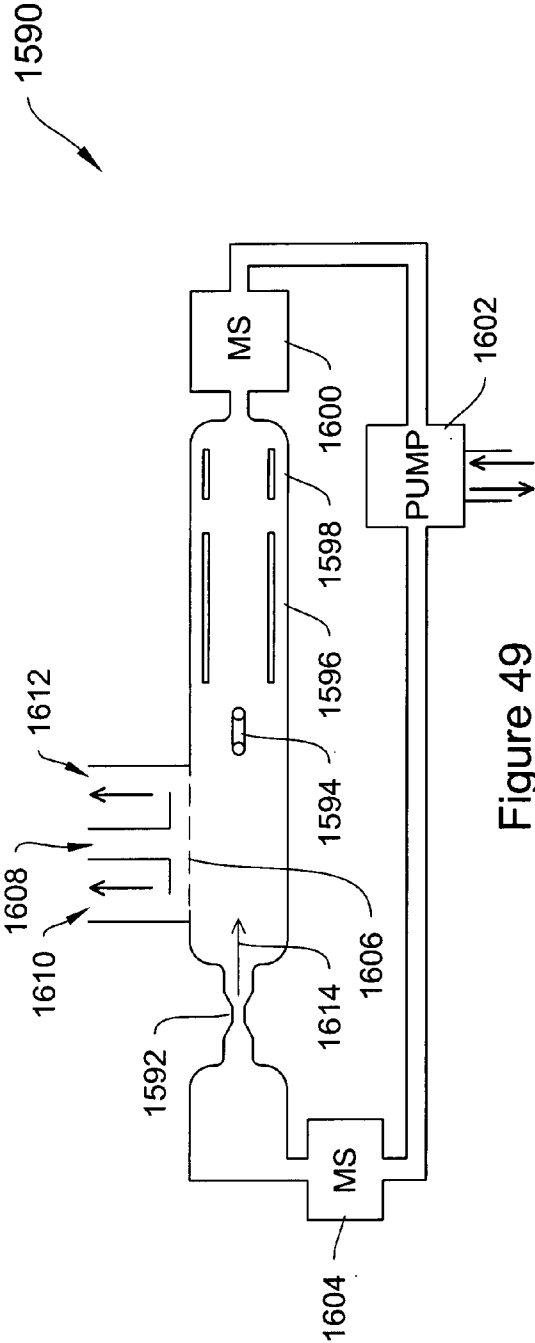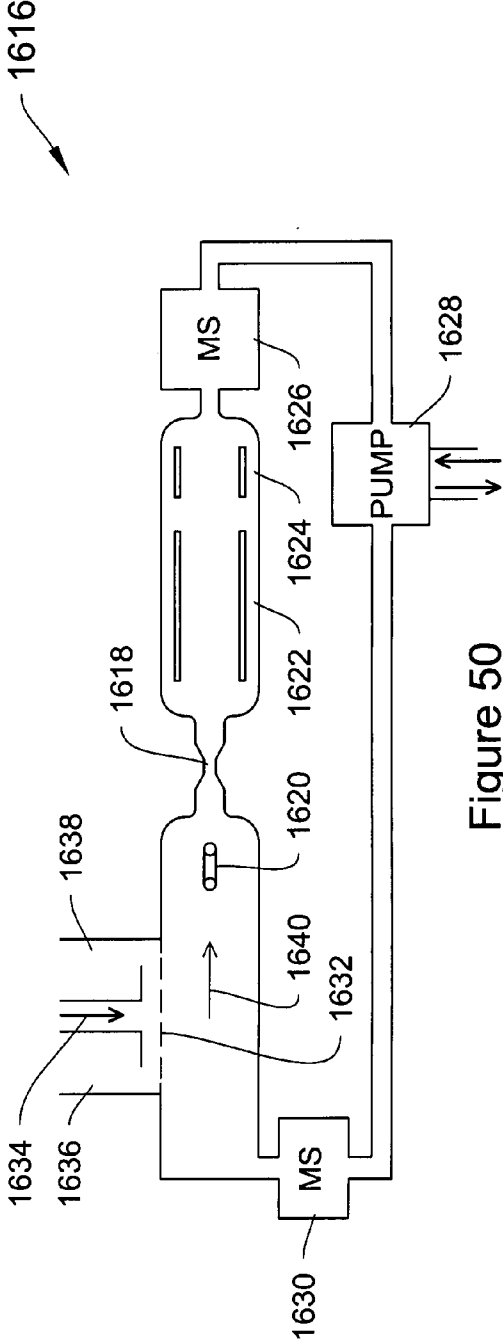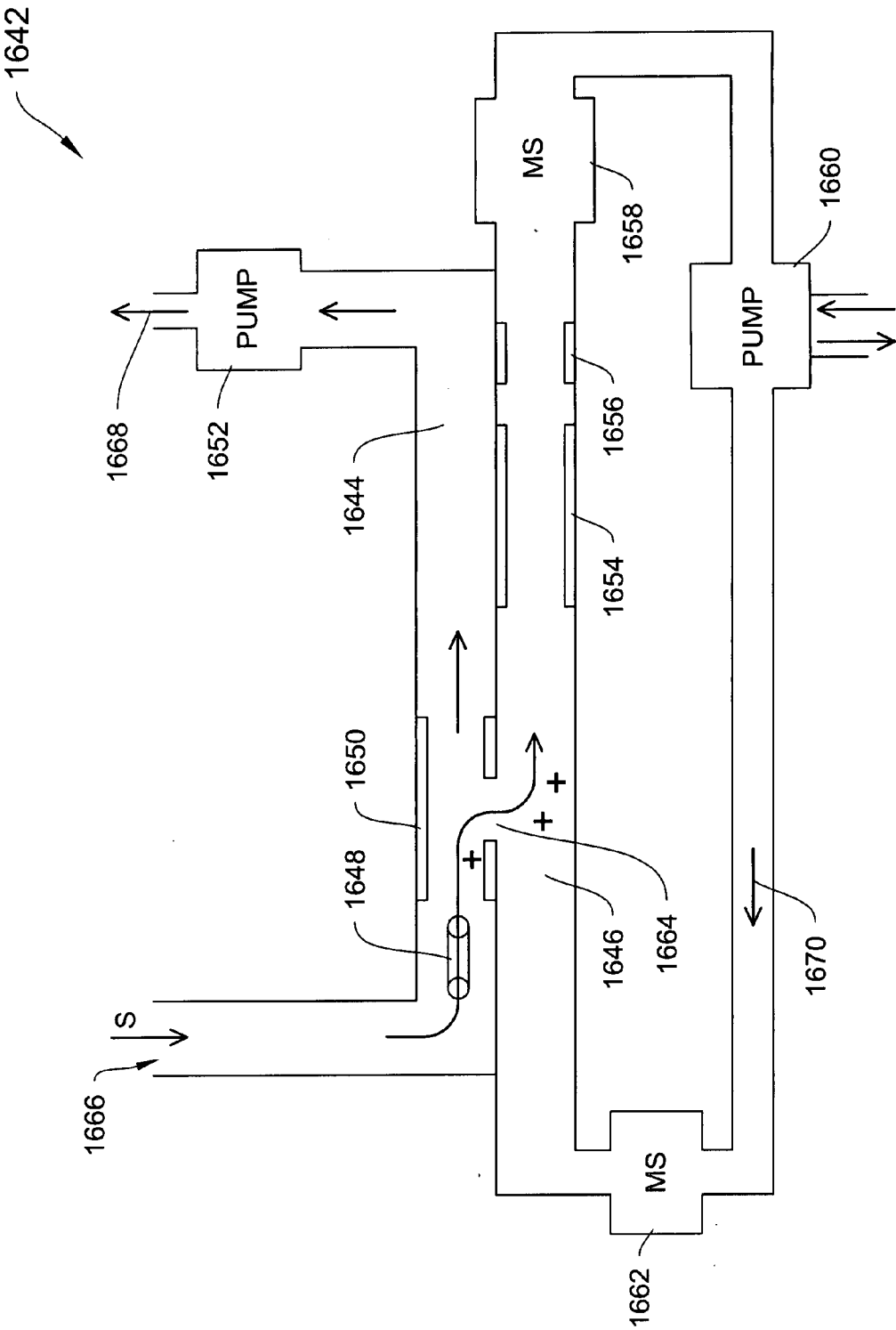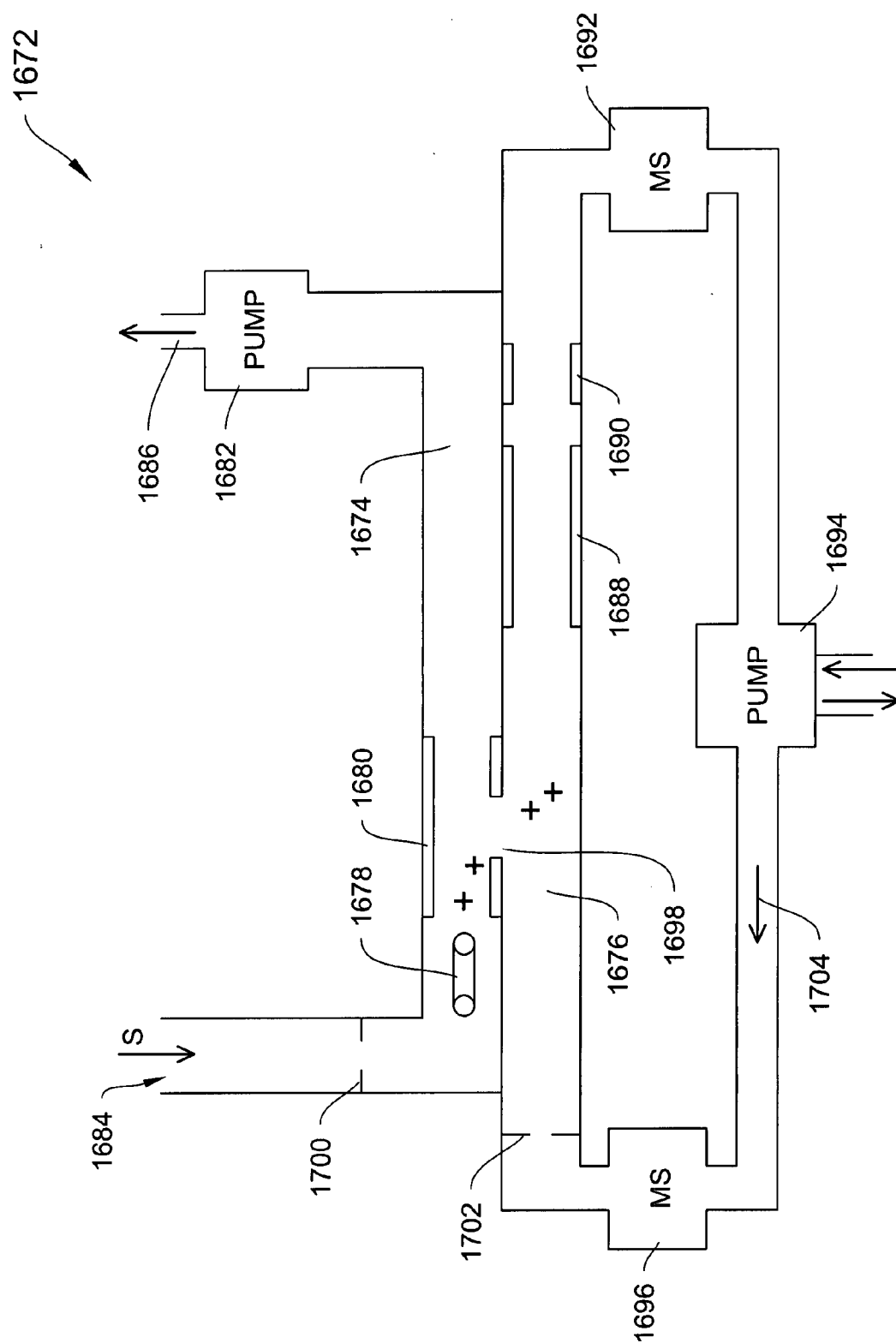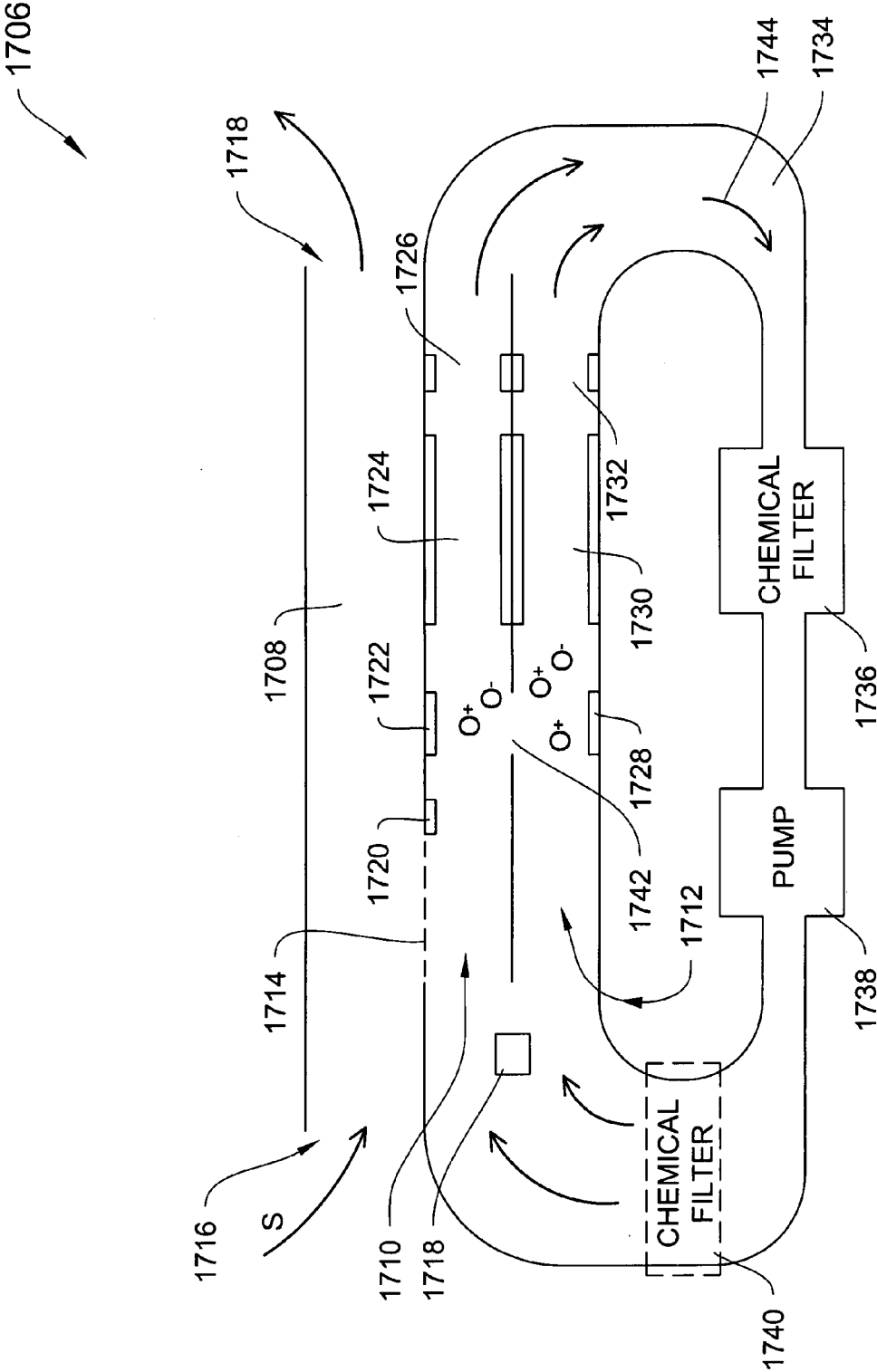eed to operate at relatively low pressures, resulting in complex support systems. They also need a highly trained operator to tend to and interpret the results. Accordingly, mass spectrometers are generally difficult to use outside of laboratories.

[0006] A class of chemical analysis instruments more suitable for field operation is known as Field Asymmetric Ion Mobility Spectrometers (FAIMS) or Differential Mobility Spectrometers (DMS), and also known as Radio Frequency Ion Mobility Spectrometers (RFIMS) among other names. Hereinafter, FAIMS, DMS, and RFIMS, are referred to collectively as DMS. This type of spectrometer subjects an ionized fluid (e.g., gas, liquid or vaper) sample to a varying high-low asymmetric electric field and filters ions based on their field mobility.

[0007] The sample flows through a filter field which allows selected ion species to pass through, according to a compensation voltage (Vcomp) applied to filter electrodes, and specifically those ions that exhibit particular mobility responses to the filter field. An ion detector then collects ion intensity/abundance data for the detected ions. The intensity data exhibits attributes, such as "peaks" at particular compensation voltages.

[0008] A typical DMS device includes a pair of electrodes in a drift tube. An asymmetric RF field is applied to the electrodes across the ion flow path. The asymmetric RF field, as shown in FIG. 1, alternates between a high or "peak" field strength and a low field strength. The field varies over a particular time period (T), frequency (f) and duty cycle (d). The field strength E varies with an applied field voltage (Vrf) and the size of the gap between the electrodes. Ions pass through the gap between the electrodes when their net transverse displacement per period of the asymmetric field is zero. In contrast, ions that undergo a net displacement eventually undergo collisional neutralization on one of the electrodes. In a given RF field, a displaced ion can be restored to the center of the gap (i.e. compensated, with no net displacement for that ion) by superimposing a low strength direct current (dc) electric field (e.g., by applying Vcomp across the filter electrodes) on the RF. Ions with differing displacement (owing to characteristic dependence of mobility in the particular field) pass through the gap at differing characteristic compensation voltages. By applying a substantially constant Vcomp, the system can be made to function as a continuous ion filter. Alternatively, scanning Vcomp obtains a spectral measurement for a sample. A recorded image of the spectral scan of the sample is sometimes referred to as a "mobility scan" or as an "ionogram."

[0009] Examples of mobility scans based on the output from a DMS device are shown in FIGS. 2A and 2B. The compounds for which scans are depicted are acetone and an isomer of xylene (o-xylene). The scan of FIG. 2A resulted from a single compound, acetone, being independently applied to the DMS analyzer. The illustrated plot is typical

of the observed response of the DMS device, with an intensity of detected ions dependent on Vcomp. For example, the acetone sample exhibits a peak intensity response at a Vcomp of approximately −2 Vdc.

[0010] FIG. 2B illustrates the results when analyzing a mixture of acetone and o-xylene. The combined response shows two peaks in approximately the same region as for the independent case. The compounds in the mixture can be detected by comparing the response against a library, for example, of stored known responses for independently analyzed compounds, or libraries of mixtures. Thus, the scans for independently analyzed compounds, such as the scan of FIG. 2A for acetone, can be stored in a computer system, and when compound responses such as that in FIG. 2B are observed, the relative locations of the peaks can be compared against the stored responses in the library to determine the constitution of the compound.

[0011] A specific RF field voltage and field compensation voltage Vcomp permits only ion species having a particular ion mobility characteristic to pass through the filter to the detector. By noting the RF level and compensation voltage and the corresponding detected signal, various ion species can be identified, as well as their relative concentrations (as seen in the peak characteristics).

[0012] Consider a plot of ion mobility dependence on Vrf, as shown in FIG. 3. This figure shows ion intensity/abundancy versus RF field strength for three examples of ions, with field dependent mobility (expressed as the coefficient of high field mobility, a) shown for species at greater, equal to and less than zero. The velocity of an ion can be measured in an electric field (E) low enough so that velocity (v) is proportional to the electrical field as v=KE, through a coefficient (K) called the coefficient of mobility. K can be shown to be related to the ion species and gas molecular interaction properties. This coefficient of mobility is considered to be a unique parameter that enables the identification of different ion species and is determined by, ion properties such as charge, size, and mass as well as the collision frequency and energy obtained by ions between collisions.

[0013] When the ratio of E/N, where N is gas density, is small, K is constant in value, but at increasing E/N values, the coefficient of mobility begins to vary. The effect of the electric field can be expressed approximately as $K(E)=K(0)[1+\alpha(E)]$, where $K(0)$ is a low voltage coefficient of mobility, and α is a specific parameter showing the electric field dependence of mobility for a specific ion.

[0014] Thus, as shown in FIG. 3, at relatively low electric field strengths, for example, of less than approximately 8,000 V/cm, multiple ions may have the same mobility. However, as the electric field strengths increase, the different species diverge in their response such that their mobility varies as a function of the applied electric field. This shows that ion mobility is independent of applied RF field voltage at relatively low RF field strengths, but is field-dependent at higher RF field strengths.

[0015] FIGS. 2A and 2B demonstrate that species can have a unique behavior in high fields according to mobility characteristics. The ions passing through the filter are detected downstream. The detection signal intensity can be plotted as a characteristic detection peak for a given RF field

voltage and field compensation voltage Vcomp. Peak intensity, location, and shape are typically used for species identification.

[0016] However, a problem occurs in that the peaks, as seen in the typical DMS spectra, are generally broad in width. Therefore, compounds exhibiting intensity peaks at similar compensation voltages may be difficult to separate from each another. Consequently, there may be particular conditions under which two different chemicals generate indistinguishable scans for a particular Vcomp and a particular RF field voltage, or for other combinations of filter field/flow channel parameters. In such a case, it is may not be possible to differentiate between the two different compounds. Another problem may occur when two or more chemical species have the same or almost the same ion mobility characteristic for a particular set of field/flow channel parameters. This is most likely to happen in the low electric field regime (referred to herein as Ion Mobility Spectrometry or IMS), where many existing ion mobility spectrometer systems operate. Therefore, if two or more chemical species have the same or almost the same mobility characteristic, then their spectroscopic peaks will overlap, and identification and quantification of individual species will be difficult or impossible.

[0017] FIG. 4 is a graph of Vcomp versus Vrf according to an illustrative embodiment of the invention, but also highlighting the above described prior art drawback. More particularly, FIG. 4 depicts a graph of Vcomp versus Vrf for four compounds: lutidine; cyclohexane; benzene; and dimethyl-methl-phosphonate (DMMP). Each curve shows the location of detected ion intensity peaks, such as those circled at 100, at the various (Vrf, Vcomp) locations, which in total provide the peak characteristics for each particular compound. As shown, there is a region 100 in which the intensity peaks and mobility curves for DMMP and cyclohexane overlap with each other. As can be seen, operating in a Vrf region of from approximately 2,500 Vpeak to approximately 2,650 Vpeak, at a Vcomp of about −6 Vdc to about −8 Vdc, one would find it virtually impossible to discriminate between the two compounds based on a single Vcomp scan at a single Vrf. Specifically, in a conventional spectral scan approach that plots intensity/abundance versus Vcomp over a range of Vcomp for a single Vrf would plot the overlapping peaks as a single peak.

[0018] Accordingly, there is a need for an improved ion mobility-based compound identification approach that addresses peak overlap issues and provides improved compound analysis features.

SUMMARY OF THE INVENTION

[0019] The invention addresses the deficiencies of the prior art by providing, in various embodiments, improved mobility-based systems, devices and methods for analyzing constituents in a sample. More particularly, in various embodiments, the invention provides improved sample collection, filtration, detection, measurement, identification and/or analysis (collectively "analysis") using, for example: dispersion characteristics; sample fragmentation; and/or sample processing variations, such as and without limitation, variations in flow channel/filter field conditions. Such conditions may include, any spectral changes, including, without limitation changes in: pressure; temperature; humidity;

field strength, duty cycle, and/or frequency; field voltage amplitude, frequency and/or duty cycle; detector bias voltage magnitude and/or polarity; and/or filter field compensation voltage magnitude and/or polarity.

[0020] In one practice, the invention employs one or more of the above to provide a library of spectral signatures for a plurality of known species, and identifies unknown species by comparing at least a portion of a spectral signature for the unknown species to at least a portion of one or more of the spectral signatures stored in the library. The spectral signature is a compilation of spectral information for a particular species. The spectral information may include, without limitation, spectral peak amplitude; spectral peak width; spectral peak slope; spectral peak spacing; spectral peak quantity; relative shifts in spectral peaks due, for example, to changes in processing conditions; spectral discontinuities; Vrf versus Vcomp characteristics or any other characteristics of any of the above described conditions plotted against any one or more other above described conditions.

[0021] According to one aspect, the invention provides improved ion-based systems, methods and devices for analyzing samples by varying a first sample processing condition over a first plurality of values, and one or more second sample processing conditions over a second plurality of values to determine spectral information for a sample. In one particular embodiment, the invention scans a field compensation voltage Vcomp over a range of values for one or more Vrf values to generate a spectral representation at each of the one or more Vrf values.

[0022] According to one feature, the invention adjusts a third sample processing condition to narrow the widths of the resulting spectral peaks of the determined ion spectral information. Such width reduction reduces spectral peak overlap for samples having similar mobility characteristics, improves resolution of an ion mobility-based analyzer, and thus, provides more accurate discrimination between sample species. In one configuration, the third sample processing condition includes pressure in a sample flow channel, and the invention reduces the pressure in the sample flow channel to decrease the width of the spectral peaks.

[0023] According to another feature, the invention adjusts a third sample processing condition to change a location of the resulting spectral peaks of the determined ion spectral information, relative to a Vcomp at which they occur. Since peaks of differing species may shift differently, such shifts can provide improved discrimination between peaks of species having similar mobility characteristics. In one configuration, the third sample processing condition includes Vrf, and the invention applies more than two field voltages Vrf to provide peak shifting information for species identification.

[0024] According to another feature, the invention adjusts a third sample processing condition to provide spectral information regarding both positive and negative ions of the sample. More particularly, in one configuration, the invention provides both a negative and a positive bias voltages to multiple detector electrodes concurrently or to a single detector electrode alternatively to provide both negative and positive mode scans. Since compounds that have similar ion mobility characteristics relative to one mode may have differing ion mobility characteristics relative to the other mode, adjusting the polarity of a bias voltage to detector electrodes can further improve sample analysis.

[0025] In a further embodiment, the invention employs various n-dimensional representations of ion spectral information, to enhance the quality of spectral signatures, improve differentiation between species having similar ion mobility characteristics, and thus, improve identification accuracy, specifically, and sample analysis, generally. By way of example, in one configuration, the invention scans Vcomp for >2 field voltages Vrf, to capture additionally, for example, spectral peak shift information. The invention then generates an n-dimensional representation of the spectral information that aggregates the spectral information captured by scanning Vcomp at each Vrf. In one example, the n-dimensional representation is a two-dimensional plot of Vrf versus Vcomp aggregating the spectral information captured by scanning Vcomp at each of the >Vrf field voltages. In a further example, the aggregated representation is a three-dimensional representation aggregating the spectral information captured from scanning Vcomp at the >2 Vrf field voltages.

[0026] According to one approach, the three-dimensional representation is a plot of ion intensity as a function of Vrf and Vcomp. According to one implementation, Vcomp and Vrf are represented in special coordinates, such as x- and y-coordinates, and variations in ion intensity at the (Vcomp, Vrf) coordinates is represented in variations of any color-related feature, including without limitation, variations in gray scale, color saturation, or color at those coordinates. Such color-related representations provide easily recognized distinctions between species that were difficult or impossible to distinguish between, without the n-dimensional aggregation of the invention.

[0027] In a related implementation, a curve circumscribing the color-related differences may be generated and the color-related differences themselves may be discarded. In this way, the invention can provide a two-dimensional representation of the spectral peaks, for example, on a Vcomp versus Vrf grid, while still incorporating the spectral information captured by scanning Vcomp over a plurality of Vrf values. In another alternative implementation, Vcomp, Vrf, and ion intensity are mapped into a three-dimensional (x,y,z) spatial representation.

[0028] According to a related embodiment, any or all of the spectral information may be represented in n-dimensional space as a function of any or all of the processing variations to create >3 dimensional spectral signatures for both known and unknown species. Conventional n-dimensional cluster matching techniques may then be employed for identifying the unknown species.

[0029] In any of the above described n-dimensional representations, any or all of the spectral information represented may be incorporated into the spectral signatures for known species and stored in the library of such signatures. Conventional pattern recognition techniques may be employed to correspond at least portions of the spectral signatures from unknown species with at least portions of the signatures from known samples stored in the library to identify the unknown species. In other implementations, both the library of signatures and the captured signatures from the unknown species are represented as mathematical descriptions, and any suitable approach for making comparisons between such mathematical descriptions may be employed to identify the unknown species.

[0030] According to another embodiment, the invention employs fragmentation to improve DMS analysis. Fragmentation includes breaking large molecules of samples into smaller molecules, molecule clusters, components, and/or base elements. The fragments may then be individually analyzed, in series and/or in parallel to generate more spectral information for the sample than would be otherwise available without fragmentation. Fragmentation may be achieved, for example and without limitation, by using any one or a combination of a chemical reaction, a high energy field strength, high Vrf, heating, laser light, colliding the sample molecules with other molecules, soft x-ray, electromagnetic waves, or the like. According to one feature, the invention incorporates any or all of the above described spectral information for the fragment spectral peaks into the spectral signature. According to a further feature, the invention incorporates the point (e.g. the temperature, pressure, field strength, Vrf, colliding molecule mass, colliding molecule velocity, laser intensity, laser frequency, x-ray intensity etc.) into the spectral signature.

[0031] According to other aspects, the invention provides various serial and parallel combinations of ion-based analyzers employing features, including those summarized above. In additional aspects, the invention provides various compact, handheld, lightweight and low power based analyzers, for example, for detecting chemical warfare agents (CWAs), Toxic Industrial Compounds (TICs), and/or Toxic Industrial Materials (TIMs).

[0032] The invention will now be described with reference to various illustrative embodiments.

BRIEF DESCRIPTION OF THE DRAWINGS

[0033] The patent or application file contains at least one drawing executed in color. Copies of this patent or patent application publication with color drawings will be provided by the Office upon request and payment of the necessary fee.

[0034] The foregoing and other objects, features, advantages, and illustrative embodiments of the invention will now be described with references to the following drawings in which like reference designations refer to the same parts throughout the different views. These drawings are not necessarily drawn to scale, emphasis instead being placed upon illustrating principles of the invention.

[0035] FIG. 1 is a graph depicting an asymmetric field having a peak RF, time period, and duty cycle.

[0036] FIGS. 2A and 2B are graphs showing ion abundance (intensity) versus applied field compensation voltage for acetone alone and for a combination of ortho-xylene and acetone, respectively, as detected in a field asymmetric ion mobility spectrometer.

[0037] FIG. 3 is a graph of ion mobility versus electric field strength for three different compounds in a differential mobility spectrometer (DMS).

[0038] FIG. 4 is a graph of Vrf versus Vcomp indicating intensity peak locations according to an illustrative embodiment of the invention and conceptualizing drawbacks of prior art approaches.

[0039] FIG. 5 is a conceptual diagram of a DMS according to an illustrative embodiment of the invention.

[0040] FIG. 6 is a graph of ion intensity versus field compensation voltage for positive mode spectra for a sample containing various amounts of ethyl mercaptan as measured in a DMS.

[0041] FIG. 7 is a graph of ion intensity versus compensation voltage for negative mode spectra of a sample containing various amounts of ethyl mercaptan.

[0042] FIG. 8 is a graph of ion intensity versus field compensation voltage illustrating negative mode separation between monomer and reactant ion peak (RIP) detections for sulfur hexafluoride (SF6).

[0043] FIG. 9 is a graph of ion intensity versus field compensation voltage illustrating the positive mode separation between monomer and reactant ion peak (RIP) detections for sulfur hexafluoride (SF6).

[0044] FIG. 10 is a graph of ion intensity versus field compensation voltage illustrating a DMS response at various RF voltage levels in the negative ion mode and also showing the RIP detected in absence of SF6.

[0045] FIG. 11 is a graph of ion intensity versus field compensation voltage illustrating a DMS response in the positive ion mode where the SF6 peak is not isolated from the RIP.

[0046] FIG. 12 is graph of ion intensity (abundance) versus field compensation voltage illustrating an ability to improve discrimination between detected ion species by observing ion spectral peak shifts corresponding to a change in field strength.

[0047] FIGS. 13A and 13B are graphs of ion intensity (abundance) versus field compensation voltage illustrating an ability to improve discrimination between detected ion species by observing ion spectral peak shifts due to reducing field strength.

[0048] FIGS. 14A and 14B are graphs of ion intensity at multiple field strengths versus field compensation voltage, showing the affect of changes in compensation voltage on specific spectra, and show the divergent behavior of monomer, cluster, and reactant ion peak (RIP) detections with changes in field strength and field compensation voltage.

[0049] FIG. 15A is a three-dimensional color dispersion plot illustrating detection of methyl salicylate over a range of field voltages and field compensation voltages with varying ion intensity represented in varying color according to an illustrative embodiment of the invention.

[0050] FIG. 15B is a two-dimensional graph of ion intensity versus field compensation voltage for mehyl salicylate at a single field voltage.

[0051] FIG. 16A is a three-dimensional color dispersion plot illustrating detection of DMMP over a range of field voltages and field compensation voltages with varying ion intensity represented in varying color according to an illustrative embodiment of the invention.

[0052] FIG. 16B is a two-dimensional graph of ion intensity versus field compensation voltage for DMMP at a single field voltage.

[0053] FIG. 17 is a three-dimensional color dispersion plot illustrating detection of DIMP over a range of field voltages and field compensation voltage with varying ion intensity

represented in varying color according to an illustrative embodiment of the invention.

[0054] FIG. 18 is a two-dimensional graph of ion intensity versus field compensation voltage for DIMP at a single field voltage.

[0055] FIG. 19 is a graph of ion intensity at a plurality of field voltages versus field compensation voltage illustrating the effects of changes in field conditions on location of individual detection peaks and the ability to separate the detection.

[0056] FIG. 20A is a graph of ion intensity versus field compensation voltage illustrating the separation of detection peaks at different compensation voltages between light and heavy molecules according to an illustrative embodiment of the invention.

[0057] FIG. 20B is a graph of ion intensity versus field compensation voltage showing the increase in number of peaks detected after sample fragmentation according to an illustrative embodiment of the invention.

[0058] FIG. 21 is a conceptual diagram of a DMS system using fragmentation operating in parallel with a DMS system not using fragmentation to improve sample analysis according to an illustrative embodiment of the invention.

[0059] FIG. 22 is a conceptual diagram of a DMS system not using fragmentation operating in series with a DMS system using fragmentation to improve sample analysis according to an illustrative embodiment of the invention.

[0060] FIG. 23A is a graph of ion intensity versus field compensation voltage showing peak detection for the DMS system of FIG. 22 not using fragmentation.

[0061] FIG. 23B is a graph of ion intensity versus field compensation voltage showing peak detection for the DMS system of FIG. 22 using fragmentation.

[0062] FIG. 24 is a conceptual block diagram of a DMS system including a fragmentation region according to an illustrative embodiment of the invention.

[0063] FIG. 25 is a three-dimensional color dispersion plot illustrating detection of agent GA according to an illustrative embodiment of the invention.

[0064] FIGS. 26A-26H are two-dimensional graphs of ion intensity versus field compensation voltage at particular field voltages, the two-dimensional graphs being of the type combinable into the three-dimensional color dispersion plot of FIG. 25, according to an illustrative embodiment of the invention.

[0065] FIGS. 27A and 27B are graphs of ion intensity at a plurality of pressures versus field compensation voltage according to an illustrative embodiment of the invention.

[0066] FIGS. 28A and 28B are graphs of ion intensity versus pressure showing a quantifiable effect on positive and negative background spectra, respectively, caused by a decrease in pressure according to an illustrative embodiment of the invention.

[0067] FIGS. 29A and 29B are graphs of ion intensity at a plurality of pressures versus field compensation voltage showing the effect of varying pressure on negative and positive tert-butylmercaptan or tert-butylithiol (TBM) spectra, respectively, according to an illustrative embodiment of the invention.

[0068] FIGS. 30A and 30B are graphs of ion intensity versus pressure showing the effect of varying pressure on negative and positive TBM ion peak parameters, respectively, according to an illustrative embodiment of the invention.

[0069] FIG. 31 is a graph that shows the effect of reduced pressure on analyte peaks for chemical warfare agents such as DMMP, DIMP, and MS.

[0070] FIGS. 32A-32D are graphs of ion intensity versus field compensation voltage showing improved detection resolution for agent GF at reduced pressures according to an illustrative embodiment of the invention.

[0071] FIG. 33 is a three-dimensional color dispersion plot illustrating detection of positive ions of 0.005 mg/m³ DIMP at about 0.65 atm and over a range of field voltages and field compensation voltages with varying intensity depicted by varying colors.

[0072] FIG. 34 is a three-dimensional color dispersion plot illustrating detection of positive ions of 0.005 mg/m³ DIMP at about 0.5 atm and over a range of field voltages and field compensation voltages with varying intensity depicted by varying colors.

[0073] FIG. 35 is a graph that shows positive (left) and negative (right) three-dimensional color dispersion plots for 0.85 mg/m³ agent GB with a relative humidity (RH)=87 in a DMS system operating at 0.5 atm and for a fragmented sample.

[0074] FIGS. 36A and 36B are graphs that show a plot of compensation versus field strength of detected monomer and cluster ion peaks for a family of ketones according to an illustrative embodiment.

[0075] FIGS. 37 and 38 are tables, each including a collection of detection data for a group of monomer and dimers (clusters) of eight ketones respectively, that were used to generate the curves in the graphs of FIGS. 36A and 36B.

[0076] FIGS. 39A and 39B are graphs of a ratio of field strength to gas density (E/N) versus field compensation voltage that illustrate the results of calculating normalized alpha parameter curves.

[0077] FIG. 40A is a flow diagram of an exemplary sequence of steps of a computer process used to acquire data concerning a particular chemical ion species.

[0078] FIG. 40B shows a diagram of a data structure for a library of stored compound data measurement information.

[0079] FIG. 40C is a flow diagram of a series of steps that may be applied to perform a chemical recognition.

[0080] FIG. 40D is a flow diagram of a series of steps that may be added to the data acquisition and chemical recognition processes using alpha curve fitting.

[0081] FIG. 40E shows a diagram of a more complex data structure.

[0082] FIG. 40F is a flow diagram of a sequence of processes that may be used to distinguish monomer and cluster peak responses.

[0083] FIG. 40G is a flow diagram of a process showing the combination of monomer and cluster scoring.

[0084] FIG. 41 is a conceptual diagram of a compact DMS analyzer system 1400 used to detect and identify chemical warfare agents (CWAs), Toxic Industrial Compounds (TICs) and Toxic Industrial Materials (TIMs) which may be released in warfare or terrorist situations according to an illustrative embodiment of the invention.

[0085] FIG. 42 is a graph of multiple plots showing experimental results for a series of warfare agent simulants selectively mixed with 1% headspace of AFFF.

[0086] FIG. 43 is a three-dimensional color dispersion plot of the detection of positive ions of agent GA over a range of field voltages and field compensation voltages with varying intensity represented in varying color according to an illustrative embodiment of the invention.

[0087] FIG. 44 is a conceptual block diagram of a chemical and/or biological agent detection system using an ion mobility analyzer system, membrane, and recirculation system according to an illustrative embodiment of the invention.

[0088] FIG. 45 is a conceptual block diagram of a chemical and/or biological agent detection system configured for reduced pressure analysis according to an illustrative embodiment of the invention.

[0089] FIG. 46 is a conceptual block diagram of a chemical and/or biological agent detection system using a cylindrical DMS analyzer system, recirculation system, and multiple flow channels according to an illustrative embodiment of the invention.

[0090] FIGS. 47-53 are conceptual block diagrams respectively of chemical and/or biological agent detection systems using various configurations of a DMS analyzer system, recirculation system, and other components according to an illustrative embodiment of the invention.

DESCRIPTION OF ILLUSTRATIVE EMBODIMENTS

[0091] As described above in summary, the invention is generally directed to systems, methods and devices for providing improved detection, measurement, discrimination and analysis (collectively "analysis") of compounds. The compounds analyzed may include any compound, both organic and inorganic, without limitation elements, chemicals, and biologicals. In particular illustrative embodiments, the invention is directed to improved ion mobility-based compound analysis. Particular features of the invention include, use of dispersion plots, sample fragmentation and/ or pressure controls to improve discrimination between compounds having similar or overlapping ion mobility characteristics.

[0092] Although the illustrative embodiments of the invention are described in terms of Field Asymmetric Ion Mobility Spectrometers (FAIMS), also known as Differential Mobility Spectrometers (DMS), or Radio Frequency Ion Mobility Spectrometers (RFIMS) among other names (col-lectively DMS), the features of the invention may be similarly employed in combination with ion mobility spectrometry (IMS), time of flight (TOF) IMS, gas chromatography (GC), Fourier transform infrared (FTIR) spectroscopy, mass spectrometry (MS), and liquid chromatography mass spectrometry (LCMS).

[0093] FIG. 5 is a block diagram of a DMS system 10 of the type that may employ the invention. The system 10 includes a flow section 15 and a processor section 40. The flow section 15 includes a flow channel 11 extending from a flow inlet 12 to a flow outlet 13. Opposing filter electrodes 20 and 21 are located within the flow channel 11. Detector electrodes 26 and 30 are also located within the flow channel 11. The processor section 40 includes an RF voltage generator 42 for providing an RF field voltage to the filter electrodes 20 and 21, and direct current (dc) voltage generator 44 for providing a dc compensation voltage Vcomp to the filter electrodes 20 and 21. The processor section 40 also includes a processor 46 for controlling the voltage generators 42 and 44, and for processing inputs from the ion detectors 28 and 30 by way of the amplifiers 36 and 38 the A/D converter 48. The processor section 40 also provides a display 49 for providing analysis information to a user. One feature of the system 10 is that it may be contained in a hand held unit weighing less than about one pound.

[0094] In operation, a sample S enters the flow channel 11 at the flow channel inlet 12. The sample S may, for example, be drawn in from the environment or received from a front end device, such as another DMS, an IMS, TOFIMS, GC, FTIR, MS, or LCMS. The sample S may be mixed with an effluent, such as a gas, liquid or vapor. In the instant example, a carrier gas CG is employed to flow the sample S through the flow channel 11. Upon entering the flow channel 11, the sample S flows into an ionization region 14. The sample is ionized by an ionization source 16 as it flows through the ionization region 14, creating a set of ionized molecules 17+, 17−, with some neutral molecules 17n, of various chemical species in the sample S. This may include, for example, monomer ions and cluster ions. Such clusters may be created when a monomer combines with water molecules or other background molecules, and the combination is ionized.

[0095] The carrier gas CG then carries the ionized sample S into the ion filter field 18 located between the opposing filter electrodes 20 and 21 of the ion filter 24. Filtering proceeds based on differences in mobility in the filter field 18 of the various ions included in the sample S. Ion mobility is influenced, for example, by ion size, shape, mass and charge. The field generator 42 applies an asymmetric field voltage Vrf across the filter electrodes 20 and 21 to cause the field strength within the filter field 18 to alternate between high and low field strengths. The ions 17+, 17− and 17n move in response to the field, based on their mobility characteristics. Typically, an ion's mobility in the high field strength condition differs from its mobility in the low field strength condition. This mobility difference produces a net transverse displacement of the ions as they travel longitudinally through the filter 24. The transverse displacement defines an ion trajectory for each of the sample S ions.

[0096] As described above, the voltage generator 44, under the control of the processor 46, applies a dc compensation voltage Vcomp across the electrodes 20 and 21. The

compensation voltage Vcomp causes particular ion species to be returned toward the center of the flow path **14**, and thus enables them to exit the filter field **18**, without colliding with either of the filter electrodes **20** or **21** and without being neutralized. Other species, for which the applied Vcomp is not sufficient ultimately collide with the filter electrodes **20** and **21** and are neutralized. The neutralized ions are purged, for example, by the carrier gas CG, or by heating the flow path **11**.

[0097] The illustrative system **10** of FIG. **5** also can discriminate between ions based on differences in polarity, as is the case with the ions **17−** and **17+**. According to one feature, the system **10** of FIG. **5** can be operated to concurrently, or in some instances, substantially simultaneously detect both positive and negative ions in the sample S. This feature enables identification of two compounds concurrently, or in some instances, substantially simultaneously. This feature also enables concurrent or substantially simultaneous detection of two modes of a single compound.

[0098] In operation, the two species of ions **17+** and **17−**, enter the detection region **25**, where further separation occurs followed by their intensity determination. In a illustrative embodiment, the electrode **28** of the detector **26** may be positively biased to attract the ions **17−** and repel the ions **17+**. Alternatively, the electrode **30** of the detector **26** may be biased negatively to attract the ions **17+** while repelling the ions **17−**. The signals generated by the ions collecting at the detector electrodes **28** and **30** are amplified by respective amplifiers **36** and **38** and provided to the processor **46** by way of the A/D converter **48**. According to one feature, the processor **46** compares the digitized signals from the A/D converter **48**, with a library of ion intensity curves for known compounds stored in the memory **47**, to identify compounds in the sample S. The results of the comparison operation can then be provided to an appropriate output device, such as the display **49**, or may be provided to an external destination by way of an interface **56**.

[0099] According to a further illustrative embodiment, the system **10** is calibrated prior to employing it for analyzing a sample. More particularly, the library of ion intensity curves for known species of ions at particular Vcomp and Vrf settings is created and stored in the memory **47**. According to one feature, once the system **100** is calibrated, it may be used continuously, without need for further calibration. However, it is also within the scope of the invention to calibrate the system **10** using the reactant ion peak (RIP) or a dopant peak, for example.

[0100] According to various illustrative embodiments, field strength within the filter field **18** resulting from an applied field voltage Vrf may have values ranging from about 1,000 V/cm to about 30,000 V/cm, or higher. The frequency of Vrf may have values ranging from about 1 to about 20 megahertz (MHz), with the higher frequencies having an approximately 30 percent duty cycle.

[0101] It should be noted that the system **10** may be tuned by employing any suitable operating values of, for example, Vrf, Vcomp, field strength, Vrf duty cycle, Vrf wavelength and Vrf frequency. Additionally, as described in further detail below, to improve analysis, the system **10** may be tuned by varying values of other flow channel conditions, such as and without limitation, temperature, pressure, humidity, flow rate, doping and carrier gas CG composition.

As also described below in more detail, multiple scans of the sample S taken, for example, by recirculating the sample S and/or processing the sample in parallel and/or in series with one or more additional DMS, IMS, TOFIMS, GC, FTIR, MS, or LCMS, at differing flow channel/filter field conditions may be employed to improve analysis of the sample S.

[0102] According to one illustrative embodiment, the processor **46** causes the voltage generator **44** to scan or sweep a range of field compensation voltages Vcomp for a particular RF field strength as controlled by the applied Vrf to obtain a first spectrum for the sample S. Then, Vrf is set to a different level and the Vcomp is once again scanned to establish a second spectrum for the sample S. This information can be compared to a library of spectral scans in a similar fashion as that described above to identify a compound in a sample.

[0103] If a particular combination of peaks in a spectral scan is known to indicate the presence of a particular compound, data representing the multiple peaks can be stored and future detection data can be compared against this stored data. For example, under controlled filter field conditions, such as at a raised field strength, a clustered compound may become de-clustered. The detection results in a signature of peaks that can be used to identify the source compound being detected even as detected in a single scan.

[0104] According to one illustrative application, the invention is used for detecting sulfur-containing compounds in a hydrocarbon background. In one example, negative and positive ions are separately detected. The detected data enables a quantitative measurement of concentration of these sulfur-containing compounds, independent of the hydrocarbon background.

[0105] In another illustrative application, the invention is used for detecting trace amounts (parts per million (ppm), parts per billion (ppb), or parts per trillion (ppt)) of mercaptan in varying and even high hydrocarbon backgrounds. The system **10** of FIG. **5** is also able to characterize hydrocarbon gas backgrounds. For example, the invention is capable of detecting mercaptans, such as ethyl mercaptan in a methane background, and is also capable of detecting a gas, such as methane, in a mercaptan background.

[0106] In this practice of the invention, where mercaptans were detected in hydrocarbon background, the asymmetric voltage applied to the ion filter electrodes ranged from about 900 to about 1.5 kV (high field condition), and a low voltage of about −400 to about −500 V (low field condition). The frequency ranged from about 1 to about 2 MHz, and the high frequency had an approximate 30% duty cycle, although other operating ranges may be employed. In one embodiment, the detector electrodes were biased at +5v and −5v. With this arrangement, the mercaptans can be detected by the negative mode (−5v) detector and the hydrocarbon gases can be detected by the positive mode (+5v) detector.

[0107] The system **10** employs various conventional components. By way of example, the amplifiers **36** and **38** may be Analog Devices model 459 amplifiers. Additionally, the A/D converter may be included on a National Instruments circuit component (model 6024E) for digitizing and storing the scans, and may include software for displaying the results as spectra, topographic plots, dispersion plots or graphs of ion intensity versus time. Alternatively, such

software may be stored in the memory **47** and may control the processor **46**. The ionization source may be, for example, a plasma, laser, radioactive, UV lamp, or any other suitable ionization source.

[0108] According to one illustrative embodiment, Vrf is applied across the filter electrodes **20** and **21**. However in some configurations, Vrf is applied to one filter electrode, e.g., electrode **20**, and the other electrode, e.g., electrode **22**, is tied to ground. Vcomp is then applied to one of the filter electrodes **20** and **21**, or alternatively, across the filter electrodes **20** and **21**, according to the ions species to be passed. According to another feature, the detector electrodes **28** and **30** are biased with a floating bias, such as with the electrode **28** being biased at −5 Vdc and the electrode **30** being biased at +5 Vdc, leads to good performance for detection of mercaptans in hydrocarbon or air backgrounds.

[0109] FIG. **6** is a graph of ion intensity versus field compensation voltage for "positive mode" spectra for a sample containing varying amounts of ethyl mercaptan as measured in a DMS system of the type depicted at **10** in FIG. **5**. For positive mode detection, the detector electrode **28** is negatively biased and attracts positive methane ions **17***m*+ for detection. FIG. **7** is a graph of ion intensity versus compensation voltage for "negative mode" spectra of a sample containing various amounts of ethyl mercaptan. For negative mode detection, the detector electrode **30** is positively biased and attracts the negative mercaptan ions **17***m*− for detection. As can by seen from FIGS. **6** and **7**, the mercaptan signatures are captured independent of the air-hydrocarbon carrier gas CG background, at various dosage levels and the detected sample peaks are fully isolated from the background. As can be seen in FIG. **6**, the reactant ion peak (RIP) is isolated; and as shown in FIG. **7**, the background (sample #9) is flat.

[0110] As mentioned above, the detector electrodes **28** and **30** can be oppositely biased to enable concurrent, or in some configurations, substantially simultaneous detection of both positive and negative ions. Even in a sample such as mercaptan, which when ionized may have predominantly negative ions, detecting both positive and negative ions provides improved analysis accuracy over a single mode detection approach. This, in turn, improves identification accuracy and confidence, and reduces the likelihood of false positives and false negatives.

[0111] For example, Sulfur hexafluoride (SF6) can be well detected in the negative mode. However, the response in the positive mode, while alone not definitive, has a profile, and thus in combination with the negative mode, is confirmative and provides a lower likelihood of a false detection. According to one feature, the invention can detect SF6 in single mode (e.g., only negative mode detection) or dual mode (both negative and positive mode detection), seriatim, concurrently, or simultaneously.

[0112] SF6 gas is used in atmospheric tracer applications to monitor air flow, as a tracer for leak detection in pipes to point detect sources of leaks, in power plants to isolate switches to reduce, or prevent breakdown of the switches, among other uses. Isolation and detection of SF6 is often found to be a difficult proposition.

[0113] According to one illustrative application, a system of the invention is employed to detect SF6 in air. According to a further illustrative embodiment, the invention provides a portable, battery powered unit for the detection of SF6 with a sensitivity of about 1×10-9 atm cc/sec SF6 (0.01 PPM). In this illustrative embodiment, the invention may be used, for example, in the power industry to ensure the leak tightness of High Voltage Switchgear and in the laboratory for testing fume hoods to the ASHREA 110 specification. Other applications include torpedo head, pipework systems, and air bag integrity testing. The high sensitivity, rugged design and ease of use and set up of the invention are advantageous for many applications that involve the detection of SF6.

[0114] FIG. **8** is a graph of ion intensity (y-axis) versus Vcomp (x-axis) for negative mode detection of SF6 according to an illustrative embodiment of the invention. As can be seen, application of the invention provides a distinct peak for the SF6, separate from the reactant ion peak. FIG. **9** provides a similar plot for SF6 for positive mode detection. As can be seen, for positive mode detection, there is no significant difference between the signal **51** without the SF6 present and the signal **53** with the SF6 present. FIG. **10** shows a plot of intensity (y-axis) versus Vcomp (x-axis) for SF6 at three different field voltages Vrf (shown at **57**, **58** and **61** for negative mode detection along with the RIP **55** detected in absence of SF6. FIG. **11** shows a similar plot to that of FIG. **10**, for positive mode detection. As would be expected the, positive mode detection curves **69**, **71** and **73**, substantially track their corresponding RIP curves **63**, **65** and **67**, respectively. As mentioned above with respect FIG. **16**, while alone this is not definitive, it is an expected detection and therefore may be used as confirmative when combined with a definitive SF6 negative mode detection.

[0115] According to another feature, the above described library data for known ion species intensity signatures for known device characteristics may be accessed for either single mode or simultaneous positive and negative mode detections. By comparison with historical detection data for the device, these peaks can be more clearly identified as the tell-tale spectra of the mercaptan. Both spectra give an indication of the mercaptan, qualitatively and quantitatively. Although the advantages of the simultaneous positive and negative mode detection is described above with respect to mercaptan, they may be employed to the analysis of any sample, and are especially useful with real-time analysis of complex samples, such as ones containing mercaptans and hydrocarbon gas, which have similar ion mobility characteristics, and are therefore, difficult to discriminate between.

[0116] The foregoing demonstrates favorably obtaining multiple detection data from a single mobility scan for identification of detected ion species in a sample. This innovation is useful in many applications. Notwithstanding this valuable innovation, a still higher level of confidence and further reduced false positives may be obtained by (1) obtaining multiple detection data from multiple ion mobility scans, and (2) further processing such data to extract device independent attributes, such as a mobility coefficient, α.

[0117] According to one illustrative "multiple scan" embodiment, ions are identified based not on a single set of field conditions, but instead on multiple ion intensity scans taken at least two and possibly additional numbers of field conditions (e.g., at least two field measurement points). Detections are correlated with the Vrf and Vcomp, at the at

least two different field conditions, to characterize a given detected compound. Because multiple detection data are associated with a given ion species of interest, more accurate detections can be made. Comparison with stored data results in reliable identification of detected compounds.

[0118] Strategies for identifying detected ions based on data in spectral peaks or in mobility curves include: curve matching, peak fitting, deconvolution (for overlapping peaks), multi-dimensional mapping, for example, employing three-dimensional representations, including (x,y,z, etc.) spatial coordinate systems and/or (x,y, etc.) coordinate systems, with z- or other values represented by color variations. These techniques enable identification of detected ion species based peaks in a single scan, including simultaneous positive and negative mode detections, and also in multiple scans. The goal is the same: analysis of multiple detection data that can be used to definitively identify, detect, measure or otherwise analyze the species of a detected ion.

[0119] As described above, different ion species of chemicals exhibit different mobility as a function of the compensated applied Vrf. Thus, by applying a set of different Vrf voltages and measuring the Vcomp at the ion abundance peak locations, for example, as detected by the detector 26 of FIG. 1, for the various compounds, a family of measurement points characteristic of a compound can be developed. This family of points can then be plotted to determine the ion mobility curve signature for specific species as a function of Vrf and Vcomp, for example, as shown in FIG. 4. As also described above, such data can be stored and compared with data from scans of unknown compounds to identify the unknown compounds. While some comparison approaches perform curve matching, other approaches determine an ion intensity for a particular ion species for two nearby field strength and Vcomp conditions. The slope between the two data points is calculated and employed as a signature for the particular ion species. The selection of measurement points and the number of measurement points may be adjusted for the specificity required for a particular application. The minimum number of measurement points is two, which at least identifies an aspect (such as slope) of the characteristic curve for a compound, given the known field values.

[0120] Although performing slope and/or curve matching for an individual or for multiple scans, where a single filter field/flow channel condition is varied, may provide sufficiently accurate results for some applications, one illustrative embodiment of the invention recognizes that multiple scans taken while varying multiple filter field/flow channel conditions can provide improved results. By way of example, according to one illustrative embodiment, the invention steps Vrf through a plurality of values and scans Vcomp at each of the plurality of Vrf values to generate unique sets of data, which better distinguish between compounds and thus, provide more accurate identification of detected compounds. This approach can be employed to create a data store of more accurate ion mobility signatures for compounds of interest.

[0121] According to one illustrative embodiment, the invention incorporates information regarding shifts in an ion abundance peak for a particular ion species at multiple filter field/flow channel conditions into the spectral signature for a compound. More specifically, at a particular Vrf (Vrf1) a ion abundance peak may be detected at a particular Vcomp

(Vcomp1). However, the ion abundance peak may shift to be detected at a second Vcomp (Vcomp2) for a second Vrf (Vrf2). One illustrative embodiment of the invention recognizes that, in many instances, the ion peak shift from Vcomp1 to Vcomp2 in response to varying Vrf from Vrf1 to Vrf2 is indicative of a particular ion species. Similar measurements of unknown compounds can be compared against this portion of the spectral signature to aid in identification of the unknown compound.

[0122] FIG. 12 depicts an example illustrating the above described ion abundance spectral shift due to a change in Vrf from 1400 Vpeak to 1450 Vpeak over a scanned Vcomp. In FIG. 12, the peaks 110-1, 110-2, 110-3, and 110-4 occur at a particular field compensation voltages Vcomp, for Vrf at 1400 Vpeak (corresponding to a field strength of 28,000 V/cm), but shift to be located at different compensation voltages in response to Vrf being changed to 1450 Vpeak (corresponding to a field strength of 29,000 V/cm). As can be seen from FIG. 12, even small changes in a field condition, such as a change in Vrf, can cause a measurable ion peak shift, and can thus provide significant additional information to the ion spectral signature. In the specific example of FIG. 12, the shift in ion peak due to the change in Vrf is employed when making a comparison to ion spectral signatures for known compounds to identify an unknown compound.

[0123] FIGS. 13A and 13B show an experimental example illustrating how ion spectral peak shifting can be employed to identify an unknown species. In FIGS. 13A and 13B, in a field strength of about 24000 V/cm, peaks for three different isomers of xylene in a sample, p-, o-, and m-, were detected. In FIG. 13A, the peaks for p- and o- are indistinguishable, while the peak for m- is well defined. To further evaluate the sample, a second detection (FIG. 13B) was performed at a lower field strength of 18000 V/cm. As can be seen in FIG. 13B, the peak shift due to the change in field strength causes the three different isomers p-, o-, and m- of xylene to be more clearly distinguishable, and thus more accurately identified. As can be seen from FIGS. 13A and 13B, better discrimination between species is not always a result of applying a higher field strength. More particularly, in this example, the p- and o- xylene isomers become more distinguishable at reduced a field strength.

[0124] According to another illustrative embodiment and as mentioned above, the invention generates detection data over a range of applied filter field/flow channel conditions. For example, FIGS. 14A and 14B show the effect of changes in field strength on the location of detection peaks at different Vcomp levels for hexanone and octanone, as detected in a DMS system of the type depicted at 10 in FIG. 1. The curves are offset on the vertical axis, with the offset increasing as electric field strength increases. While various operating ranges are possible, as an illustration, FIGS. 14A and 14B may be understood as presenting peak Vrf between a low of about 620 Vpeak (lowermost plot in each) and a high of around 1450 Vpeak (uppermost plot in each). Several attributes are noted in this series of responses. For example, referring specifically to the hexanone plot of FIG. 14A, a monomer peak of 601-1 of particular interest is somewhat obscured in the lowest field strength condition. However, at the highest applied field strength, the peak 601-m corresponding to hexanone is clearly discernable from the other peaks.

[0125] Several phenomena have occurred with the increase in increasing applied field strength. First, a reactant ion peak (RIP) 605-1 is relatively dominant in the low field strength detection. However, as electric field strength is increased, the RIP 605-m shifts to the left at a more rapid rate than the monomer ion peak 601-m of interest. This is because the α parameter for the mobility coefficient for the reactant ion species is different than the α parameter for the monomer ion of interest.

[0126] In addition, the relative amplitude of the RIP 605 decreases markedly with the increase in the electric field strength. Thus, RIP 605-m is observed at much lower amplitude and well separated from the monomer peak 601-m of interest at a specific field condition. While the monomer peaks 601 also shift, they do not shift by the same amount, or by as much. Thus, by analyzing the compound over a range of applied field conditions, a condition can be discovered at which the RIP 605 shifts away from or off the scale of other observed peak voltages. In some cases, this allows easier detection of the monomer ion peak 601 of interest.

[0127] Similar behavior is observed in the monomer peaks 610-1, 610- . . . , 610-n observed for octanone and the resulting reactant ion peaks 615-1 to 615-m. This information can thus be used to identify a species by comparing a family of response curves to a stored family of known response curves.

[0128] Another observed effect shown in both FIGS. 14A and 14B is that a group of cluster ions 608 and 610 are seen. The cluster ions 608 represent clusters of chemical materials in the sample. Typical cluster ions, having a heavier chemical weight, have peaks that are shifted differently from monomer ion peaks of interest. In this example, the cluster peaks shift in a direction away from the direction of shift of the monomer peaks with increasing applied field strength. This characteristic feature of cluster ions, observed with this sample, can also be stored and utilized in recognizing the hexanone and/or octonone ions. The curves shown in FIGS. 14A and 14B are but one example of how applying a range of field/flow channel conditions to detect a given sample can be utilized to an advantage.

[0129] As mentioned above briefly, according to one illustrative embodiment, the invention employs multi-dimensional compound signatures for comparison with multi-dimensional representations of unknown compounds to identify and more generally analyze the unknown compounds. Such multi-dimensional representations may arise, for example, from plotting ion abundancy as a function of a plurality of varying filter field/flow channel conditions. Such conditions may include, without limitation, Vrf, Vcomp, filter field strength, Vrf duty cycle, Vrf wavelength and Vrf frequency; temperature, pressure, humidity, flow rate, doping and carrier gas CG composition. Multi-dimensional representations may also result from taking multiple scans of the sample S taken, for example, by recirculating the sample S and/or processing the sample S in parallel and/or in series with one or more additional DMS, IMS, TOFIMS, GC, FTIR, MS, or LCMS, at the same or differing flow channel/filter field conditions. The multi-dimensional representation, according to one illustrative embodiment, is a three-dimensional dispersion plot, employing x- and y- spatial coordinates, with a z-coordinate being represented by a variation in color.

[0130] FIG. 15A shows a three-dimensional color dispersion plot 620 depicting detection of methyl salicylate over a range of field voltages Vrf (y-axis) and field compensation voltages Vcomp (x-axis), with varying ion intensity (abundance) represented in varying colors, according to and illustrative embodiment of the invention. Although, particular color coordination may vary, the dispersion plot of FIG. 15A represents the highest ion intensity in blue with yellow representing the lowest. The three-dimensional color dispersion plot 620 represents an aggregation of data from a plurality of two-dimensional graphs, such as that shown in FIG. 15B. More specifically, FIG. 15B shows a plot 622 of ion intensity (y-axis) versus Vcomp (x-axis) at a particular Vrf for methyl salicylate. A plurality, illustratively more than two, of such graphs taken at a plurality, illustratively more than two, of field voltages Vrf are aggregated to provide the color plot 620 of FIG. 11A. Aggregating a plurality of scans taken at a plurality of filter field voltages Vrf (and thus, field strengths) provides a more discriminating scan than a single scan taken at a single Vrf. One reason for this is that the aggregated scans incorporate the above discussed peak shifting that occurs due to the changes in Vrf. As can be seen, the three-dimensional representation of FIG. 15A provides three signature peaks 621, 623, and 625, as opposed to the two peaks 627 and 629 of FIG. 15B.

[0131] The effect of the increased resolution provided by employing dispersion plots, is even more evident, when trying to distinguish between compounds having similar ion mobility characteristics. By way of example, FIGS. 16A and 16B show positive mode plots 624 and 626 for DMMP, while FIGS. 17 and 18 show positive mode plots 628 and 630 for DIMP. More specifically, FIGS. 16B and 18, plot ion intensity (y-axis) versus Vcomp (x-axis) at a particular Vrf for DMMP and DIMP, respectively. As shown, both FIGS. 16B and 18 included three peaks of similar magnitude, located at a approximately the same field compensation voltages, and similarly spaced apart. Distinguishing between DMMP and DIMP, based solely on the individual plots 626 and 630 of FIGS. 16B and 18 is at best unreliable, and at worst impossible. However, referring to FIGS. 16A and 17, the three-dimensional plots 624 and 636 are easily visually distinguishable.

[0132] More particularly, the DMMP color plot 624 of FIG. 16A shows three clear peaks 638, 639 and 640, while the DIMP color plot 628 shows four clear peaks 631, 632, 634 and 636. While the peaks 638, 639 and 640 nearly overlay the peaks 631, 634 and 636, the fourth blue peak 632 for DIMP, which is lacking for DMMP, easily distinguishes the DMMP scan from the DIMP scan. Also, the branches 634 and 636 of the color plot 628 are closer together than the branches 638 and 640 of the color plot 624. Additionally, the color distribution (e.g., saturation) throughout the branches of the three-dimensional color plot 624 is not the same as the color distribution throughout the branches of the plot 628. As in the case of previously discussed signature scans, three-dimensional signature scans of the type depicted in FIGS. 15A-18 may be stored in a library for known compounds. At least portions of one or more of the stored scans may be compared with at least portions of similar scans of unknown species to identify and generally analyze the unknown species. Any suitable pattern matching approach, including conventional pattern matching approaches, may be employed for such comparison.

11

[0133] It should be noted that although the above discussed dispersion plots of FIGS. **15A, 16A** and **17** employ color changes to indicate intensity, changes in any color-related feature, such as changes in color saturation, gray scale or black and white may be employed instead or in combination. Additionally, in a further illustrative embodiment, the invention generates a curve circumscribing the intensity peaks, and the color-related information may be discarded. By way of example, in this illustrative embodiment, the outlines, for example, for the intensity peaks **632**, **634** and **636** would remain, without the color-related information. Removing the color-related information provides a two-dimensional dispersion representation of, for example, Vrf versus Vcomp that also takes into account the spectral information gained from aggregating a plurality of Vcomp scans at a plurality of Vrf values. Any or all of this two-dimensional information may be incorporated into the above discussed signature information.

[0134] As described above, various illustrative comparison approaches may employ pattern matching using, for example, the above described two- and/or three-dimensional dispersion plots. However, in other illustrative embodiments, the information provided by the dispersion plots is stored in the library as mathematical relationships, and suitable conventional approaches for comparing such mathematical relationships are employed to identify the unknown species.

[0135] According to another illustrative embodiment, Vcomp may be plotted on the x-axis, Vrf on the y-axis, and ion intensity on the z-axis. Thus, instead of showing ion intensity as color, saturation, gray scale or black and white variations, as in the three-dimensional color plots **620**, **624**, and **628**, ion intensity may be depicted/conceptualized in a topographical manner. Multi-dimensional signature representations of this sort may also stored in the library of known species and used in the same fashion as the above described ion mobility signatures. In other embodiments of the invention, more than three dimensions may be employed, for example, plotting spectral data as clusters in n-dimensional space and employing known cluster matching algorithms.

[0136] A processor, such as the processor **46** of FIG. **5**, may be programmed in a conventional fashion to automatically step an analyzer, such as the system **10**, through a range of field voltages Vrf and a scanned Vcomp, and provide the data to a display or other system for processing and generation of a three-dimensional dispersion plot.

[0137] Another analysis improving effect can be observed with the application of relatively high field strengths. Specifically, complex ion groupings can be fragmented, for example, by applying a high field strength to the sample. Sample fragmentation is a useful technique for enhancing species separation, detection, and identification. Fragmentation includes a process in which large molecules of samples are broken up into smaller molecules, components, or fragments prior to sample detection. This enables the components of the group to be individually detected and more generally analyzed.

[0138] FIG. **19** is an example of such an effect on a mercaptan sample. In particular, a range of background voltages (from 620-1450 Vpeak) were applied to an ethyl mercaptan spectra in which a general shift of ion peak behavior can be seen as an electric field conditions are strengthened. However, a fragmentation condition can also be observed. Specifically, at lower applied field conditions, strong single peak is observed, such as at **701-1**. However, as electric field strength is increased, multiple peaks **701-n**, **702**, . . . **710** are observed in a spectra. By observing and recording the peak locations, not only at the low voltage field conditions, but also at a range of field conditions, this fragmentation behavior can be further exploited to better identify compounds. According to one feature, data indicating the peak RF voltage at which fragmentation occurs is incorporated into the stored spectral signatures for the known samples. According to another feature, the locations of the fragment peaks are also or instead incorporated into the stored spectral signatures for further use for matching detection data with known data.

[0139] FIG. **20A** is a graph **712** of ion intensity (y-axis) versus field compensation voltage Vcomp (x-axis) illustrating the separation of detection peaks at different compensation voltages between light and heavy molecules according to an illustrative embodiment of the invention. The graph **712** shows that light molecules associated with the RIP background peak **714** may be identified at an arbitrary −30 Vdc compensation voltage, while heavier molecules tend to be clustered and form a peak **716** at about 0 Vdc compensation. By fragmenting a sample of heavy molecules and detecting the fragments using, for example, a DMS or IMS system, a plurality of ion intensity peaks, each associated with a fragment, may be used create a unique signature of the sample to enable subsequent identification of that sample. Fragmentation of a sample may be achieved, for example and without limitation, by using any one or a combination of a chemical reaction, a high energy field at high strength, high field voltage, heating, laser light, colliding the sample molecules with other molecules, soft x-ray, or the like.

[0140] FIG. **20B** is a graph **718** of ion intensity (y-axis) versus field compensation voltage (x-axis) showing the increase in number of peaks detected after sample fragmentation according to an illustrative embodiment of the invention. The graph **718** shows that fragments are lighter, and therefore, have lower mass and higher associated compensation voltages, resulting in improved resolution of and differentiation between the fragments. Also, the graph **718** shows an increased number of peaks **720** associated with the fragmented sample, which increases the collective data that may be used to fingerprint the compound. The additional detection data enable a more accurate identification of the detected species, such as by comparing the signature detected with a set of signatures in a look up table and by other techniques disclosed herein.

[0141] FIG. **21** is a conceptual block diagram of a dual channel detection system **748** including a first DMS system **722** using fragmentation and forming a first channel operating in parallel with a second DMS system **124** not using fragmentation and forming a second channel to improve sample analysis according to an illustrative embodiment of the invention. As shown, the DMS system **724** includes a sample inlet **726**, ionization region **728**, ion source **730**, analyzer region **732**, and outlet **734**. Similarly, the DMS system **722** includes a sample inlet **736**, ionization region **738**, ion source **740**, analyzer region **742**, and outlet **744**. The DMS system **722**, however, also includes a fragmentation energy source **746** within the ionization region **738**. The

analyzer regions **732** and **742**, respectively, include a DMS filter and detector to enable detection and identification of samples. In operation, the dual channel detection system **748** operates DMS systems **722** and **724** concurrently, simultaneously or alternatively. With respect to the DMS system **724**, a sample S is introduced into ionization region **728** via the sample inlet **726**. The ionization source **730** may then ionize the sample S into positive and/or negative ions that are then delivered to the analyzer region **732**. The analyzer region **732** performs filtering and detection of the sample which then exits the DMS system **724** via the outlet **734**. The DMS system **722** operates in a similar manner as the DMS system **724**, but with an additional fragmentation source **746**. Thus, when the sample S enters ionization region **738** of DMS system **724**, the fragmentation source **746** breaks up/fragments the sample S molecules into lighter, less massive molecules. These lighter molecules are then delivered to analyzer region **742** for filtering and detection.

[0142] Thus, the dual channel detection system **748** using DMS systems **722** and **724** may improve sample analysis by substantially simultaneously analyzing a sample S and its fragments to create a more complete signature of the sample. Alternatively, the dual channel detection system **748** may selectively compare the fragmentation spectra, depending on the sample species to be detected and the need for better discrimination from other interferants or compounds.

[0143] FIG. **22** is a conceptual diagram of a DMS system **750**, not using fragmentation, and operating in series with a DMS system **752** using fragmentation to improve sample analysis according to an illustrative embodiment of the invention. The combination of the DMS systems **750** and **752** form a serial detection system **754**. As shown, the serial detection system **754** includes a sample inlet **756**, the DMS system **750**, the DMS system **752**, and an outlet **758**. The DMS system **750** includes an ionization region **760**, ion source **762**, ion filter **764**, and detector **766**. The DMS system **752** includes an ionization region **768**, ion source **770**, fragmentation source **772**, ion filter **774**, and detector **776**.

[0144] In operation, a sample S is introduced into the serial detection system **754** via the sample inlet **756**. The DMS system **750** ionizes the sample S using the ionization source **762** within the ionization region **760**. Then, the ionized sample S is delivered to the ion filter **764**. The ion filter **764** applies a combination of field and field compensation voltage to the sample S to allow select ion species to reach and be detected by the detector **766**.

[0145] FIG. **23**A is a graph **778** of ion intensity (y-axis) versus Vcomp (x-axis) showing peak detection for the DMS system **750**. As shown previously, when no fragmentation occurs, the relatively heavy sample molecules cluster to form a peak **780** at Vcomp=approximately 0 Vdc.

[0146] After analysis by the DMS system **750**, the sample S is delivered to the DMS system **752**, where the sample S is ionized by an ionization source **770**, and also fragmented by the fragmentation source **772**. The fragmentation source **772** may be a radioactive source, a high energy voltage source or the like with enough energy to break up the relatively large sample molecule into a plurality of fragment molecules, fragments, components, or atoms. Then, the fragments are delivered to the ion filter **774** whereupon a combination of filter field voltages Vrf and field compensa-

tion voltages Vcomp applied a plurality of filter field conditions to the fragments to filter them before detection by the detector **776**.

[0147] FIG. **23**B is a graph **782** of ion intensity versus compensation voltage showing peak detection for the DMS system **752** of FIG. **22** using fragmentation. As shown previously, when fragmentation occurs, the relatively lighter fragments form a plurality of ion intensity peaks **784** at various distinct field compensation voltages Vcomp.

[0148] Thus, the serial detection system **754** using the DMS systems **750** and **752** may improve sample analysis by serially detecting a sample S and its fragments to create a more complete signature or fingerprint of the sample. Alternatively, the serial detection system **754** may selectively compare the fragmentation spectra depending on the sample species to be detected and the need for better discrimination from other interferants or compounds.

[0149] FIG. **24** is a conceptual block diagram of a DMS system **786** including a fragmentation region **792** according to an illustrative embodiment of the invention. As shown, the DMS system **786** includes a sample introduction region **788**, ionization region **790**, fragmentation region **792**, fragmentation source **806**, fragmentation effluent inlet **794**, transport effluent inlet **796**, ion filter **798**, detector **800**, and controller **812**. An ionization source **802** may optionally be located within the fragmentation region **792**. An ionization source **804** may optionally be located within ion filter **798**.

[0150] In operation, a sample S is introduced into sample introduction region **788**. The sample introduction region **788** may perform pre-separation of the sample S to reduce the amount of interferants or unwanted compounds. The ionization source **808** then ionizes the sample S in the ionization region **790**. Once the sample S is delivered to the fragmentation region **792**, the fragmentation source **806** fragments the relatively heavy molecules of the sample S into a plurality of lighter fragments. Alternatively, a fragmentation gas including fragmentation molecules may be introduced into fragmentation region **792** via fragmentation gas inlet **794**. The fragmentation gas molecules, upon colliding with the sample S molecules, cause a portion of the sample S molecules to break up into sample S fragments.

[0151] After fragmentation, a transport effluent, such as a carrier gas CG may be introduced via the transport effluent inlet **796** to deliver the sample S fragments to the ion filter **798**. After filtering, the fragments are then detected by the detector **800**. The ionization source **802** may optionally be located in the fragmentation region **792**. Furthermore, as in the case of all of the previously described illustrative embodiments, the fragmentation source **806** may function additionally as a ionization source. The ionization source **804** may optionally be located in the ion filter **798**. Furthermore, the ion filter **798** may also act as either a fragmentation source **810** or an ionization source **804**.

[0152] It should be noted that although the previously described embodiments refer to separate ionization and fragmentation sources, in other illustrative embodiments, a single source may attend to both fragmentation and ionization. Additionally, any of the previously described fragmentation approaches may be employed in addition to or in replacement of the fragmentation sources of FIGS. **21**, **22** and **24**. The controller **821** may switch fragmentation on and

off as needed by activating or deactivating the fragmentation source **806** or by introducing or not introducing a fragmentation effluent via fragmentation effluent inlet **794**.

[0153] The foregoing fragmentation techniques and system implementing these fragmentation techniques may be used to enhance the detection of a sample S, such as without limitation, Sarin gas, also known as:

[0154] GB

[0155] Zarin

[0156] Phosphonofluoridic acid, methyl-, isopropyl ester

[0157] Phosphonofluoridic acid, methyl-, 1-methylethyl ester

[0158] Isopropyl methylphosphonofluoridate

[0159] Isopropyl ester of methylphosphonofluoridic acid

[0160] Methylisoproposfluorophosphine oxide

[0161] Isopropyl Methylfluorophosphonate

[0162] 0-Isopropyl Methylisopropoxfluorophosphine oxide

[0163] 0-Isopropyl Methylphosphonofluoridate

[0164] Methylfluorophosphonic acid, isopropyl ester

[0165] Isoproposymethylphosphonyl fluoride

[0166] Sarin, a colorless and odorless gas, has a lethal dose of 0.5 milligram for an adult. It is 26 times more deadly than cyanide gas and is 20 times more lethal than potassium cyanide. Just 0.01 milligram per kilogram of body weight in a pinprick sized droplet will kill a human.

[0167] FIG. **25** is a three-dimensional color dispersion plot **814** of the type described above with respect to FIGS. **15A-18** and illustrating detection of agent GA over a range of field voltages Vrf and field compensation voltages Vcomp with varying ion intensity presented in varying color according to an illustrative embodiment of the invention. The color dispersion plot **814** includes branches **816**, **818**, **820**, and **822** that represent the detection of fragments of agent GA using, for example, DMS system **786** having a Ni63 ionization source for fragmentation of the GA sample at 0.14 ng/l. The branch **840** represents an original peak before fragmentation.

[0168] FIGS. **26A-26H** depict two-dimensional graphs **824**, **826**, **828**, **830**, **832**, **834**, **836**, and **838** of ion intensity (y-axis) versus Vcomp (x-axis), each at a particular Vrf. As described above with respect to FIGS. **15A-18**, the two-dimensional graphs **824**, **826**, **828**, **830**, **832**, **834**, **836**, and **838** are aggregated into the three-dimensional color dispersion plot **814** of FIG. **25**. As discussed previously, the color dispersion plot **814** improves the analysis process of a particular species such as agent GA or GB, for example, because it takes into account peak shifts due to changes in Vrf, and because the color nature of the three-dimensional dispersion plot **814** makes more evident the signature behavior of particular ion species in relation to other ion species, especially after fragmentation.

[0169] As described above with respect to FIGS. **15A**, **16A**, and **17**, the dispersion plot of FIG. **25**, may employ

color saturation, gray scale variations, black and white variations and/or peak outlines in place of the color variations depicted.

[0170] The fragmentation techniques described herein are not limited to DMS systems and may be employed with other mobility-based detection systems such as ion mobility spectrometry (IMS), time of flight (TOF) IMS, gas chromatography (GC), Fourier transform infrared (FTIR) spectroscopy, mass spectrometry (MS), liquid chromatography mass spectrometry (LCMS), surface acoustic wave (SAW) sensors, and the like.

[0171] Another technique for improving ion species detection, identification and analysis generally is operating the mobility-based detection system, such as any of the systems described herein, below atmospheric pressure. By operation below atmospheric pressure, the separation between ion intensity detection peaks is increased and the width of the peaks is narrowed. This provides for improved the resolution, resulting in improved system discrimination and sensitivity. By operating, for example a DMS system at various pressure conditions, the change in ion species behavior with respect to pressure may be measured and used as another characteristic for identifying ion species. According to various illustrative embodiments, the invention performs ion scans at pressures between about 0.2 and about 0.9 atmospheres, less than about 0.3 atmospheres, less than about 0.4 atmospheres, less than about 0.5 atmospheres, less than about 0.6 atmospheres, less than about 0.7 atmospheres, or less than about 0.8 atmospheres.

[0172] FIG. **27A** is a graph **840** of background (RIP) ion intensity versus field compensation voltage at a plurality of pressures for a DMS system in positive ion detection mode according to an illustrative embodiment of the invention. The graph **840** shows that the field voltage may be adjusted to maintain the ion intensity peak within the same compensation voltage position as the pressure within a DMS system is adjusted. More specifically, according to the graph **840**, as the pressure decreases, the field voltage decreases to maintain the ion intensity peak for a species at the same compensation voltage. Furthermore, changes in pressure at lower pressures result in the need for greater changes in field voltage to maintain a constant compensation voltage. For example, when reducing the pressure by approximately 100 mmHg from 760 mmHg to 655 mmHg, the reduction in field voltage is approximately 40 Vpeak from about 1050 Vpeak to about 1010 Vpeak. For approximately the same pressure reduction from 655 mmHg to 556 mmHg, the reduction in Vrf is approximately 90 volts from about 1100 Vpeak to about 920 Vpeak. Thus, the field voltage decrease is approximately twice as great for changes in pressure in the 600 mmHg range, which indicates that the resolution is improved at reduced pressure.

[0173] FIG. **27B** is a graph **842** of background (RIP) ion intensity versus field compensation voltage at a plurality of pressures for a DMS system in negative ion detection mode according to an illustrative embodiment of the invention. Like positive mode graph **840**, the graph **842** shows that, in negative detection mode, the field voltage may be adjusted to maintain the ion intensity peak within the same compensation voltage position as the pressure within a DMS system is adjusted.

[0174] As shown by comparing the graph **840** with the graph **842**, there is an offset in the ion intensity peak between

14

the positive mode ion intensity peaks of graph **840** and negative mode ion intensity peaks of graph **842** at the same pressure and field voltage. This offset may indicate a difference in the alpha parameter between positive and negative mode detection for an ion species. The alpha parameter is discussed in further detail below. The DMS flow rate is approximately 300 cc/min in graphs **840** and **842**.

[0175] FIGS. **28**A and **28**B depict graphs **844** and **846**, respectively, of ion intensity (y-axis) versus pressure (x-axis) showing a quantifiable effect on positive and negative background spectra, respectively, caused by a decrease in pressure according to an illustrative embodiment of the invention. More specifically, the graph **844** shows that field voltage is decreased by about 50% when pressure is decreased to about 0.3 atmosphere (atm). The graph **846** also shows a similar field voltage decrease of about 50% when pressure is decreased to about 0.3 atm.

[0176] FIGS. **29**A and **29**B depict graphs **848** and **850**, respectively, showing ion intensity (y-axis) versus field compensation voltage (x-axis) for a plurality of pressures and showing the effect of varying pressure on negative and positive tert-butylmercaptan and tert-butylithiol (TBM) spectra, respectively. While the graphs **848** and **850** show that field voltage decreases as pressures decreases for a particular field compensation voltage, the graphs **848** and **850** also show that the ion intensity peak positions for TBM spectra shift in the opposite direction as the ion intensity peak shifts for the background (RIP) spectra of graphs **840** and **842**. Furthermore, the level of change of the ion intensity peaks in graphs **848** and **850** for TBM spectra is less than the level of change of the ion intensity peaks in graphs **840** and **842** for background spectra.

[0177] FIGS. **30**A and **30**B depict graphs **852** and **854** showing ion intensity (y-axis) versus pressure (x-axis) and showing the effect of varying pressure on negative and positive TBM ion peak parameters, respectively. More specifically, the graph **852** shows that the ion intensity peak remains relatively constant as the pressure is varied for negative ion spectra. The graph **854** shows that the ion intensity peak remains relatively constant with the level decreasing slightly at a lower pressure for positive spectra. Because changes in pressure impact the background (RIP) and analyte spectra differently, pressure may be manipulated, regulated, or otherwise controlled in such a manner as to improve the ability of a DMS system to detect and identify ion species with better resolution while minimizing the negative effects of background spectra interference.

[0178] In certain embodiments, it may be desirable to maintain uniform detection results by maintaining a constant ratio of electric field strength to gas density N or pressure P where the ratio is expressed as E/N or E/P. Thus, when the gas operating pressure within a DMS system is decreased, the field voltage is correspondingly lowered to maintain a constant E/N or E/P. This reduction in field voltage results in a reduction in power consumption which, in turn, results in smaller, lighter weight, and lower cost detection systems.

[0179] FIG. **31** is a graph **856** showing the effect of reduced pressure on analyte peaks for chemical warfare agents, such as DMMP, DIMP, and MS. The top graph **857** show the ion intensity results at atmospheric pressure, while the bottom two graphs **859** and **861** show the results at 0.65 and 0.5 atm, respectively. At 1 atm with field voltage at

Vrf=about 1000 Vpeak, the top spectra shows the overlap **858** of monomer and dimmer cluster peaks for DIMP over a range of about 10 Vdc field compensation voltage. But at 0.65 atm and Vrf=about 800 Vpeak, the monomer peak **860** and cluster peak **862** are separated with the monomer peak **860** at Vcomp=about −3 Vdc and cluster peak **862** at Vcomp=about +1 volt. At 0.5 atm and Vrf=about 650 Vpeak, the DIMP monomer peak **864** and DIMP cluster peak **866** are each narrower with the peaks **864** and **866** at Vcomp= about −2.5 Vdc and about +1 Vdc, respectively. The narrower peaks **864** and **866** at 0.5 atm result in higher resolution for a DMS system.

[0180] FIGS. **32**A-**32**D depict graphs **868**, **870**, **872**, and **874**, respectively, showing ion intensity (y-axis) versus Vcomp (x-axis). The graphs **868**, **870**, **872** and **874** show improved detection resolution for agent GF at reduced pressures, according to an illustrative embodiment of the invention. The graphs **868** and **870** show the ion intensity spectra of agent GF at Vrf of 1500 and 1000 Vpeak, respectively, at 1 atm. The graphs **872** and **874** show the ion intensity spectra of agent GF at Vrf of 1000 and 750 Vpeak, respectively, at 0.5 atm. According to the graph **870**, the monomer and dimer peaks overlap at peak **876** at Vrf=about 1000 Vpeak. According to the graph **868**, however, the monomer peak **878** and dimer peak **880** are separated at Vrf=about 1500 Vpeak. Thus, DMS system resolution may be increased by increased the field voltage (Vrf).

[0181] In the graph **872**, the DMS system pressure is reduced to about 0.5 atm with Vrf at about 1000 Vpeak. The graph **872** shows the monomer peak **882** clearly isolated from any dimer peak, because the cluster or dimer RIP peaks are off-scale of the graph **872**. In the graph **874**, the field voltage Vrf is reduced to about 750 Vpeak, with a system pressure at about 0.5 atm. The graph **874** shows clear separation of the GF monomer peak **884** from the dimer peaks **886** and RIP peak **888**. Thus, GF may be detected and identified by the signature peaks illustrated in graph **874** in a DMS system utilizing reduced pressure, reduced field voltage, and, therefore, reduced power.

[0182] As described above, three-dimensional color dispersion plots may be used to significantly enhance the ability of a DMS system to detect and identify ion species of interest by allowing a user or pattern recognition program to match the color patterns against a library of similar color pattern for known compounds.

[0183] FIG. **33** is a three-dimensional color dispersion plot **890** depicting intensity of positive ions of 0.005 mg/m^3 DIMP at about 0.65 atm and over a range of field strengths, gas densities (E/N) and field compensation voltages Vcomp. As shown, gas density is plotted on the x-axis, Vcomp is plotted on the y-axis, and variations in intensity depicted by variations in color. The plot **890** includes several prominent branches **892**, **894**, and **896**.

[0184] FIG. **34** plots the same information as FIG. **33**, except as obtained at a decreased pressure of about 0.50 atm. As shown in plot **898**, the reduction in pressure in relation to plot **890**, results in significantly more prominent branches **900**, **902**, and **904**, thus providing enhanced resolution.

[0185] FIG. **35** is a graph depicting positive (**906**) and negative (**908**) mode three-dimensional color dispersion plots for about 0.85 mg/m^3 of agent GB RIP, at a relative

humidity (RH)=about 87%, in a DMS system operating at about 0.5 atm for a fragmented sample. The negative mode plot **908** shows only a single strong RIP branch **909**, while the positive mode plot **906** shows two strong trace analyte peaks **901** and **903** to the right of the heavy background RIP branch **905**. Thus, plotting three-dimensional graphs for both the positive and negative ion species of a sample provides further enhanced ion species identification over three-dimensional plots of positive or negative mode measurements alone.

[0186] The three-dimensional color dispersion plots **906** and **908**, as illustrated above, may also show discontinuities in the branches, i.e., peak plots or traces, that are also useful for species identification. For example, the plot **906** includes a break in the trace or branch **901** that may be included as part of the stored signature for future comparisons.

[0187] As described above with respect to FIGS. **15A**, **16A**, **17** and **25**, the dispersion plots of FIGS. **33** and **35**, may employ color saturation, gray scale variations, black and white variations and/or peak outlines in place of the color variations depicted.

[0188] According to another feature, the identification above described analysis approaches may be made device-independent. FIGS. **36A** and **36B** show experimental detection data for a homologous group of ketones, including: acetone, butanone, pentanone, hexanone, heptanone, octanone, nonanone, decanone. FIGS. **37** and **38** are tables showing monomers and clusters, respectively, for the above listed keytone species. As shown in FIGS. **36A** and **36B**, each species has a unique mobility curve, and thus a unique mobility signature, for the given set of field conditions. As described above, the mobility signatures may be obtained and enhanced in any of a plurality of ways. However, the identification process can be further enhanced by making it device-independent. With device independence, signature data can be created that can be used on any device. According to one illustrative embodiment, the invention accomplishes this by determining the parameters of a function derived from the fundamental mobility coefficient associated with each species.

[0189] Therefore, for example, the multiple data represented in FIGS. **36A**, **36B**, **37** and **48** each can be used to provide positive identification of a detected species by the unique and inherent mobility characteristic that identifies that species. According to one feature, the comparison can be made to a lookup library specific to the device in question, but also can be made to a universal set of data that is device-independent. Thus, in general, one does not wish to only compare the plot of abundance curves versus compensation voltage individually, but rather generate a plot of observed peak locations for specific compensation voltages, so that curves, slopes, signs, and various details can be discerned for each of the detected ions for comparison to a library of lookup data.

[0190] More specifically, in computing mobility signatures, we have found that an expression of the field-dependence of ion mobility, the so-called a coefficient, expressed as a function of field, can be used to generate a unique a function that is inherent for that species and is device independent. Thus the a function can be used as the unique signature of a species; this function expresses both a characteristic signature for the ion species and is device inde-

pendent. In short, according to one feature, the invention recognizes that peaks change position in signature ways because they have different alpha signatures.

[0191] In one illustrative embodiment, the invention employs the a function as a mobility signature for detected species. The signature can be determined for a detected unknown compound, based on the field conditions that are used, and then this can be used to make an identification according to a lookup table of stored known signature data associated with known compounds. More particularly, in practice of a preferred embodiment of the invention, ion species are identified based on the mobility dependence of the species under various field conditions. Data is collected for the sample under test for at least two field conditions, the data is processed, and a comparison of detection data computed as an a function for the sample under test versus the stored data enables identification of the compounds in the sample.

[0192] Referring again to the discussion of the a parameter, FIG. **3** is a plot of mobility versus electric field strength for three examples of ions, with field dependent mobility (expressed as the coefficient of high field mobility, α) shown for species at a greater, equal to and less than zero. For any given set of field conditions, the field strength and compensation can be correlated with an α value. This is shown in the work of Buryakov et. al., *A New Method Of Separation Of Multi-Atomic Ions By Mobility At Atmospheric Pressure Using A High-Frequency Amplitude Asymmetric Strong Electric Field, Intl J MassSpec and Ion Proc.* (1993), at p. 145.

[0193] We have observed that knowing the α parameter alone at a particular field strength does not prevent false positives. This would occur at the intersection of the two plots in FIG. **4**, at the point indicated by reference numeral **100**. Without more information, knowledge of the α parameter for the respective ion species at that location does not provide unique mobility signatures for both compounds. Thus, without doing more, any number of readings at this intersection is likely to result in a detection error.

[0194] However, we have also found that we can express an ion's a mobility characteristic as a function of field, i.e., as $\alpha(E)$, and can define a unique mobility signature for the ion species which is device-independent. This $\alpha(E)$ or "alpha function" relates the size, effective cross-section, shape, and mass of the ion to field conditions. It is understood that as the applied electric field increases, the increasing electric field tends to displace, stretch, and/or breaks the bonds of the ion such that the stronger the field, the greater the induced dipole, quadripole, or higher order moments of the ion. These, in turn, affect the relative mobility of the specific ion. The result of relating these aspects is to define a unique mobility signature for the ion species of interest. This also turns out to be device-independent.

[0195] The relationship of the $\alpha(E)$ function to field conditions is shown in the following:

$$V_c(E) = \frac{<\alpha E_s f(t)>}{1 + <\alpha> + <\frac{d\alpha}{dE}E_s f(t)>} \tag{1}$$

where: Vcomp (peak position); Es-electric field strength; f(t)-waveform parameters (wave shape and so forth).

[0196] Thus, for each spectral detection, we can compute a as a function of field conditions, i.e., $\alpha(E)$. Specifically, the asymmetric waveform in a planar field asymmetric waveform mobility spectrometer, $E_{max}(t)=E_{max}f(t)$, is designed to satisfy the following conditions:

$$1/T \int_0^T E_s(t)dt = <E_s f(t)> = 0 \qquad (3a)$$

$$< f^{2n+1}(t) > \neq 0 \qquad (3b)$$

where $f(t)$—is a normalized function which describes the waveform, and E_{max} is the maximum amplitude of the waveform. The waveform is designed such that its average value is zero (equation 3a) while the polarity of the electric field during one period is both positive and negative. The addition of the compensation field, C, to the waveform $E_s(t)$ yields Equation 4:

$$E(t)=E_s(t)+C=E_s f(t)+C \qquad (4)$$

so the average ion velocity over a period of the asymmetric waveform can be written as:

$$V=<V(t)>=<K(E)E(t)> \qquad (5)$$

Only ions with average velocity of zero, v=0, will pass through the gap without neutralization. An expression for the compensation field required to enable an ion to pass through the gap can be obtained by substituting Equations 2, 3, and 4 into Equation 5 as shown in Equation 6:

$$C = \frac{<\alpha E_s f(t)>}{1 + <\alpha.> + <\frac{d\alpha}{dE}E_s f(t)>}. \qquad (6)$$

The value of this compensation electric field can be predicted precisely when the alpha parameter for the ion species, the waveform $f(t)$, and the amplitude of the asymmetric waveform E_{max} are known.

[0197] A procedure for extraction of $\alpha(E)$ from experimental measurements of the electric field dependence of the mobility scans is thus known. In this section, some additional considerations regarding the alpha parameter and methods to determine this parameter described. First, emphasis must be given that the alpha parameter is a function (not a number) and the physical and chemical information about an ion is contained in the shape of the $\alpha(E)$ curve. The method of representing this curve is incidental to the topic. The only criterion critical in these methods is that the calculated values for mobility (i.e. $K(E)=K_o\{1+\alpha(E)\}$) should be as close as possible to the experimental values. The function for $\alpha(E)$ can be represented as an even power series or in complex form. In either instance, the curves of experimental results and calculated should agree closely. Thus, the quality of the approximation is limited by the accuracy of the experimental results and has been illustrated. Discerning the quality of a model based upon two parameters, three parameters, or a nonlinear

function with five parameters was difficult. All approximations were located within the error of ΔC_1 (at $\pm 9\%$).

[0198] In this work, a simple uniform method is described to represent the function of $\alpha(E)$, which will be suitable for comparison of results obtained under different experimental conditions. These methods could be used for differing asymmetric waveforms or different designs of IMS drift tubes: linear, cylindrical, or planar DMS.

[0199] In general then, the criteria for choosing the level of approximation of alpha is first to ensure that the method of extracting the alpha parameter uses the least number of individual parameters of the experimental device. Second, the result should contain the fewest number of adjustable parameters, and the approximation curves should be within the experimental error bars. In the next section, the general method to extract the alpha parameter is described and then applied in the subsequent section.

[0200] The function of $\alpha(E)$ can be given as a polynomial expansion into a series of electric field strength E degrees as shown in Equation 7:

$$\alpha(E) = \sum_{n=1}^{\infty} \alpha_{2n} \cdot E^{2n} \qquad (7)$$

Substituting Equation 7 into Equation 6 provides a value of the compensation voltage as shown in Equation 8 where an uneven polynomial function is divided by an even polynomial function. Therefore an odd degree polynomial is placed after the identity sign to approximate experimental results:

$$C = \frac{\sum_{n=1}^{\infty} \alpha_{2n} S^{2n+1} \langle f^{2n+1}(t) \rangle}{1 + \sum_{n=1}^{\infty} (2n+1)\alpha_{2n}S^{2n}\langle f^{2n}(t)\rangle} \equiv \sum_{n=1}^{\infty} c_{2n+1}S^{2n+1}\langle f^{2n+1}\rangle \qquad (8)$$

This allows the a comparison of the expected coefficient (approximated) to be compared to the values of alpha parameter as shown in Equation 9:

$$c_{2n+1} = \alpha_{2n}\langle f^{2n+1}\rangle - \sum_{k=1}^{n-1} (2(n-k)+1)c_{2k+1}\alpha_{2(n-k)}\langle f^{2(n-k)}\rangle \qquad (9)$$

Alternatively, alpha parameters can be calculated by inverting the formula by using an approximation of the experimental results per Equation 10:

$$\alpha_{2n} = \frac{1}{\langle f^{2n+1}\rangle}\left\{ c_{2n+1} + \sum_{k=1}^{n-1} (2(n-k)+1)c_{2k+1}\alpha_{2(n-k)}\langle f^{2(n-k)}\rangle \right\} \qquad (10)$$

[0201] Any number of polynomial terms (say 2n), in principle, can be determined from Equation 10 though a practical limit exists as the number of polynomial terms in

the experimental result of the approximation c_{2n+1} should be higher than the expected number of alpha coefficients α_{2n}. Since the size of n depends on the experimental error, the power of the approximation of the experimental curves $C(E_s)$ cannot be increased without limit. Usually N experimental points of $C_i(E_{si})$ exist for the same ion species and experimental data can be approximated by the polynomial using a conventional least-square method. Finally, the number series terms cannot exceed the number of experimental points so increasing the number of series terms above the point where the fitted curves are located within the experimental error bars in unreasonable. In practice, two or three terms are sufficient to provide a good approximation shown in prior findings. The error in measurements must be determined in order to gauge the order of a polynomial for alpha. The sources of error in these experiments (with known or estimated error) were:

[0202]   1. Error associated with measurement and modeling of the RF-field amplitude (~5%);

[0203]   2. Error in $C(E_s)$ from a first-order approximation of Equation 4 (~3%), and

[0204]   3. Error in measuring the compensation voltage (~5-8%).

An approximate error may be ~10% and there is no gain with approximations beyond two polynomial terms; thus, alpha can be expressed as $\alpha(E/N)=1+\alpha^1(E/N)^2\alpha_2(E/N)^4$ with a level of accuracy as good as permitted

by the measurements.

[0205]   A standard least-square method (regression analysis) was used to approximate or model the experimental findings. For N experimental points with $C_i(E_{si})$ and for $C=C^3S^3+c_5S^5$ a function $y=c_3+c_5x$ can be defined where $y=C/S^3$; $x=S^2$ so c_5 and c_3 are given by Equations 11 and 12, respectively:

$$c_5 = \frac{\sum_{i=1}^{N} x_i \sum_{i=1}^{N} y_i - N \sum_{i=1}^{N} x_i y_i}{\left(\sum_{i=1}^{N} x_i\right)^2 - N \sum_{i=1}^{N} x_i} \tag{11}$$

$$c_3 = \frac{1}{N}\left(\sum_{i=1}^{N} y_i - c_5 \sum_{i=1}^{N} x_i\right) \tag{12}$$

Through substituting experimental value C_3, C_5, values for α_2 and α_4 can be found per Equations 13 and 14:

$$\alpha_2 = c_3 / \langle f^3 \rangle \tag{13}$$

$$\alpha_4 = \frac{c_5 + 3c_3\alpha_2\langle f^2 \rangle}{\langle f^5 \rangle} \tag{14}$$

In order to calculate α_{2n}, knowledge is needed for the approximations of experimental curves for $C(E_s)$ and for the function $f(t)$—which is a normalized function describing the asymmetric waveform.

[0206]   For example, nine data points were identified for each of the eight ketones of FIGS. 36A, 36B, 37, and 38, based on the data collected in the tables of FIGS. 37 and 38. These can be used to compute the α curve for that species, such as with a piecewise linear approximation to the α curve. For example, two data points for butanone are a(Vcomp-a, Vrf-a) and b(Vcomp-b, Vrf-b). Between these two points, the slope and sign of the butanone curve can be computed. More complete characterization of the curve, such as with polynomial curve fitting, is also possible.

[0207]   Now this data set becomes part of a data store for use in identification of the species of an unknown detected ion species for which two data points are collected and the corresponding curve data is computed. In short, in an illustrative practice of the invention, we collect data on at least two closely associated points (peaks) for a given ion sample and generate the curve data accordingly. Once we have the detected and computed data, we assume this approximates the alpha curve and therefore do a lookup to our stored data. Upon finding a match, we can then positively identify the sample.

[0208]   In FIGS. 39A and 39B (monomers and clusters, respectively) we computed unique a curves for keytone ions (acetone, butanone, pentanone, hexanone, heptanone, octanone, nonanone, decanone) based on data collected in the tables of FIGS. 37 and 38, plotting the percent change in a against the change of field strength for the various data collected. These plots of percent change in a against field strength express a unique signature for each of these ion species. This is loaded in our data store for later comparison: the signature data includes the RF field strength and the compensation voltage at which the peak is detected, we also associate with it the identifying data for the known a function associated with that detected peak location and field conditions for each species.

[0209]   FIGS. 39A and 39B thus express the α function for individual ketones spanning electric fields of 0 to 80 Td (~23 kV/cm), expressed as a percentage change in alpha as a function of field conditions. These plots are fundamental signature features of these ion species that are independent of the drift tube parameters and can be used in other mobility spectrometers. Thus, the α function can be favorably used in practice of the invention to provide a mobility identification data set that is device-independent.

[0210]   These results are surprising and demonstrate that for chemicals with the same functional group, protonated monomers of a single type exhibit a broad range of behavior vis-á-vis the dependence of coefficients of mobility on electric fields. This difference in behavior for a common moiety suggests that the effect from the electric field must be associated with other aspects of molecular structure. One possible interpretation is that ions are heated during the high field and the effect on the protonated monomer should be striking. These ions with structures of $(H_3O)^+M (H_2O)_n$ or perhaps $(H_3O)^+M (H_2O)_n(N_2)_2$, should be prone to dissociations with slight increases in ion temperature caused by the high field conditions. Thus, ion cross-sections and mobilities would accompany declustered small ions at high fields.

[0211]   Referring again to FIG. 39A, it should be noted that there is approximately a 20% increase in $\alpha(E)$ for the protonated monomer of acetone with high fields. As the

molecular weight of the keytone is increased, ion heating is less pronounced and reflected in the $\alpha(E)$ function. The $\alpha(E)$ function for proton bound dimers (clusters) is consistent with decreases in mobility under high field conditions. Consequently, the basis for the $\alpha(E)$ function differs from that of protonated monomers. Indeed, the proton bound dimer for decanone undergoes about a 5% decrease at high fields. The cause for a decrease in mobility at high fields has no existing model but should be due to increased collisional size or increased strength of interaction between the ion and the supporting gas.

[0212] Furthermore, if we were to do the same for the cyclohexane and DMMP in FIG. 4, the computed alpha curves would differ accordingly. In this manner, the invention can distinguish ion species even when their mobility curves overlap, as long as we have at least a second detection data set to associate with each detected species in question. Therefore, the invention achieves a high level of assurance for the accuracy of identifications.

[0213] Thus we have shown that the fundamental dependence of mobility for ions in high electric field can be obtained from field asymmetric ion mobility spectrometry. Functions of dependence can be extracted from experiments using known methods to treat imperfect waveforms. These findings show an internal consistency with a homologous series of ketones, and also indicates a mass dependence not previously reported.

[0214] Focusing attention now on FIGS. 40A-40F a specific sequence of steps is described that may be carried out to perform species identification in several of the embodiments of the invention. These steps are provided by way of illustration and not limitation. In this illustration, the sequence of steps may be performed by the microprocessor 46 of the ion mobility spectrometer device 10 of FIG. 5. The microprocessor 46 provides digital control signals to the RF dispersion voltage (Vrf) generator 42 and compensation voltage (Vcomp) generator 44 to control the drive voltages for the filter 24. The voltage generators 42 and 44 may also include, for example, digital-to-analog converters, not shown in detail in FIG. 5.

[0215] The microprocessor 46 coordinates the application of specific RF dispersion voltages Vrf and compensation voltages Vcomp, also taking into account the function of observing responses from the detector 26 as read through the analog to digital converter 48. By detecting attributes (such as the peaks) of observed abundances of a particular ion species across a range of Vrf voltages, the microprocessor 46 can thus take steps to identify particular compounds. These may include, for example, comparing or correlating particular "response curve" data against a library of response curve data as stored in the memory 47. They can also include computation of a curve parameters. The results of the comparison operation can be provided in the form of an appropriate output device such as a display or personal computer or the like, or maybe provided by electrical signals through an interface to other data processing equipment.

[0216] As shown more particularly in FIG. 40A, a state 1000 is entered into the microprocessor 46 in which a compound is to be analyzed. Here, the compound is known and identified, such as by a user supplying an identifying text string to the computer. A sequence of steps is then performed by which data is to be acquired concerning the

known chemical compound. From this state 1000, a next state 1002 is entered in which a range of dispersion voltages Vrf and compensation voltages Vcomp are determined by the processor 46. These ranges include a beginning voltage (b) and an end voltage (s) and step voltage(s) to be applied to each of the ranges Vrf is thus varied from an initial value Vrf(b) to a final value Vrf(e) by a step amount Vrf(s). Similarly, Vcomp is to be varied from Vcomp(b) to a final value Vcomp(e) by a step amount Vcomp(s).

[0217] The voltage ranges are then applied in the following steps. Specifically, step 1004 is entered in which the Vrf is allowed to step through a range of values. A state 1008 is entered next in which the compensation voltage Vcomp is also swept or stepped through a series of values or ranges. In state 1010, the response to each applied voltage is stored as a value, (a).

[0218] If the last compensation voltage has not yet been tested, then processing returns to state 1008 in which the next compensation voltage is applied. However, in state 1012, if all of the compensation voltages have been applied, then processing proceeds to a state 1014 wherein a test is made to see if all of the dispersion have been applied.

[0219] The loop continues until all of the compensation and dispersion voltages have been applied. The resulting set of data is then analyzed in a state 1018 to identify features of interest. In the specific example being described, it is the peak locations that are of interest. For each such peak in an observed response for a given applied dispersion voltage Vrf, a response value for a specific Vcomp is determined and its corresponding amplitude (a) is detected and stored.

[0220] The response curve data, or certain attributes thereof such as the peak locations are then stored as a data object P (or table) as shown in FIG. 40B. Such an object illustratively contains an identification of the tested compound such as a text string. Also stored are a set of the applied dispersion voltages Vrf. For each such dispersion voltage Vrf, a corresponding peak compensation voltage is stored. Specifically, at least the compensation voltage Vcomp at which a peak was observed, and preferably, the corresponding amplitude of the response (abundance) observed at that peak is stored.

[0221] As previously described in detail, for a given Vrf, there may be a set of compensation voltages at which a number of "peaks" are observed. For example, as was described in connection with FIG. 14A, the sample analyzed can be made up of a compound of specific ions, including monomers, cluster ions, and reactant ion peaks. Thus, illustratively, there is an accommodation in the structure of object P to anticipate that there will be more than one peak observed in any particular mobility scan, and that the number of peaks per response curve may not always be the same number.

[0222] An example, the illustrative object P of FIG. 40B includes a data element, where for a single RF dispersion voltage Vrf-1, peaks may be observed at compensation voltages Vc11, ..., Vcmn having corresponding amplitudes a11, ..., amn. This may correspond to the case of the lowest applied dispersion voltage in FIG. 14A, where numerous peaks 601-, 605-1, 608-1 are detected. However, at another dispersion voltage Vrf-m, only a single peak at Vcomp-m, am was detected. This might correspond to a case such as in the uppermost curve of FIG. 6A, where only a single peak 601-*m* was detected.

[0223] In an illustrative application, a library of data objects P (reference vectors) is developed by performing the steps of FIG. **40A** for a plurality of known compounds of interest. This then permits an instrument to eventually enter a chemical recognition state **1200** as shown in FIG. **40C**. Next, a series of measurements are taken in states **1202-1214**. This series is similar to the measurements taken in FIG. **40A**. Specifically, a series of measurements are taken for a specified compensation and RF voltages. It should be understood that an entire set of all of the same measurements need not be taken in this mode as were taken in the chemical data acquisition mode. Specifically, not all points on a relatively dense response curve need to be taken, only enough to identify each compound.

[0224] Once the measurements are taken, a state **1220** is entered in which features, such as peaks of the response are identified for each peak a corresponding compensation voltage and amplitude may be identified and these stored to a candidate measurement vector P'. The candidate vector P' thus represents a series of data that need to be tested against a number of candidate compounds. The candidate vector P' is then analyzed in states **1230** and/or **1240** by looking up corresponding counterparts in the library of reference vector objects P, and scoring a match between P and P'. These steps may be iterated until such time as a match or a best match is determined in a state **1250**.

[0225] It should be understood that any number of techniques may be used to determine a degree of match between P and P'. For example, if the elements (Vcomp, a) of P and P' are considered to be data points in Euclidian geometry space, a distance can be computed. The comparison with the smallest Euclidian distance can then be selected as the best match. However, other recognition techniques may be used to determine an identity of an unknown compound, for example, more sophisticated signal processing techniques such as correlation may be used to resolve peaks; or other known pattern recognition algorithms, neural networks or artificial intelligence techniques may be used to find a best match for P'. This best match is then identified to a user, such as by looking up the compound identifier field and displaying in state **1260**.

[0226] FIG. **40D** shows a series of steps, which may be added to the data acquisition phase and the chemical recognition phase to take advantage of second order data processing characteristics. For example, in the data acquisition state, a series of states **1020**, **1022**, **1024** and **1026** may be added to curve-fit specific attributes of the measured response. Specifically, a state **1020** may be entered in which for each data element of the object P a vector, z, is formed consisting of the peak compensation voltages vc**11**, vc**12**, . . . vc1*m*.

[0227] This vector is a vector of point locations for the peaks observed for a range of compensation voltages. Returning attention to FIG. **14A**, briefly, this may correspond, for example, to locating the points **601**-1, . . . **601**-*m*, . . . **601**-*n* corresponding to peak height and locations for the monomer ions of interest. A curve may then be fit through these peaks such as by applying a curve fitting algorithm, in state **1024**. In the illustrated example it is assumed that a quadratic equation is fitting the peaks of the form $y^2 = \beta x^2 + \gamma$. The β and γ coefficients can then be stored in the state **1026**

associated with the vector. The chemical is thus identified by a curve fit to its peak locations approximating its mobility (α coefficient) behavior.

[0228] If this is done, a corresponding set of steps **1270**, **1272** and **1274** can be added to the recognition process to identify peaks by performing a curve fit to observe data, and then, determining γ and β coefficients, rather than comparing raw data values in states **1270** and **1272**. In state **1274**, the β and γ coefficients are tested to determine closest matches in the P object library.

[0229] FIG. **40F** shows a series of steps that may be used to identify or distinguish peaks in the acquisition phase. Here initial data may be added to the objects P by identifying peaks as a cluster peak or monomer peak. Specifically, if a peak shift over a range of field condition voltages (e.g., FIG. **14A**) increases (i.e., shifts to the right), then this may be identified as a cluster peak. If the peak does not meet specific shifting criteria, it may be identified as a monomer peak. States **1310**, **1331**, and **1332** may thus be added to the identification process. The results of these steps adds an additional parameter L associated with each data point in the object P to further identify each peak as a monomer cluster or other peak type, as shown in FIG. **40E**.

[0230] Other approaches to this may be used to label peaks. For example, reactant ion peaks (RIP) may also be identified by performing an analysis on a response of the instrument, with no sample S applied. In this mode, only the RIPs occur, and in their behavior across a range of compensation voltages can be stored. Information concerning the particular type of peak may be stored in pointer data in a state **1320**, at which such a peak is detected. This information can then be added to the objects P, specifically as shown in FIG. **40E**.

[0231] FIG. **40G** shows additional processing steps, which may be performed in the compound recognition state to take advantage of the situation of FIGS. **36A-38** in which monomer and cluster ion behavior is observed. Specifically, the steps of FIG. **40G** may be added as further steps **1280** in the recognition phase. Here, for every candidate peak P', a corresponding monomer peak in the reference array P is compared. A score is then associated with the closest of the match in state **1284**. Similarly, in state **1286**, a cluster peak may be compared with its corresponding in the peak library P. A score sc is then determined in step **1288**, depending on the closest of this match. In a state **1290**, a final score sf can be associated with weighting the monomer peak score and the cluster peak score by weighting factors wm and wc. For example, in an instance where cluster peaks are expected to provide more information than monomer peaks, cluster peaks may be weighted highly and monomer peaks relatively low or zero factor. Using this weighting, both monomer and cluster peak identification can be combined to further refine compound analysis.

[0232] In various applications, the above described approaches to ion-based sample analysis may be employed in relatively compact, such as handheld, analyzer systems. FIG. **41** is a conceptual diagram of such a compact DMS analyzer system **1400**. The DMS system may be used, for example, to analyze compounds, such as chemical warfare agents (CWAs), and Toxic Industrial Compounds (TICs), and Toxic Industrial Materials (TIMs) according to an illustrative embodiment of the invention. By operating the

compact DMS analyzer system **1400** at less than atmospheric pressure, e.g., 0.5 atm, as described above, the system **1400** approximately doubles its resolution over existing state-of-the-art systems, while reducing its power consumption and size. By performing sample fragmentation, as described above, sample analysis may be further enhanced. By utilizing three-dimensional color dispersion plots, as also described above, analysis of CWAs, TICs, and TIMs is further enhanced.

[0233] The DMS analyzer system **1400** may employ an electromechanical pump, compressed gas or air, or the solid-state flow generator **1402**, which includes an ion source **1404**, an ion attractor **1406**, and a constrained flow channel **1408** for controlling sample flow and/or pressure within the system **1400**. The ion source **1404** provides a source of ions and the ion attractor **1406** attracts either positive or negative ions, depending on an applied bias voltage. The ion flow created in the constrained channel **1408** due to the ion flow generated by the interaction of the ion source **1404** with the ion attractor **1406** creates a fluid, e.g., a sample effluent, flow. In some illustrative embodiments, the DMS analyzer system **1400** may be miniaturized, such that the analyzer unit **1410** is included in application-specific integrated circuits (ASICs) embedded on a substrate **1412**. A solid state flow generator of the type employed by the invention is described in further detail in co-pending and co-owned U.S. patent application Ser. No. 10/943,523, filed on 17 Sep. 2004, the entire contents of which are incorporated above by reference.

[0234] The constrained channel **1408** includes an inlet end **1414** and an outlet end **1416**. The constrained channel **1408** also includes a sample introduction inlet **1418** to enable the analyzer **1410** to collect the sample gas for analysis. A pre-concentrator **1420** may be employed at the sample introduction inlet **1418** to concentrate the sample .and improve analysis accuracy. An ionizer **1422** provides ionization of the sample using, for example, a radioactive Ni^{63} foil, or non-radioactive plasma ionizer, or other suitable ionization source within ionization region **1424**. A plasma ionizer has the advantage of enabling precise control of the energy imparted to the sample gas for ionization. Ideally, the ionizer **1422** imparts only enough energy to ionize the sample gas, without producing nitric oxides (NOx's) and ozone. A fragmentation region may also be included in the system **1400**. NOx's and ozone are undesirable because they can form ion species that interfere with the ionization of CWA agents. Because diffusion and mobility constants generally depend on pressure and temperature, the DMS analyzer system **1400** may include a temperature sensor **1426** and/or a pressure sensor **1428** for regulating the temperature and/or pressure of the sample gas within the analyzer unit **1410** for more accurate analysis. The analyzer **1410** may also include a humidity sensor. The analyzer **1410** also includes an analytical region **1440** with filter plates **1442** and detector plates **1444**. A molecular sieve **1446** may be employed to trap spent analytes.

[0235] The controller **1446** provides control of filtering and detection while also providing an output of the detection results. The power supply **1448** provides power to the filter plates **1442**, solid-state flow generator **1402**, and any other component requiring electrical power. The controller electronics **1446** for Vcomp, Vrf, the ion heater pumping, the DMS ion motion, and the pre-concentrator **1420** heater may

be located with the analyzer unit **1410**. Also, the detector **1444** electronics, pressure **1426** and temperature **1428** sensors, and the processing algorithm for a digital processor may reside within analyzer **1410**.

[0236] At atmospheric pressure, to realize the benefits of mobility nonlinearity, the DMS analyzer system **1400** illustratively employs RF electric fields of about 10^6 V/m, and a Vrf of about 200 Vpeak at about a 200×10^{-6} μm gap. However, any suitable RF electric field parameters may be employed. The power supply **1448** may be remotely located relative to the analyzer unit **1410** to generate RF voltage for filter the plates **1442**. At less than atmospheric pressure, the RF electric field may be reduced as described above to further reduce the power consumption and size of the DMS analyzer system **1400**.

[0237] The DMS analyzer system **1400** may also interface with a personal computer (PC) or controller **1446** to utilized signal-processing algorithms that convert analyzer **1410** outputs into detection, identification, and/or measurement of analytes and concentration levels. The controller **1446** or an interfacing PC may also facilitate control and power management for the DMS analyzer system **1400**. The supporting electronics for the DMS analyzer system **1400** may be implemented, for example, on an ASIC, a discrete printed circuit board (PCB), or System on a Chip (SOC).

[0238] In operation, the solid-state flow generator or electromechanical transport pump **1402** draws samples into the DMS analyzer system **1400** at the inlet **1414** and past a CWA-selective chemical membrane concentrator **1420** having an integrated heater. The CWA-selective chemical membrane pre-concentrator **1420** may also serve as a hydrophobic barrier between the analytical region **1440** of the analyzer system **1400** and the sample introduction region **1450**. The membrane of the pre-concentrator **1420**, illustratively, allows CWA agents to pass, but reduces the transmission of other interferants and act as a barrier for moisture.

[0239] The pre-concentrator **1420** may use selective membrane polymers to suppress or block common interferences (e.g., burning cardboard) while allowing CWA agents or CWA simulants to pass through its membrane. Although many selective membrane materials are available, polydimethyl siloxane (PDMS) may be a preferred membrane/concentrator/filter to reject water vapor and collect CWA analytes. At high concentration levels, water vapor molecules may cluster to the analytes, altering the analytes' mobilities. Membrane materials such as hydrophobic PDMS tend to reduce the vapor to acceptable levels while absorbing and releasing analyte atoms. The thin membrane of the pre-concentrator **1420** may also be heated periodically to deliver concentrated analytes to the ionization region **1424** and analytical region **1440**.

[0240] Except for diffusion of analytes through the membrane/filter/pre-concentrator **1420**, the analytical region **1440** is generally sealed to the outside atmosphere. Thus, the analyzer system **1400** may employ elements for equalizing the pressure inside analytical region **1440** with the atmospheric pressure outside the analyzer system **1400** or maintain pressure in the analytical region **1440** at less than atmospheric pressure for improved ion intensity peak resolution. Once the sample gas molecules are ionized, the ions are driven longitudinally in the direction indicated by the

arrow **1452** through the ion filter plates **1442** by static or traveling electrostatic fields, as opposed to being driven by the carrier gas. The filter plates **1442** apply transverse radio frequency (RF) field voltages and dc excitation electric compensation fields to the ions moving through analytical region **1440** to separate the species within a sample.

[0241] With water vapor removed, interferants (e.g., hydrocarbons and others) typically comprise roughly 0.10% of the incoming air volume by weight. Depending on the collection efficiency of the pre-concentrator **1420**, the molecular sieve **1446** may be sized to support about 6, 9, 12 or more months of substantially continuous or continuous operation before saturating. The molecular sieve **1446** may also be configured to allow movement of air in a circulatory fashion through the ion filter electrodes **1442** and back to the ionization region **1424**.

[0242] The DMS analyzer system **1400** may be used for detecting low concentrations (e.g., parts per trillion (ppt)) of CWAs, such as, without limitation, nerve and blister agents. In one illustrative embodiment, the DMS analyzer system **1400** includes a high-sensitivity, low-power, sample gas analyzer **1404** that builds on MEMS technology, but further miniaturizes the DMS analyzer system **1400** to achieve parts-per-trillion sensitivity, about 0.25 W overall power consumption (i.e., 1 Joule measurement every 4 seconds), and a size of about 2-cm³ or less.

[0243] Because of the smaller analytical region **1440** and the resulting lower flow rate requirements, a low-power (e.g., mW) solid-state gas transport pump **1402**, using ionic displacement, may be employed to draw an air sample into the DMS analyzer system **1400** and onto the CWA-selective chemical membrane pre-concentrator **1420**. Compact DMS analyzer systems according to the invention have shown very high sensitivities to CWA simulants. By way of example, a compact DMS analyzer system according to the invention has been shown to detect methyl salycilate at parts-per-trillion (ppt) levels. The DMS analyzer system **1400** has the ability to resolve CWA simulants from interferants that cannot be resolved by current field-deployed detection technologies.

[0244] FIG. **42** is a graph depicting a DMS spectra showing resolution of dimethylmethylphosphonate (DMMP) from aqueous firefighting foam (AFFF) as measured in a DMS analyzer system **1400**. AFFF is one interferant that has proved extremely challenging for conventional IMS systems to resolve CWAs or other simulants. The AFFF ion intensity peak tends to overlap with the agent peak during sample detection in DMS or IMS systems.

[0245] FIG. **42** is a graph of multiple plots showing experimental results for a series of CWA simulants selectively mixed with 1% headspace of AFFF. The top plot **1460** of FIG. **42** shows RIP for a DMS analyzer system **1400** with background air but no sample present with the sensor at atmospheric pressure. In the next plot **1462**, the AFFF interferant is added. This results only in a slight shift to the left (more negative compensation voltage) of the RIP ion intensity peak. Then, in plot **1464**, the CWA stimulant DMMP is introduced into the spectrometer and the typical monomer and dimmer peaks appear together with a corre-

sponding reduction in the RIP peak ion intensity. When 1% AFFF is added according to plot **1468**, the DMMP peaks are not effected and only a slight leftward shift of the RIP is observed. The same experiment was repeated with DIMP in plots **1468** and **1470**, and the effect of AFFF was negligible. In plot **1472**, MS is introduced, and according to monitored negative ion peaks, gives similar data illustrating the lack of interference with AFFF. The conclusion is that 1% AFFF has virtually no effect. Thus, FIG. **42** illustrates the ability of the DMS analysis system **1400** to resolve CWA simulants from interferants.

[0246] In one illustrative embodiment, the compact hand-held DMS analyzer system **1400** is achieved by combining the following design characteristics: (a) using the analyzer/filter/detector **1410** with improved sensitivity and size reduction; (b) using the solid-state flow generator or electromechanical pump as a gas transport pump **1402** to sample and move analytes; (c) using the CWA-selective chemical membrane pre-concentrator **1420** with integrated heater (in some configurations provided by using a solid-state generator or electromechanical pump to transfer heat from other analyzer system components to the pre-concentrator **1420**) to remove water vapor and to concentrate; and/or (d) using electric field propulsion of the ions **1454** through the analytical region **1440** of analyzer **1410**.

[0247] According to various illustrative embodiments, the invention improves the resolution of species identification over conventional systems, while decreasing size and power to achieve parts-per-trillion sensitivity, a less than about 0.25 mW overall power dissipation, and a size of about a 2-cm³ or less in an entire system not including a power source or display, but including an RF field generator. According to some embodiments, an analyzer system of the invention has a total power dissipation of less than about 15 W, about 10 W, about 5 W, about 2.5 W, about 1 W, about 500 mW, about 100 mW, about 50 mW, about 10 mW, about 5 mW, about 2.5 mW, about 1 mW, and/or about 0.5 mW. According to further embodiments, an analyzer system according to the invention, optionally including a display (e.g., indicator lights and/or an alphanumeric display) and a power source (e.g., a rechargeable battery) compartment, along with an RF field generator, may have a total package outer dimension of less than about 0.016 m³, 0.0125 m³, 0.01 m³, 0.0056 m³, 0.005 m³, 0.002 m³, 0.00175 m³, 0.0015 m³, 0.00125 m³, 0.001 m³, 750 cm³, 625 cm³, 500 cm³, 250 cm³, 100 cm³, 50 cm³, 25 cm³, 10 cm³, 5 cm3, 2.5 cm³, with the package being made, for example, from a high impact plastic, a carbon fiber, or a metal. According to further embodiments, an analyzer system, for example, according to the invention, including an RF generator, and optionally including a display, keypad, and power source compartment, may have a total package weight of about 5 lbs, 3 lbs, 1.75 lbs, 1 lbs, or 0.5 lbs.

[0248] Table 1 provides a comparison of drift tube (e.g., the constrained channel) dimensions, fundamental carrier gas velocities, and ion velocities for a various illustrative embodiments of a DMS analyzer system **1400** depending on the flow rate (Q) available to the analysis unit. Designs **1-4** provide flow rates of varying orders of magnitude ranging from about 0.03 l/m to about 3.0 l/m. Table 1 illustrates that

as the flow rate is decreased through the DMS analyzer system **1400**, the filter plate dimensions and power requirements are reduced. Table 1 is applicable to a DMS analyzer system **1400** using either a sample gas or longitudinal field-induced ion motion. The time to remove an unwanted analyte is preferably less than about the time for the carrier to flow through the filter region (tratio). Also, for a particular target agent, the lateral diffusion as the ion flows through the analyzer **1410** is preferably less than about half the plate spacing (difratio). Based on this criteria, the plate dimensions may be reduced to about 3×1 mm² or smaller, while the ideal flow power may be reduced to less than about 0.1 mW. Thus, even for design **4**, the number of analyte ions striking the detectors is sufficient to satisfy a parts-per-trillion detection requirement.

over a range of RF voltage versus compensation voltage with varying intensity represented in varying color that illustrates the enhanced identification (selectivity) of a compound using a three-dimensional dispersion plot by, for example, DMS system **1400**. Both measurements were performed with a concentration of GA at 0.14 ng/l, a Ni⁶³ source, 50% RH, 3 scan averaging, and 350 cc/min carrier gas flow. The differences between the three-dimensional plots **814** of FIGS. **25** and **1750** of FIG. **50** illustrate that performing both positive and negative ion mode detection provides enhanced signature identification of ion species.

[0252] In certain illustrative embodiments, the compact DMS system **1400** of FIG. **41** and various other figures may employ features and/or be incorporated into systems

TABLE 1

Illustrative DMS Analyzer System Design Specifications and Characteristics

Description	Units	Symbol	Design 1 Q = 3 l/m Baseline	Design 2 Q = 0.3 l/m Base dimen	Design 3 Q = 0.3 l/m scaled	Design 4 Q = 0.03 l/m
plate dimensions						
*length	m	L	0.025	0.025	0.005	0.001
*width	m	b	0.002	0.002	0.001	0.0004
*air gap	m	h	0.0005	0.0005	0.0005	0.0002
*volume flow rate	l/min	Qf	3	0.3	0.3	0.03
Flow velocity	m/s	Vf	50	5	10	6.25
pressure drop	Pa	dPf	1080	108	43.2	33.75
flow power	W	Powf	0.054	0.00054	2.16E−04	1.69E.05
RF excitation	V	Vrf	650	650	650	260
design ratios						
Time to remove unwanted analyte divided by carrier time	s	tratio	0.0128	0.0013	0.0128	0.0160
wanted ions-lateral diffusion divided by half gap	s	difratio	0.200	0.632	0.200	0.283
ions to count per cycle	—	Nout	1.22E+07	1.22E+06	1.22E+06	1.22E+05

[0249] For sample/carrier gases, there does not appear to be an electromechanical pump that operates at the preferred flow characteristics with an efficiency better than about 0.5%. With a 0.5% efficiency, an ideal flow loss of about 0.05 mW results in an actual power consumption of about 10 mW, about a factor of 100 greater than in the above discussed illustrative embodiment of the invention.

[0250] The DMS system **1400** may simultaneously detect both positive and negative ion intensity peaks which further improves detection selectivity. The combination of the positive and negative ion channel information, the shift in spectral peak as a function of applied field strength or voltage, and the display is this information in a three-dimensional manner provide a novel mechanism for chemical identification.

[0251] FIG. **43** is a three-dimensional dispersion plot **1750** of the detection of positive ions of agent GA over a range of field voltages and field compensation voltages with varying intensity represented in varying color according previously described illustrative embodiments of the invention. The plot **1750** illustrates the enhanced identification (selectivity) of a compound using a three-dimensional dispersion plot by, for example, a DMS system **1400**. In comparison, FIG. **25** is a three-dimensional dispersion plot of negative ions of GA

described in further detail in U.S. Pat. Nos. 6,495,823 and 6,512,224, the entire contents of both of which are incorporated herein by reference.

[0253] FIGS. **44-53** are conceptual block diagrams of chemical and/or biological agent detection systems using various configurations of a mobility detection analyzer system such as those depicted and described herein, a recirculation system, and other components according to illustrative embodiments of the invention. More particularly, FIG. **44** is a conceptual block diagram of a CWA and/or biological agent detection system **1476** according to an illustrative embodiment of the invention. The system **1476** employs a mobility detection system **1478**, molecular sieve **1480**, pump **1482** with optional vent **1484**, optional second molecular sieve **1486**, circulating channel **1488**, sample inlet **1490**, exhaust **1492**, membrane **1494**, and orifice **1496**. The system **1476** may also employ filtered air or gas **1498** to circulate or transport a sample through the system **1476**. The mobility analyzer system **1478** may be a compact DMS analyzer system **1400** of FIG. **48**, DMS system **10** of FIG. **5**, an IMS, a TOF-IMS, a GC-IMS, an MS or the like. The system **1476**, like all of the previously described illustrative systems, may employ one or more dopants to enhance analysis.

[0254] In operation, the system **1476** receives a sample S at inlet **1490** and passes it through the membrane **1494** into the circulation channel **1498**. The membrane **1494** may filter out unwanted interferants, if desired, in the same or similar manner as the pre-concentrator **1420** of FIG. **48**. The orifice **1496** may, in a fixed, controlled, or adjustable manner, regulate the gas and/or sample flow into the analyzer system **1478** and thereby regulate or control the pressure within the analyzer system **1478**. Thus, the analyzer system **1478** may operate at atmospheric pressure, below atmospheric pressure, or above atmospheric pressure. The pump **1482** maintains gas flow in the analyzer system **1478** and pressure control either independently or in coordination with the orifice **1496**. Thus, in one example, the pump **1482** draws sample flow through the orifice **1496** into the analyzer system **1478** to enable detection and identification of select ion species. The analyzer system **1478** may be a DMS system **1400** that tunably detects certain ion species by adjusting its field/flow channel conditions, such as, its Vrf and Vcomp, parameters and in some configurations, controlling the pump **1484** and/or the orifice **1496** to control pressure within the system **1400**.

[0255] Once detection and identification are performed, the molecular sieve **1480** may trap spent analytes from the analyzer system **1478**. Again, the pump **1484**, whether electromechanical or solid-state, propels the gas, optionally through a second molecular sieve **1486**, through the circulating channel **1488**. The sample gas is then expelled through the membrane **1494** and the outlet **1492** or mixed and re-circulated with more sample S back into the orifice **1496**.

[0256] FIG. **45** is a conceptual block diagram of a CWA and/or biological agent detection system **1500**, configured for reduced pressure analysis, according to an illustrative embodiment of the invention. The system **1500** is similar to the system **1476** except that an additional sample flow channel **1502** is employed instead of a membrane. The system **1500** includes sample S inlet **1504**, orifice **1506**, ionization region **1508**, deflector plate **1510**, attractor plate **1512**, channel **1502** pump **1514**, second channel **1516**, analyzer system **1518**, molecular sieve **1520**, pump **1522**, and optional second molecular sieve **1524**.

[0257] In operation, the system **1500** draws sample S through the sample inlet **1504** and through the orifice **1506**. The orifice **1506** may be controlled, fixed, or adjustable to regulate sample gas flow and/or pressure in the channel **1502**. The pump **1514** may also be used in coordination with the orifice **1506** to regulate gas flow and/or pressure within the channel **1502**. The deflector plate **1510** may force, push, or selectively separate ions into the channel **1516** through the opening **1526** while the attractor **1512** may attract ions from the channel **1502** into the channel **1516**. A pressure drop across the opening **1526** may be adjusted so that only sample ions enter the channel **1516** while sample neutrals are prevented from entering. The sample ions may be directly introduced into the analyzer system **1518** or the ions may be neutralized and then re-ionized in the analyzer system **1518**. The analyzer system **1518** may be a DMS system, IMS system, or the like. The analyzer system **1518** may include multiple DMS, IMS, or other like systems or a combination of such systems to perform sample detection and identification. For example, system **748** of FIG. **21** or

system **754** of FIG. **22** may be employed to apply conventional DMS detection in combination with fragmentation to enhance sample analysis.

[0258] The channel **1516** pump **1524** may then draw the sample S from the analyzer system **1518** through the molecular sieve **1520** and then propel the sample S, optionally through the second molecular sieve **1524**. The molecular sieves **1520** and **1524** will capture most of the spent sample S analytes. Any remaining sample S is mixed with new sample S gas and returned to the analyzer system **1518** via the channel **1516**. The outlet **1528** expels sample S gas from the channel **1502**.

[0259] FIG. **46** is a conceptual block diagram of a cylindrical or coaxial CWA and/or biological agent detection system **1530** according to an illustrative embodiment of the invention. The system **1530** includes a sample S inlet **1532**, constrictor **1534**, inner channel **1536**, opening **1538**, clean transport gas inlet **1540**, outer channel **1542**, analyzer system **1544**, channel **1542** outlet **1546**, and channel **1536** outlet **1548**.

[0260] In operation, the system **1530** draws the sample S into the channel **1536** through the constrictor or orifice **1534**. The constrictor **1534** may be adjustable, controllable or fixed to enable a pressure reduction below 1 atm, for example to 0.5, 0.65, or 0.85 atm, in the channel **1536**. The clean transport gas inlet **1540** receives clean transport gas into the channel **1542**. The channel **1542** may operate at pressures below 1 atm. The sample S maybe drawn or attracted into the channel **1542** through the opening **1538** by a pressure differential with the channel **1536**, an ion attractor in channel **1542**, gas flow into channel **1542**, or other like technique. The analyzer system **1544** then detects and identifies the ion species of the sample S and expels the sample S through the outlet **1546**. The sample neutrals in the channel **1536** may be expelled through the outlet **1548**.

[0261] FIG. **47** is a DMS system **1550** including an orifice **1552** at the system **1550** inlet to control pressure within the system **1550** in coordination with a pump **1554**. The system also includes the molecular sieve **1556**, ion source **1558**, filter **1560**, and detector **1562**. In operation, the pump **1554** has sufficient power to draw a sample S through the orifice **1552** to then enable detection of the sample at a reduced pressure.

[0262] FIG. **48** is a DMS system **1564** including an orifice **1566**, ionization source **1568**, filter **1570**, detector **1572**, molecular sieve **1574**, pump **1576**, a second molecular sieve **1578**, an inlet **1582**, and outlets **1584** and **1586**. Because the membrane **1580** is positioned upstream of the orifice **1566** and the sample flow is in direction **1588**, the membrane **1580** operates at atmospheric pressure while the ionization source **1568**, filter **1570**, and detector **1572** operate below atmospheric pressure due to a pressure drop across the orifice **1566**. It may be advantageous to operate the membrane **1580** at atmospheric pressure to prolong its useful life.

[0263] FIG. **49** is a DMS system **1590** including an orifice **1592**, ionization source **1594**, filter **1596**, detector **1598**, molecular sieve **1600**, pump **1602**, a second molecular sieve **1604**, a membrane **1606**, an inlet **1608**, and outlets **1610** and **1612**. Because the membrane **1606** is positioned downstream of the orifice **1592** and the sample flow is in the

direction **1614**, the membrane **1606** operates below atmospheric pressure along with the ionization source **1594**, filter **1596**, and detector **1598** due to a pressure drop across the orifice **1592**. It may be advantageous to operate the membrane **1606** below atmospheric pressure.

[0264] FIG. **50** is a DMS system **1616** including an orifice **1618**, ionization source **1620**, filter **1622**, detector **1624**, molecular sieve **1626**, pump **1628**, a second molecular sieve **1630**, a membrane **1632**, an inlet **1634**, and outlets **1636** and **1638**. Because the membrane **1632** and the ionization source **1620** are positioned upstream of the orifice **1618** and the sample flow is in direction **1640**, the membrane **1632** and the ionization source **1620** operate at atmospheric pressure while the filter **1622** and detector **1624** operate below atmospheric pressure due to a pressure drop across the orifice **1618**. It may be advantageous to operate the membrane **1632** and ionization source **1620** at atmospheric pressure.

[0265] FIG. **51** is a DMS system **1642** including a first channel **1644** and a second channel **1646** operating at atmospheric pressure. The first channel **1644** includes an ionization source **1648**, deflector electrode **1650**, pump **1652**, inlet **1666**, and outlet **1668**. The second channel **1646** includes a filter **1654**, detector **1656**, molecular sieve **1658**, pump **1660**, and molecular sieve **1662**. An opening **1664** provides fluid communication between the channels **1644** and **1646**.

[0266] In operation, the system **1642** receives a sample S at the inlet **1666** into the channel **1644**. The ionization source **1648** ionizes the sample S. The ionized portions of the sample S, e.g., the positive ions, are deflected through the opening **1664** into the channel **1646** by the deflector **1650** having a positive charge. When the deflector **1650** is negatively charged, the deflector **1650** may deflect negative ions of sample S through the opening **1664** into the channel **1646**. The neutrals and non-deflected ions of sample S are then drawn by the pump **1652** to the outlet **1668** and expelled from the system **1642** while the ions in the channel **1646** are filtered by the filter **1654** and detected by the detector **1656**. The pump **1660** creates circulation flow in the direction **1670** within the channel **1646** to draw the sample S through the molecular sieve **1658** which collects spent analytes and then through a second molecular sieve **1662**.

[0267] FIG. **52** is a DMS system **1672** including a first channel **1674** and a second channel **1676** operating below atmospheric pressure without a membrane. The first channel **1674** includes an ionization source **1678**, deflector electrode **1680**, pump **1682**, inlet **1684**, outlet **1686**, and orifice **1700**. The second channel **1676** includes a filter **1688**, detector **1690**, molecular sieve **1692**, pump **1694**, molecular sieve **1696**, and orifice **1702**. An opening **1698** provides fluid communication between the channels **1674** and **1676**.

[0268] In operation, the system **1672** receives a sample S at the inlet **1684** into the channel **1674** and through the orifice **1700**. The orifice **1700** provides a pressure drop within the channel **1674** caused by the gas and/or air flow generated by the pump **1682**. The ionization source **1678** ionizes the sample S. The ionized portions of the sample S, e.g., the positive ions, are deflected through the opening **1698** into the channel **1676** by the deflector **1680** having a positive charge. When the deflector **1680** is negatively charged, the deflector **1680** may deflect negative ions of

sample S through the opening **1698** into the channel **1676**. The neutrals and non-deflected ions of sample S are then drawn by the pump **1682** to the outlet **1686** and expelled from the system **1672** while the ions in the channel **1676** are filtered by the filter **1688** and detected by the detector **1690**. The pump **1694** creates circulation flow in the direction **1704** within the channel **1676** to draw the sample S through the molecular sieve **1692** which collects spent analytes and then through a second molecular sieve **1696**.

[0269] FIG. **53** is a DMS system **1706** including a first channel **1708**, a second channel **1710**, and a third channel **1712** with the second channel **1710** and third channel **1712** capable of operating at or below atmospheric pressure using a membrane **1714**. The first channel **1708** includes an inlet **1716** and an outlet **1718**. The second channel **1710** includes an ionization source **1718**, optional ionization source **1720**, deflector electrode **1722**, filter **1724**, and detector **1726**. The third channel **1712** includes an attractor electrode **1728**, filter **1730**, and detector **1732**. The combined circulation channel **1734** includes the chemical filter **1736**, pump **1738**, and optional chemical filter **1740**. An opening **1742** provides fluid communication between the channels **1710** and **1712**.

[0270] In operation, the system **1706** receives a sample S at the inlet **1716** into the channel **1708**. The sample S may be introduced from a GS column. The membrane **1714** may filter a portion of the sample S and provide a pressure barrier to enable a pressure below atmospheric pressure in the channels **1710** and **1712**. The channels **1710** and **1712**, along with the combined circulation channel **1734**, circulate filtered and clean carrier gas. The ionization source **1718** ionizes the sample S within this clean carrier gas. Optionally, a second ionization source **1720** may be employed in the channel **1710** to enhance the ability of the deflector **1722** and attractor **1728** to transfer select ions from the channel **1710** to the channel **1712**. For example, the ionized portions of the sample S, e.g., the positive ions, are deflected through the opening **1742** into the channel **1712** by the deflector **1722** when the deflector **1722** is positively charged. When the deflector **1722** is negatively charged, the deflector **1722** may deflect negative ions of sample S through the opening **1728** into the channel **1712**.

[0271] The neutrals and non-deflected ions of sample S are then drawn by the pump **1738** through the channel **1710**, filter **1724** and detector **1726** while the selected ions are drawn through the channel **1712**, filter **1730**, and detector **1732**. The pump **1738** creates circulation flow in the direction **1744** within the channels **1710**, **1712**, and **1734** to draw the carrier gas from the channels **1710** and **1712** into the channel **1734** and through the chemical filter **1736** and, optionally, the second chemical filter **1740**. The chemical filters **1736** and **1740** remove unwanted contaminants from the carrier gas. A make up gas may also optionally be introduced into the channel **1734** from an outside system.

[0272] The deflector **1722** and the attractor **1728** may be activated in a controlled manner to transport ions from the channel **1710** to the channel **1712**. In the channel **1710**, the non-deflected ions are filtered by filter **1724** and detected by detector **1726** while, in the channel **1712**, the deflected and attracted ions are filtered by the filter **1730** and detector **1732**. The resulting detected measurements from the channels **1710** and **1712** can then be compared, added, or subtracted from each other to enhance the identification of

ion species. The controlled ionization of the sample S which is performed in a clean carrier gas, the detection in the channel **1712** of monomer or de-clustered ions, and the detection of clustered ions in the channel **1710** provide enhanced compound and ion species identification.

[0273] Although the invention has been described with regard to particular illustrative embodiments, it should be appreciated that the invention is broader in scope and can be applied to any system for identification of unknown species of ions traveling through a varying controlled excitation field, the identification being based on the known characteristic travel behavior of the species under the varying field conditions. The ion or ions to be identified may be traveling alone or in a group of ions of same or differing characteristic travel behavior. The filter field may be compensated in any of various manners as long as a species of interest is returned to the center of the flow and permitted to pass through the filter while all other species are retarded or neutralized. Identification is made based on known field-dependent differential mobility behavior of at least one species of ions traveling in the field at known field conditions.

[0274] It should also be appreciated that in various practices, the invention provides improved systems, methods and devices for ion species identification. According to some features, the invention varies one or more filter field/flow channel conditions to improve species discrimination. For example, according to some illustrative embodiments, the invention determines changes in ion mobility, based, for example, on changes in: Vrf; Vcomp; field strength; Vrf duty cycle; Vrf wavelength; Vrf frequency; and/or flow channel temperature, pressure, humidity, flow rate, doping and/or carrier gas CG composition. According to other features, the invention takes multiple scans of the sample S, for example, by recirculating the sample S and/or processing the sample S in parallel and/or in series with one or more additional DMS, IMS, TOFIMS, GC, FTIR, MS, or LCMS, at differing flow channel/filter field conditions.

[0275] According to further features, the invention employs approaches, such as, fragmenting, lowering pressure, and three-dimensional dispersion plotting to enhance detection resolution. According to other features, the invention stores a library of signatures for known compounds and pattern matches data from unknown compounds with the stored library to identify the unknown compounds. It should be understood that the invention is applicable not only to planar DMS systems, but may be applied in general to ion mobility spectrometry devices of various types, including various geometries, ionization arrangements, detector arrangements, and the like, and brings new uses and improved results even as to structures that are all well known in the art.

[0276] Thus, the invention is not limited to configurations of the illustrative embodiments and may be practiced in any other suitable configurations, including radial and cylindrical DMS devices. Additionally, various modifications and variations may be made to the invention without departing from the spirit and scope herein.

What is claimed is:

1. A device for displaying ion mobility based analysis information comprising:

a processor for processing data from an ion mobility based analyzer, and

a display for displaying the processed data in a three-dimensional representation.

2. The device of claim 1, wherein the processing includes receiving the data.

3. The device of claim 1, wherein the data includes detection data.

4. The device of claim 3, wherein the detection data includes ion intensity information.

5. The device of claim 1, wherein the data is associated with a plurality of processing conditions of the ion mobility based analyzer.

6. The device of claim 5, wherein the processing conditions include at least one of Vrf, Vcomp, field strength, duty cycle of Vrf, frequency of Vrf, time, flow channel pressure, flow channel temperature, and an amount of dopant.

7. The device of claim 1, wherein processing includes comparing a set of data from the ion mobility based analyzer with a library of data to identify one or more ion species.

8. The device of claim 1, wherein the processing includes generating a three-dimensional spectral signature based on the data.

9. The device of claim 8, wherein the processing includes comparing the three-dimensional spectral signature based on the data with a library of three-dimensional spectral signatures to identify on or more ion species.

10. The device of claim 8, wherein the spectral signature includes a set of information associated with at least two processing conditions and associated detection data of the ion mobility analyzer.

11. The device of claim 1, wherein a change in value of at least one of the first, second and a third dimension of the three-dimensional representation is displayed as a change in at least one of gray scale, black and white patterning, color, and color saturation.

12. The device of claim 1, wherein the thee-dimensional representation includes a first dimension as a length, the second dimension as a width, and a third dimension as a height.

13. The device of claim 1, wherein the three-dimensional representation is a dispersion plot.

14. The device of claim 1, wherein the three-dimensional representation comprises an x-axis for field voltage, a y-axis for Vcomp, and varying aspects of a color-related feature for ion intensity.

15. The device of claim 1, wherein the three-dimensional representation includes an x-axis corresponding to field voltage, a y-axis corresponding to field compensation voltage, and a z-axis corresponding to ion intensity.

16. A method for displaying ion mobility based analysis information comprising:

processing data from an ion mobility based analyzer, and

displaying the processed data in a three-dimensional representation.

17. The method of claim 16, wherein the processing includes receiving the data.

18. The method of claim 16, wherein the data includes detection data.

19. The method of claim 18, wherein the detection data includes ion intensity information.

20. The method of claim 16, wherein the data is associated with a plurality of processing conditions of the ion mobility based analyzer.

21. The method of claim 20, wherein the processing conditions include at least one of Vrf, Vcomp, field strength, duty cycle of Vrf, frequency of Vrf, time, flow channel pressure, flow channel temperature, and an amount of dopant.

22. The method of claim 16, wherein processing includes comparing a set of data from the ion mobility based analyzer with a library of data to identify one or more ion species.

23. The method of claim 16, wherein the processing includes generating a three-dimensional spectral signature based on the data.

24. The method of claim 23, wherein the processing includes comparing the three-dimensional spectral signature based on the data with a library of three-dimensional spectral signatures to identify on or more ion species.

25. The method of claim 23, wherein the spectral signature includes a set of information associated with at least two processing conditions and associated detection data of the ion mobility analyzer.

26. The method of claim 16, wherein a change in value of at least one of the first, second and a third dimension of the three-dimensional representation is displayed as a change in at least one of gray scale, black and white patterning, color, and color saturation.

27. The method of claim 16, wherein the three-dimensional representation includes a first dimension as a length, a second dimension as a width, and a third dimension as a height.

28. The method of claim 16, wherein the three-dimensional representation is a dispersion plot.

29. The method of claim 16, wherein the three-dimensional representation comprises an x-axis for field voltage, a y-axis for Vcomp, and varying aspects of a color-related feature for ion intensity.

30. The method of claim 16, wherein the three-dimensional representation includes an x-axis corresponding to field voltage, a y-axis corresponding to field compensation voltage, and a z-axis corresponding to ion intensity.

* * * * *